

# **A Tale of Two Barrels: Import of $\beta$ -Barrel Proteins into Yeast Mitochondria**

## **Dissertation**

der Mathematisch-Naturwissenschaftlichen Fakultät  
der Eberhard Karls Universität Tübingen  
zur Erlangung des Grades eines  
Doktors der Naturwissenschaften  
(Dr. rer. nat.)

vorgelegt von  
Anasuya Moitra  
aus Durgapur, Indien

Tübingen

2022



Gedruckt mit Genehmigung der Mathematisch-Naturwissenschaftlichen Fakultät  
der Eberhard Karls Universität Tübingen.

Tag der mündlichen Qualifikation:	10.01.2023
Dekan:	Prof. Dr. Thilo Stehle
1. Berichterstatter:	Prof. Dr. Doron Rapaport
2. Berichterstatter:	Prof. Dr. Ralf-Peter Jansen



Erklärung / Declaration: Ich erkläre, dass ich die zur Promotion eingereichte Arbeit mit dem Titel:

**„A tale of two barrels: Import of  $\beta$ -barrel proteins into yeast mitochondria”**

Selbständig verfasst, nur die angegebenen Quellen und Hilfsmittel benutzt und wörtlich oder inhaltlich übernommene Stellen als solche gekennzeichnet habe. Ich versichere an Eides statt, dass diese Angaben wahr sind und dass ich nichts verschwiegen habe. Mir ist bekannt, dass die falsche Abgabe einer Versicherung an Eides statt mit Freiheitsstrafe bis zu drei Jahren oder mit Geldstrafe bestraft wird.

I hereby declare that I have produced the work entitled:

**“A tale of two barrels: Import of  $\beta$ -barrel proteins into yeast mitochondria”**

submitted for the award of a doctorate, on my own (without external help), have used only the sources and aids indicated and have marked passages included from other works, whether verbatim or in content, as such. I swear upon oath that these statements are true and that I have not concealed anything. I am aware that making a false declaration under oath is punishable by a term of imprisonment of up to three years or by a fine.

Tübingen, den



# Table of Contents

<b>List of abbreviations</b>	<b>1</b>
<b>Summary</b>	<b>3</b>
<b>Zusammenfassung</b>	<b>5</b>
<b>List of publications contained in this thesis</b>	<b>7</b>
a) <b>Accepted publications</b>	
b) <b>Manuscript ready for submission</b>	
<b>Personal contribution to the publications contained in this thesis</b>	<b>9</b>
<b>Chapter 1 – Introduction</b>	<b>11</b>
<b>1.1 Diversity of outer membrane <math>\beta</math>-barrel proteins</b>	<b>12</b>
1.1.1 Bacterial $\beta$ -barrel proteins	12
1.1.2 Mitochondrial $\beta$ -barrel proteins	13
1.1.3 Chloroplast $\beta$ -barrel proteins	13
1.1.4 Synthetic $\beta$ -barrel proteins	14
<b>1.2 Biogenesis pathways of bacterial <math>\beta</math>-barrel proteins</b>	<b>14</b>
<b>1.3 Biogenesis of mitochondrial <math>\beta</math>-barrel proteins</b>	<b>15</b>
1.3.1 Early cytosolic events of newly synthesized mitochondrial $\beta$ -barrel precursors	15
1.3.2 Targeting of $\beta$ -barrel precursors to the mitochondrial surface	18
1.3.3 Membrane integration of mitochondrial $\beta$ -barrels by the TOM and TOB/SAM complexes	19
<b>1.4 Biogenesis of chloroplast <math>\beta</math>-barrel proteins</b>	<b>23</b>
<b>Chapter 2 – Research Objectives</b>	<b>25</b>
<b>Chapter 3 – Materials and Methods</b>	<b>27</b>
<b>3.1 Yeast strains and growth conditions</b>	<b>28</b>
<b>3.2 Recombinant DNA techniques</b>	<b>28</b>
<b>3.3 Isolation of mitochondria</b>	<b>28</b>
<b>3.4 Subcellular fractionation</b>	<b>29</b>
<b>3.5 Protease protection assay</b>	<b>29</b>
<b>3.6 Alkaline (carbonate) extraction</b>	<b>30</b>

<b>3.7 Western blotting and immunodecoration</b>	<b>30</b>
<b>3.8 Blue-native (BN) PAGE</b>	<b>31</b>
<b>3.9 Analysis of growth of yeast cells</b>	<b>31</b>
<b>3.10 Relevant tables</b>	<b>32</b>
<b>Chapter 4 – Yeast can express and assemble bacterial secretins in the mitochondrial outer membrane</b>	<b>35</b>
<b>4.1 Introduction</b>	<b>36</b>
<b>4.2 Results</b>	<b>38</b>
4.2.1 Assembly of the T3SS secretin InvG in yeast mitochondria	<b>38</b>
4.2.2 Assembly of the T3SS secretin SsaC in yeast mitochondria	<b>41</b>
<b>4.3 Discussion</b>	<b>42</b>
<b>Chapter 5 – Yeast mitochondria can process <i>de novo</i> designed <math>\beta</math>-barrel proteins</b>	<b>45</b>
<b>5.1 Introduction</b>	<b>46</b>
<b>5.2 Results</b>	<b>46</b>
5.2.1 TMBs can localise to and integrate into the mitochondrial outer membrane	<b>46</b>
5.2.2 The biogenesis of the synthetic TMBs does not depend on the import receptors Tom20 and Tom70	<b>53</b>
5.2.3 The assembly of the TMBs depends to a variable extent on the TOB complex	<b>56</b>
5.2.4 Single amino acid mutation in the $\beta$ -signal does not significantly alter the biogenesis of both TMBs	<b>60</b>
<b>5.3 Discussion</b>	<b>63</b>
<b>References</b>	<b>66</b>
<b>Acknowledgements</b>	<b>75</b>
<b>Appendix</b>	<b>79</b>
<b>A.1 Author contributions</b>	<b>79</b>
<b>A.2 Accepted publications</b>	<b>80</b>

## List of abbreviations

BAM	$\beta$ -barrel assembly machinery
BN-PAGE	Blue native polyacrylamide gel electrophoresis
BSA	Bovine serum albumin
CE	Carbonate extraction
DHFR	Dihydrofolate reductase
DNA	Deoxyribonucleic acid
DTT	Dithiothreitol
EDTA	Ethylenediaminetetraacetic acid
EM	Electron microscopy
ER	Endoplasmic reticulum
ERMES	Endoplasmic reticulum-mitochondria encounter structure
FL	Full-length
GFP	Green fluorescent protein
HA	Haemagglutinin
Hsp	Heat shock protein
IM	Inner membrane
IMS	Intermembrane space
LPS	Lipopolysaccharides
Mdm	Mitochondrial distribution and morphology
MOM	Mitochondrial outer membrane
NMR	Nuclear Magnetic Resonance
OD	Optical density
OEP	Outer envelope protein
OM	Outer membrane
PCR	Polymerase chain reaction
PK	Proteinase K
POTRA	Polypeptide-transport-associated
PVDF	Polyvinylidene fluoride
SAM	Sorting and assembly machinery
SDS-PAGE	Sodium dodecyl sulfate polyacrylamide gel electrophoresis
SPI	<i>Salmonella</i> pathogenicity island

T2SS	Type II secretion system
T3SS	Type III secretion system
T4P	Type IV pili
TBS	Tris buffer saline
TCA	Trichloroacetic acid
TIC	Translocase of the inner membrane of chloroplast
TIM	Translocase of the inner membrane
TMB	Transmembrane $\beta$ -barrel
TOB	Topogenesis of outer membrane $\beta$ -barrel protein
TOC	Translocase of the outer membrane of chloroplast
TOM	Translocase of the outer membrane
TPI	Triosephosphate isomerase
VDAC	Voltage-dependent anion channel
WCL	Whole cell lysate
WT	Wild type
YadA	<i>Yersinia</i> adhesin A

## Summary

Membrane-embedded  $\beta$ -barrel proteins are found in the outer membranes (OM) of Gram-negative bacteria, mitochondria and chloroplasts. They form a barrel shaped hydrophilic pore in the membrane, which can be composed of 8-26 H-bonded, mostly anti-parallel  $\beta$ -strands. These proteins constitute an essential part of the OM proteome by functioning as transporters, enzymes, or subunits of protein translocons and membrane insertion machineries. Mitochondrial and chloroplast  $\beta$ -barrel proteins are transcribed in the nucleus and translated on cytosolic ribosomes, from where they are targeted to the correct subcellular organelle and ultimately integrated with the help of dedicated import machineries into the respective outer membrane.

The biogenesis pathways for  $\beta$ -barrel proteins have been quite conserved over the course of evolution due to the endosymbiotic origins of mitochondria and chloroplasts from ancient Gram-negative bacterial endosymbionts ( $\alpha$ -proteobacterium and a photosynthetic cyanobacterium, respectively). Such conserved mechanisms prompted studies to investigate the evolutionary lineage of these pathways. Bacterial and chloroplast  $\beta$ -barrel proteins have been shown to be targeted and integrated into mitochondria upon their expression in yeast cells.

In this study, I aimed to study the extent of evolutionary conservation of  $\beta$ -barrel biogenesis pathways. To this end, I started my work by testing the destiny of the bacterial secretins InvG and SsaC upon their expression in yeast cells. My findings demonstrate that they are capable of mitochondrial localization in these cells and their biogenesis is variably dependent on the TOM import receptors and the TOB complex.

Next, I investigated whether *de novo* designed synthetic eight-stranded transmembrane  $\beta$ -barrel (TMB) proteins (Tmb2.3 and Tmb2.17) could be expressed in yeast cells and integrated into their mitochondria. I further assessed the role of components of yeast mitochondrial import and assembly machinery in their proper biogenesis.

My results demonstrate that both *de novo* designed synthetic TMBs, Tmb2.3 and Tmb2.17, can be successfully expressed as HA-tagged proteins in yeast cells without being detrimental to their growth. Subcellular fractionation experiments show that both TMBs can be targeted to the mitochondria, with partial ER localization as well. They are embedded into the mitochondrial OM with a topology that exposes part of them to the cytosol.

I further observed that the absence of either one of the import receptors (Tom20 or Tom70), did not impair their biogenesis. Moreover, deficiency in certain critical components of the TOB complex, namely Mas37 and Tob55, differentially affected the assembly of these synthetic TMBs. In the absence of Mas37, the mitochondrial steady state levels of the TMBs decreases, similar to *bona fide* mitochondrial  $\beta$ -barrel proteins. Depletion of Tob55 leads to decreased mitochondrial levels of Tmb2.3-HA, while the levels of Tmb2.17-HA are further stabilized. Interestingly, Tmb2.3-HA can assemble into higher oligomers in a TOB complex dependent manner. In contrast, the biogenesis of Tmb2.17-HA seems to be independent of the TOB complex.

Collectively, my findings indicate that different  $\beta$ -barrel proteins can be dependent to a variable extent on the proper function of the TOB complex. Such distinctions might be mapped to the dissimilarities in their sequence, hydrophobicity patterns of the  $\beta$ -strands, and/or different sequence of the classical  $\beta$ -signal at the last  $\beta$ -strand. My results further suggest the strong evolutionary conservation of pathways and machineries that recognize  $\beta$ -barrel structural elements and facilitate the biogenesis of  $\beta$ -barrel proteins across the spectrum of life.

## Zusammenfassung

$\beta$ -Fass-Proteine, die in die Membran eingebettet werden, kommen in den äußeren Membranen (OM) von Gram-negativen Bakterien, Mitochondrien und Chloroplasten vor. Sie bilden eine röhrenförmige hydrophile Pore in der Membran, die aus 8-26  $\beta$ -Strängen zusammengesetzt sein kann, die meist antiparallel angeordnet werden und über Wasserstoffbrücken miteinander verbunden werden. Diese Proteine sind ein wesentlicher Bestandteil des OM-Proteoms, da sie als Transporter, Enzyme oder Untereinheiten von Proteintranslokatoren und Membraninsertionsmaschinerie fungieren. Mitochondriale und chloroplastische  $\beta$ -Fass-Proteine werden im Zellkern transkribiert und auf zytosolischen Ribosomen translatiert, von wo aus sie zu den richtigen subzellulären Organellen transportiert und schließlich mit Hilfe spezieller Importmaschinerie in die jeweilige äußere Membran integriert werden.

Die Biogenesewege für  $\beta$ -Fass-Proteine blieben im Laufe der Evolution ziemlich konserviert, da Mitochondrien und Chloroplasten aus ursprünglichen Gram-negativen bakteriellen Endosymbionten ( $\alpha$ -Proteobakterium bzw. photosynthetisches Cyanobakterium) endosymbiotisch entstanden sind. Diese konservierten Mechanismen haben Studien veranlasst, die evolutionäre Verknüpfung dieser Signalwege zu untersuchen. Es hat sich gezeigt, dass bakterielle und chloroplastische  $\beta$ -Fass-Proteine nach ihrer Expression in Hefezellen gezielt in Mitochondrien integriert werden.

In dieser Studie wollte ich das Ausmaß der evolutionären Erhaltung der  $\beta$ -Fass-Biogenesewege untersuchen. Zu diesem Zweck begann ich meine Arbeit, indem ich das Schicksal der bakteriellen Sekretine InvG und SsaC nach ihrer Expression in Hefezellen testete. Meine Ergebnisse zeigen, dass sie in diesen Zellen zur mitochondrialen Lokalisierung fähig sind und ihre Biogenese in unterschiedlicher Weise von den TOM-Importrezeptoren und dem TOB-Komplex abhängig ist.

Als nächstes untersuchte ich, ob *de novo* entworfene synthetische achtsträngige Transmembran- $\beta$ -Fass-Proteine (TMB) (Tmb2.3 und Tmb2.17) in Hefezellen exprimiert und in ihre Mitochondrien integriert werden können. Darüber hinaus habe ich die Rolle von Komponenten der mitochondrialen Import- und Assemblierungsmaschinerie in Hefezellen bei deren korrekter Biogenese untersucht.

Meine Ergebnisse zeigen, dass beide *de novo* entworfenen synthetischen TMBs, Tmb2.3 und Tmb2.17, erfolgreich als HA-markierte Proteine in Hefezellen exprimiert werden können, ohne

ihr Wachstum zu beeinträchtigen. Subzelluläre Fraktionierungsexperimente zeigen, dass beide TMBs zu den Mitochondrien lokalisiert werden können, wobei sie teilweise auch zum ER lokalisiert werden. Sie sind in das mitochondriale OM mit einer Topologie eingebettet, die einen Teil von ihnen dem Zytosol aussetzt.

Ich habe außerdem beobachtet, dass das Fehlen eines der Importrezeptoren (Tom20 oder Tom70) ihre Biogenese nicht beeinträchtigt. Darüber hinaus wirkte sich das Fehlen bestimmter kritischer Komponenten des TOB-Komplexes, nämlich Mas37 und Tob55, unterschiedlich auf den Aufbau dieser synthetischen TMBs aus. In Abwesenheit von Mas37 nimmt der mitochondriale Steady-State-Spiegel der TMBs ab, ähnlich wie bei echten mitochondrialen  $\beta$ -Fass-Proteinen. Die Deletion von Tob55 führt zu einer Abnahme des mitochondrialen Tmb2.3-HA-Spiegels, während der Tmb2.17-HA-Spiegel weiter stabilisiert wird. Interessanterweise kann sich Tmb2.3-HA in Abhängigkeit vom TOB-Komplex zu höheren Oligomeren zusammensetzen. Im Gegensatz dazu ist die Biogenese von Tmb2.17-HA unabhängig vom TOB-Komplex.

Insgesamt deuten meine Ergebnisse darauf hin, dass verschiedene  $\beta$ -Fass-Proteine in unterschiedlichem Maße von der ordnungsgemäßen Funktion des TOB-Komplexes abhängig sein können. Solche Unterschiede könnten auf die Unähnlichkeiten in ihrer Sequenz, die Hydrophobizitätsmuster der  $\beta$ -Stränge und/oder die unterschiedliche Sequenz des klassischen  $\beta$ -Signals am letzten  $\beta$ -Strang zurückzuführen sein. Meine Ergebnisse deuten außerdem darauf hin, dass die Wege und Mechanismen, die  $\beta$ -Fass-Strukturelemente erkennen und die Biogenese von  $\beta$ -Fass-Proteinen im gesamten Spektrum des Lebens diktieren, evolutionär stark erhalten sind.

## List of publications contained in this thesis

### a) Accepted publications

1. Natarajan, J., **Moitra, A.**, Zabel, S., Singh, N., Wagner, S., & Rapaport, D. (2019). Yeast can express and assemble bacterial secretins in the mitochondrial outer membrane. *Microbial Cell*, 7(1), 15–27. <https://doi.org/10.15698/mic2020.01.703>
2. **Moitra, A.**, & Rapaport, D. (2021). The Biogenesis Process of VDAC - From Early Cytosolic Events to Its Final Membrane Integration. *Frontiers in Physiology*, 12, 732742. <https://doi.org/10.3389/fphys.2021.732742>

### b) Manuscript ready for submission

3. **Moitra, A.**, Tiku, V., & Rapaport, D. (2022). Yeast mitochondria can process *de novo* designed  $\beta$ -barrel proteins.



## Personal contribution to the publications contained in this thesis

### a) Accepted publications

1. Natarajan, J., **Moitra, A.**, Zabel, S., Singh, N., Wagner, S., & Rapaport, D. (2019). Yeast can express and assemble bacterial secretins in the mitochondrial outer membrane. *Microbial Cell*, 7(1), 15–27. <https://doi.org/10.15698/mic2020.01.703>

I performed experiments for the revised version of this contribution. I analysed the whole cell extracts from the different strains expressing InvG-HA and SsaC-HA (Figure 6D and Figure 7C). I furthermore edited the final manuscript. This publication comprises a part of Chapter 4 of this thesis.

2. **Moitra, A.**, & Rapaport, D. (2021). The Biogenesis Process of VDAC - From Early Cytosolic Events to Its Final Membrane Integration. *Frontiers in Physiology*, 12, 732742. <https://doi.org/10.3389/fphys.2021.732742>

I wrote the original draft of this mini-review, made all the figures, and edited the final manuscript. This publication is a section of Chapter 1 of this thesis.

### b) Manuscript ready for submission

3. **Moitra, A.**, Tiku, V., & Rapaport, D. (2022). Yeast mitochondria can process *de novo* designed  $\beta$ -barrel proteins.

I designed and performed the vast majority of experiments, analyzed the data, prepared all the figures and wrote the manuscript. This manuscript is integrated into Chapter 3 and Chapter 5 of this thesis.



# Chapter 1

## Introduction

This chapter consists of sections adapted from the following published Mini Review:

(DOI: <https://doi.org/10.3389/fphys.2021.732742>)

### **The biogenesis process of VDAC – from early cytosolic events to its final membrane integration**

Anasuya Moitra<sup>1</sup> and Doron Rapaport<sup>1,\*</sup>

<sup>1</sup>Interfaculty Institute of Biochemistry, University of Tübingen, Tübingen, Germany

\*Corresponding author

#### **Author Contributions**

I wrote the original draft, made all the figures and edited the final manuscript. Doron Rapaport co-wrote and edited the final manuscript.

# Introduction

Most of the outer membrane (OM) proteins in Gram-negative bacteria are membrane-embedded  $\beta$ -barrel proteins that are composed of 8-26 anti-parallel  $\beta$ -strands forming a barrel shaped hydrophilic pore in the membrane. These proteins perform a variety of functions ranging from active transporters of solutes, enzymes, structural proteins to protein translocons and membrane insertion machinery (Wimley 2003). In eukaryotes, the presence of  $\beta$ -barrel proteins is restricted to the OM of mitochondria and chloroplasts that were derived from prokaryotic ancestors (Gray 1999). The assembly of these proteins into their corresponding OM is in each case facilitated by a dedicated protein complex that contains a highly conserved central  $\beta$ -barrel protein termed BamA/YaeT/Omp85 in Gram-negative bacteria, Tob55/Sam50 in mitochondria, and OEP80 in plastids (Ulrich and Rapaport 2015; Gross et al. 2021). These central components are related to each other and belong to the Omp85 superfamily (Gentle, Burri, and Lithgow 2005).

## 1.1 Diversity of outer membrane $\beta$ -barrel proteins

### 1.1.1 Bacterial $\beta$ -barrel proteins

Gram-negative bacteria are enveloped by two membranes, the inner and the outer. The space between these membranes, the periplasm, contains the peptidoglycan. While the inner membrane is a regular phospholipid bilayer, the OM is an asymmetrical bilayer consisting of phospholipids and lipopolysaccharides (LPS) in the inner and outer leaflets, respectively (Walther, Rapaport, and Tommassen 2009). Bacterial  $\beta$ -barrel proteins constitute different functional groups within the OM proteome including porins, lysins, efflux pumps and membrane insertion machinery. Prominent members of Porin class of proteins include phosphoporin (PhoE), maltoporin (LamB) and Matrixporin (OmpF) (Pauptit et al. 1991). Lysins such as  $\alpha$ -haemolysin from *Staphylococcus aureus* function as pore forming toxins. Proteins like OmpA found in *E. coli*, that play key structural and functional roles for the bacteria (Krishnan and Prasadarao 2012), are also a member of this group of proteins. This class also includes the type II secretion system secretin GspD in *Vibrio cholerae* and the *Salmonella typhimurium* SPI-1 type III secretion injectisome secretin InvG (Natarajan, Singh, and Rapaport 2019).

### 1.1.2 Mitochondrial $\beta$ -barrel proteins

Mitochondria are double membrane organelles consisting of an outer and inner membrane, which sandwiches the intermembrane space and encapsulates the matrix (Nunnari and Suomalainen 2012). Mitochondrial  $\beta$ -barrel proteins reside in their OM and include mitochondrial voltage-dependent anion channel (VDAC/Porin); components of the translocase of outer membrane (TOM) and topogenesis of outer membrane  $\beta$ -barrel protein (TOB) machinery namely Tom40 and Tob55, respectively; as well as mitochondrial distribution and morphology (Mdm)10 (Paschen, Neupert, and Rapaport 2005). VDACs are abundant mitochondrial  $\beta$ -barrel proteins. Their pore is composed of 19 anti-parallel  $\beta$ -strands whereas strands 1 and 19 are in parallel orientation to each other. VDAC, which was previously known as mitochondrial porin, functions as a channel for transport of metabolites, nucleotides, ions, and even small peptides (Benz 1989). VDACs are found in mitochondria across the spectrum of life, from unicellular yeasts to plants and all higher eukaryotes. Bakers' yeast (*Saccharomyces cerevisiae*) has two genes encoding VDACs, *POR1* and *POR2*, while higher eukaryotes like humans have at least three isoforms, VDAC1, VDAC2 and VDAC3 and plants have up to five such genes (Young et al. 2007; Raghavan et al. 2012). Tob55/Sam50 in mitochondria belongs to the Omp85 superfamily comprising of 16-stranded  $\beta$ -barrel with a single polypeptide-transport-associated (POTRA) domain extending into the intermembrane space (Diederichs et al. 2020). Tob55 is important for the membrane integration of  $\beta$ -barrel proteins. Tom40 forms the 19-stranded barrel core of the TOM complex and is required for the import of the vast majority of precursor proteins into mitochondria. Mdm10 is part of the ERMES complex (Michel and Kornmann 2012) and facilitates the assembly of Tom40 in the OM (Takeda et al. 2021).

### 1.1.3 Chloroplast $\beta$ -barrel proteins

Chloroplast OM contains several  $\beta$ -barrel proteins including outer envelope proteins (OEP) such as OEP7, OEP16, OEP21, OEP24, OEP37 and OEP40 which function as high-conductance solute channels (Schleiff et al. 2003; Goetze et al. 2006; Hemmler et al. 2006). The outer envelope protein of 21 kDa (OEP21) constitutes an ATP-regulated anion selective channel (Bölter et al. 1999), while the outer envelope proteins of 24, 37, and 40 kDa (OEP24, OEP37, and OEP40, respectively) function as cation-selective solute channels with distinct substrate specificities (Pohlmeyer et al. 1998; Schleiff et al. 2003; Harsman et al. 2016). In addition, the  $\beta$  barrel protein Toc75-III forms the protein conducting channel of the translocase of the OM of chloroplasts (TOC complex) (Schleiff and Becker 2011) while Toc75-V, also

known as OEP80, belongs to the Omp85 superfamily and is probably involved in the chloroplast OM  $\beta$ -barrel protein biogenesis (Gross et al. 2021). Other Omp85 homologs include the non-essential proteins P36 (Nicolaisen et al. 2015) and P39 (Hsueh et al. 2017).

#### **1.1.4 Synthetic $\beta$ -barrel proteins**

A recent study from the Baker lab showed that *de novo* designed synthetic  $\beta$ -barrel proteins could fold and assemble into barrel structures in artificial lipid membranes (Vorobieva et al. 2021). These rather small proteins, named Tmb2.3 and Tmb2.17, are around 13.5 kDa and composed of eight anti-parallel  $\beta$ -strands. These proteins were designed using a combination of geometric models, Rosetta protein structure simulations, and extensive *in vitro* and *in vivo* testing of expression and folding capabilities. The key to the successful design of these proteins was the careful balance of hydrophobicity and  $\beta$ -sheet propensity of the sequences and the presence of important structural features like glycine kinks,  $\beta$ -bulges, and register-defining side-chain interactions.

## **1.2 Biogenesis pathways of bacterial $\beta$ -barrel proteins**

Precursors of bacterial  $\beta$ -barrel proteins are synthesized in the cytoplasm with N-terminal signal sequences that are recognised by the cytosolic SecB chaperone. SecB binding to the precursor prevents their aggregation and maintains them in a translocation-competent state. The signal sequence and bound chaperone target the precursor to the bacterial inner membrane where the precursor traverses through the SecYEG translocon and reaches the periplasm (Papanikou, Karamanou, and Economou 2007). The signal sequences are then cleaved off and the precursors are stabilized by the periplasmic chaperone Skp and assisted in folding by the periplasmic chaperone SurA (Walther, Rapaport, and Tommassen 2009). Ultimately, the  $\beta$ -barrel precursors are assembled into the outer membrane, potentially through lateral release, with the help of the  $\beta$ -barrel assembly machinery (BAM) complex composed of the  $\beta$ -barrel protein, BamA and four lipoproteins BamB-E (Noinaj et al. 2014) (Figure 1.1). Many bacterial  $\beta$ -barrel proteins contain a signature sequence at the C-terminus. This signature sequence consists of a highly conserved Phe (or Trp) residue at the ultimate C-terminal position, Tyr or a hydrophobic residue at position 3, and also hydrophobic residues at positions 5, 7, and 9 from the C-terminus. The Phe residue is essential for optimum assembly into the OM (Struyvé, Moons, and Tommassen 1991).

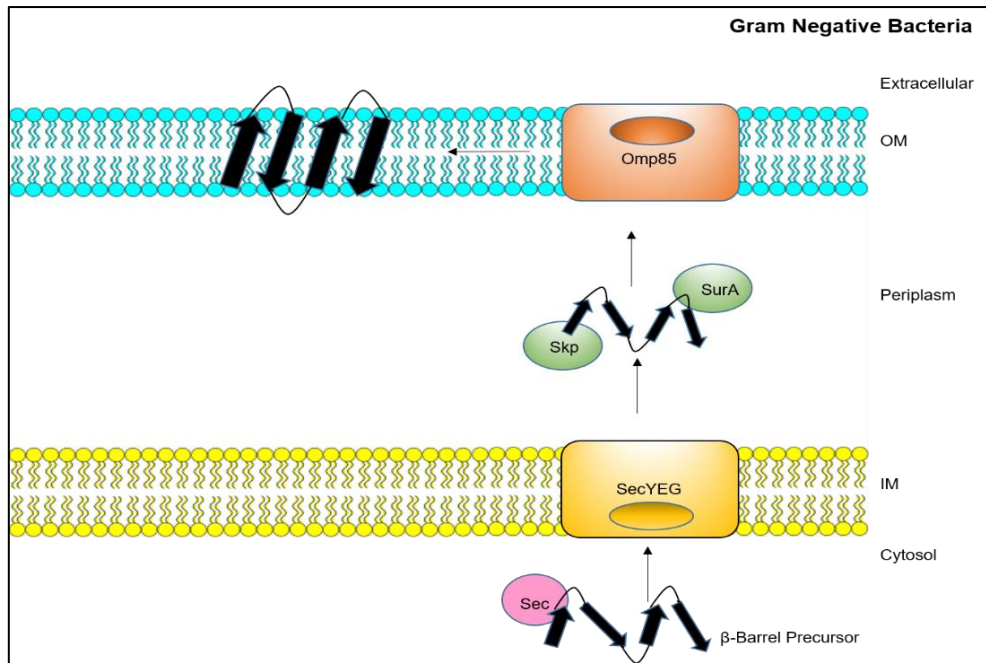


**Figure 1.1 – Biogenesis pathway of bacterial  $\beta$ -barrel proteins.**

Precursors of bacterial  $\beta$ -barrel proteins are synthesized in the cytoplasm with signal sequences, which are recognized by Sec chaperones, who in turn guide them to the SecYEG translocon, which eventually translocates them across the inner membrane (IM). Signal sequences are cleaved in the periplasm and the periplasmic chaperones SurA and Skp mediate the transfer to the BAM machinery (Omp85) that ultimately integrate the  $\beta$ -barrel protein into the outer membrane (OM).

### 1.3 Biogenesis of mitochondrial $\beta$ -barrel proteins

During the evolution of mitochondria from an ancient endosymbiont, most of the organellar genes, including those encoding predecessors of  $\beta$ -barrel proteins, were transferred to the nucleus, with the mitochondrial genome retaining the codes for only few key proteins, mostly components of the respiratory chain complexes (Gray, Burger, and Lang 1999). Mitochondrial  $\beta$ -barrel proteins are thus transcribed in the nucleus and translated on cytosolic ribosomes. Then, they need to be targeted to the correct sub-cellular organelle, namely the mitochondria, and ultimately integrated into the mitochondrial OM (MOM) with the help of dedicated import machineries.

#### 1.3.1 Early cytosolic events of newly synthesized mitochondrial $\beta$ -barrel precursors

The first challenge in the biogenesis of mitochondrial  $\beta$ -barrel proteins is to keep the newly synthesized molecules in an import competent conformation (Freitag, Neupert, and Benz 1982; Rapaport and Neupert 1999). The rather hydrophobic  $\beta$ -strands that build the transmembrane

segments are prone to aggregation in the cytosol. Thus, the newly synthesized  $\beta$ -barrel precursors must be bound by cytosolic chaperones to shield these hydrophobic patches, preventing the emerging nascent chain from engaging in unfavourable intra- and intermolecular interactions (Kim et al. 2013). This association with chaperones maintains them in an import-competent conformation. Recent studies, using yeast as a model system, demonstrate that newly synthesized  $\beta$ -barrel precursors like VDAC dynamically interact with Hsp70 chaperones (Ssa1/2) and their Hsp40 co-chaperones Ydj1 and Sis1 (Figure 1.2) (Jores et al. 2018). Inhibiting the activity of the cytosolic Hsp70 chaperone, preventing its docking to the mitochondrial receptor Tom70, or co-depleting both co-chaperones Ydj1 and Sis1 resulted in a significant reduction in the *in vivo* and *in vitro* import of VDAC into yeast mitochondria. Experiments utilizing Hsp70 inhibitors and pull-down assays demonstrated that the interactions between VDAC and Hsp70 chaperones and their physiological role are also conserved in mammalian cells. Moreover, a  $\beta$ -hairpin motif of VDAC, hypothesized to be the mitochondrial targeting signal (see below), was sufficient for the interaction with these (co-)chaperones. It should be emphasized that these (co-)chaperones support the import of not only  $\beta$ -barrel proteins but are also involved in the biogenesis of many additional proteins. Hence, so far, a targeting factor, which is dedicated solely to  $\beta$ -barrel proteins was not identified. The abovementioned chaperones and the mitochondrial targeting information contribute to the relay of the nascent precursors to the receptors of the translocase of the outer membrane (TOM) of mitochondria. Other  $\beta$ -barrel proteins like Tom40 and Tob55/Sam50 appear to follow the same route as VDAC (Jores et al. 2018).

Currently, it is not clear whether the aforementioned cytosolic factors support biogenesis solely by preventing premature unfavourable aggregation or whether they also facilitate specific targeting. The contribution of the chaperone anchor Tom70, located at the mitochondrial surface, to the overall import process suggests that association with chaperones also increases the specificity of organellar targeting.

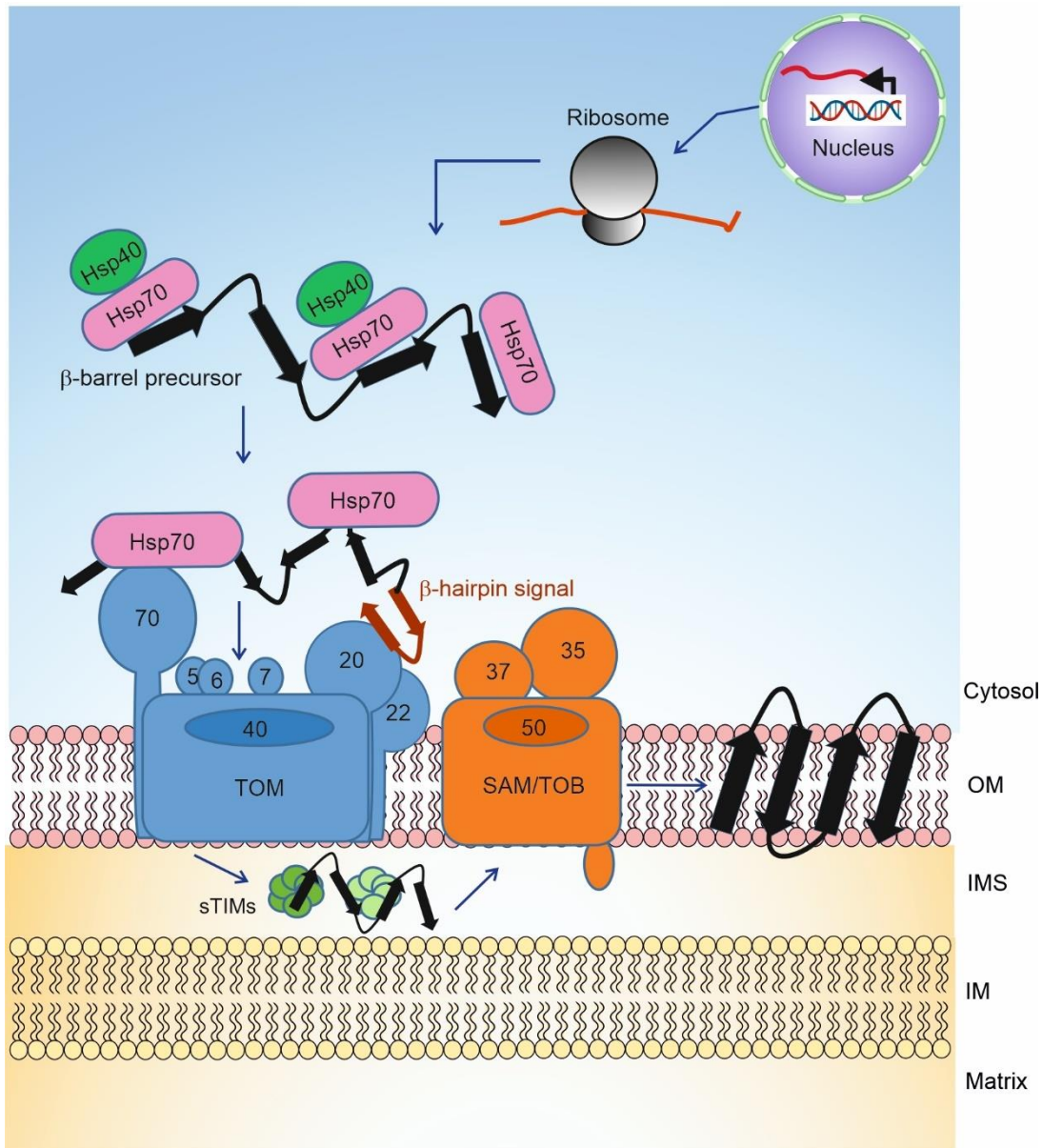


**Figure 1.2 – Biogenesis pathway of mitochondrial  $\beta$ -barrel proteins.**

Mitochondrial  $\beta$ -barrel proteins are transcribed in the nucleus, translated on cytosolic ribosomes, transported to the mitochondrial surface in an import competent fashion by chaperones, where the precursors are initially recognized by receptors of the TOM complex. The import and assembly of the  $\beta$ -barrel precursors is facilitated by the TOM and TOB complexes together with the small translocase of inner membrane (sTIM) chaperones [Figure from (Moitra and Rapaport 2021)].

### 1.3.2 Targeting of $\beta$ -barrel precursors to the mitochondrial surface

Most mitochondrial precursor proteins contain a cleavable N-terminal presequence that targets them to mitochondria. However, mitochondrial  $\beta$ -barrel proteins lack a cleavable targeting signal. Hence, it remained unclear how the targeting information for mitochondrial  $\beta$ -barrel proteins was encoded. Various studies showed that bacterial and chloroplast  $\beta$ -barrel proteins could be targeted and assembled into yeast mitochondria (Walther et al. 2009; Ulrich et al. 2012; Ulrich et al. 2014). Conversely, VDAC could also be integrated into bacterial OM and form pores there (Walther et al. 2010), suggesting that the targeting information for  $\beta$ -barrel proteins is conserved from bacteria to mitochondria and thus functional in both systems. Since none of the studies could identify a definitive linear amino acid sequence as the targeting signal, it was hypothesized that the targeting signal may be a structural feature of the  $\beta$ -barrel proteins. Truncation studies showed that the last C-terminal  $\beta$ -strand of mitochondrial  $\beta$ -barrel proteins contains a stretch of amino acids that facilitate their interaction with the TOB complex. These residues were called the  $\beta$ -signal (Kutik et al. 2008). However, deletion or mutation of the  $\beta$ -signal did not interfere with the initial targeting of newly synthesized  $\beta$ -barrel proteins to mitochondria. Studies involving a bacterial trimeric autotransporter *Yersinia* adhesin A (YadA), where each subunit contributes four  $\beta$ -strands to a 12-mer  $\beta$ -barrel structure, demonstrated that such proteins can be targeted to mitochondria upon their expression in yeast cells (Müller et al. 2011). This finding implies that even a partial  $\beta$ -barrel structure (like four  $\beta$ -strands) is sufficient for specific mitochondrial targeting. Hence, it was further tested whether a  $\beta$ -hairpin structural motif, which is composed of two  $\beta$ -strands and a loop and represents the most basic repeating structural motif of  $\beta$ -barrel proteins, could be the elusive mitochondrial targeting signal. To support this possibility, it was shown that a peptide corresponding to the last  $\beta$ -hairpin of human VDAC1 could competitively inhibit the *in vitro* import of mitochondrial  $\beta$ -barrels (Jores et al. 2016).

Moreover, hybrid proteins of this  $\beta$ -hairpin fused to soluble passenger domains like GFP or DHFR were targeted to mitochondria upon their expression in yeast cells. Such  $\beta$ -hairpin motif has an amphipathic characteristic as eventually, upon its incorporation into a membrane-embedded  $\beta$ -barrel, one phase of the motif will face the lipid core and hence is hydrophobic, whereas the opposite one will be exposed to the pore lumen and thus is rather hydrophilic. Importantly, it was discovered that optimal mitochondrial targeting depends on relative elevated hydrophobicity of those amino acid residues that face the lipid core of the membrane (Jores et al. 2016).

In most eukaryotic cells, mitochondria are the only organelles containing  $\beta$ -barrel proteins. The problem of specific targeting gets an interesting twist in plant cells where plastids can be an alternative destination for such proteins. Klinger et al. addressed this issue and found that the hydrophobicity is not sufficient for the discrimination of targeting to chloroplasts or mitochondria. By domain swapping between mitochondrial (atVDAC1) and chloroplast (psOEP24) targeted  $\beta$ -barrel proteins, they could demonstrate that the presence of a hydrophilic amino acid at the C-terminus of the penultimate  $\beta$ -strand is also required for mitochondrial targeting. A variant of the chloroplast  $\beta$ -barrel protein psOEP24, which mimics such profile, was efficiently targeted to mitochondria (Klinger et al. 2019).

Collectively, it seems that the combined contribution of several  $\beta$ -hairpin motifs with a highly hydrophobic face assures proper mitochondrial targeting of  $\beta$ -barrel proteins.

### **1.3.3 Membrane integration of mitochondrial $\beta$ -barrels by the TOM and TOB/SAM complexes**

Once the chaperone-associated  $\beta$ -barrel precursors are targeted to mitochondria via the  $\beta$ -hairpin signal, they interact with the TOM complex at the mitochondrial surface to initiate organellar import (Figure 1.2). The TOM complex is comprised of the core complex and its peripheral import receptors. The core complex has a central translocon channel, formed by the integral  $\beta$ -barrel protein Tom40, along with several transmembrane accessory proteins namely Tom5, Tom6, Tom7, and Tom22 (Bausewein et al. 2017; Araiso et al. 2019; Tucker and Park 2019). Tom20 and Tom70 are the receptors involved in the initial recognition of multiple mitochondrial proteins (Neupert and Herrmann 2007) (Figure 1.2). Several studies hinted at the role of Tom20 in the recognition of  $\beta$ -barrel precursors (Rapaport and Neupert 1999; Schleiff, Silvius, and Shore 1999; Krimmer et al. 2001; Yamano et al. 2008). Using NMR, photo-crosslinking and fluorescence complementation assays, it was recently shown that the  $\beta$ -hairpin element of VDAC interacts with the mitochondrial import receptor Tom20 via the presequence binding region of the latter (Jores et al. 2016). Moreover, direct cross-linking of the  $\beta$ -hairpin motif to Tom70 and the observation that blocking this receptor interferes with the import of VDAC suggested that Tom70 also plays a role in the initial recognition of VDAC (Jores et al. 2016). The involvement of Tom70 can be either via direct recognition of the substrate protein or by serving as a docking site for the chaperone-substrate complex.

Following recognition by the import receptors, the  $\beta$ -barrel precursors are translocated across the MOM via the Tom40 channel by interacting with a series of binding sites, probably with increasing affinities (Hill et al. 1998). Upon its emergence at the intermembrane space (IMS),

the translocated  $\beta$ -barrel precursor interacts with the small chaperones of the translocase of the inner membrane (small TIMs). The IMS chaperone system includes the small Tim proteins, Tim8, Tim9, Tim10, and Tim13 (Koehler et al. 1998). These small chaperones form alternating circular hexamers comprised of three subunits of Tim9 and Tim10, or three subunits of each Tim8 and Tim13 (Webb et al. 2006; Beverly et al. 2008). Site-specific cross-linking indicated that the small TIMs interact with the IMS-exposed part of the N-terminal extension of Tom40 (Shiota et al. 2015).

The small TIMs play an important role in the transfer of the  $\beta$ -barrel precursors from the TOM complex to the sorting and assembly machinery (SAM) complex, which is also known as the topogenesis of outer-membrane  $\beta$ -barrel proteins (TOB) complex (Hoppins and Nargang 2004; Wiedemann et al. 2004; Habib et al. 2006) (Figure 1.2). Structural and mechanistic studies revealed that TIM chaperones hold the VDAC protein precursors in a nascent chain-like extended conformation via multiple clamp-like binding sites (Weinhäupl et al. 2018). Such multiple weak and constantly reshuffling interactions ultimately allow for the efficient release of the precursor to the actual insertase, the TOB/SAM complex (Figure 1.2) (Paschen et al. 2003; Wiedemann et al. 2003; Gentle et al. 2003). The Tim9/10 binding cleft for the  $\beta$ -barrel precursors has conserved hydrophobic residues for these interactions, and mutations in these residues are detrimental to the  $\beta$ -barrel biogenesis and overall cell growth.

To facilitate a smooth transfer, the TOM and the TOB/SAM complex can form a super-complex bridged by the cytosolic domain of Tom22 and the peripheral TOB/SAM component, Mas37/Sam37 (Qiu et al. 2013). The core subunit of the TOB/SAM complex is the 16-stranded  $\beta$ -barrel protein Tob55/Sam50, that belongs to the Omp85 superfamily of proteins. Tob55/Sam50 has an N-terminal POTRA domain, which can bind the incoming substrate but is not essential for the  $\beta$ -barrel assembly process. In addition, the TOB/SAM complex harbors two cytosol-exposed peripheral subunits that are involved in formation of a TOM-TOB super-complex (Mas37/Sam37) and stabilization of the TOB/SAM bound form of the precursor (Tob38/Sam35).

Our understanding of the final steps in the biogenesis of the mitochondrial  $\beta$ -barrel precursors, particularly VDAC, evolved dramatically in the last five years. Structural studies indicate the formation of a lateral gate between  $\beta$ -strands 1 and 16 of Sam50. Accordingly, and supported by intensive cross-linking assays, the lateral gate insertion model was put forward. This model suggests that the C-terminal  $\beta$ -signal of the precursor initiates opening of the gate by exchange with the endogenous Sam50  $\beta$ -signal. In addition, loop 6 of Sam50 was found to be crucial for the VDAC precursor transfer to the lateral gate (Höhr et al. 2018). An increasing number of  $\beta$

hairpin-like loops of the precursor insert and fold sequentially and accumulate at the lateral gate (Figure 1.3A). Finally, hydrogen bonds are formed between the first and last  $\beta$ -strand to close the newly folded VDAC  $\beta$ -barrel. Upon folding at Sam50, the full-length newly formed  $\beta$ -barrel protein is laterally released into the outer membrane and the Sam50 lateral gate closes (Figure 1.3A). The opening of the putative lateral gate obtained further support from a recent report on the atomic structure of the SAM complex (Diederichs et al. 2020). Membrane thinning in the vicinity of the lateral gate can further facilitate insertion of the  $\beta$ -barrel protein into the lipid bilayer.

The membrane integration model recently obtained a new twist from structural studies. Based on detailed atomic structure of the SAM complex, the barrel swapping model was suggested. This scenario envisions the SAM complex as formed by a SAM monomer (Sam50a along with Sam35 and Sam37) and a Sam50b second barrel (Figure 1.3B) (Takeda et al. 2021). The precursor protein  $\beta$ -signal binds Sam50a as in the lateral gate insertion model. Then, the folded VDAC  $\beta$ -barrel slowly displaces Sam50b and takes its place. Sam37 that originally also interacts with Sam50b, gets gradually involved in interactions with the newly formed VDAC barrel (Figure 1.3B). Finally, this barrel dissociates from the SAM complex and is integrated into the MOM.

Of note, most of our current knowledge regarding the biogenesis of mitochondrial  $\beta$ -barrel proteins is based on biochemical and structural studies on fungal elements. While the atomic structure of the mammalian TOM complex appears to be rather similar to its fungal counterpart (Wang et al. 2020), not much is known about the SAM complex in higher eukaryotes. It is rather clear that the mammalian SAM50 is the central component of the complex. However, the precise functions of Metaxins1/2/3, which are homologous to yeast Sam35 and Sam37, is not clear yet.

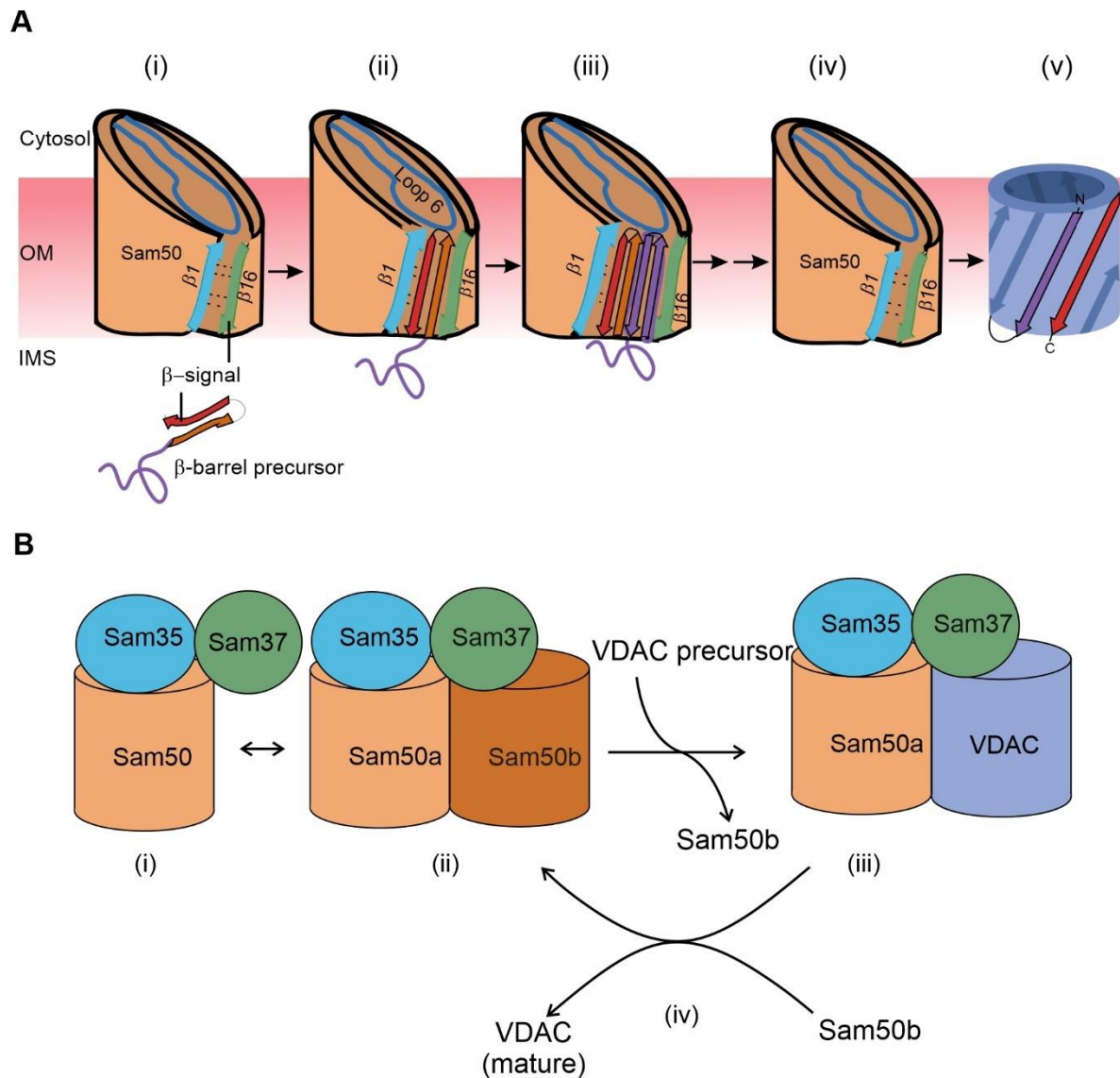


**Figure 1.3 - A working model for the final steps of the membrane integration of VDAC, a mitochondrial  $\beta$ -barrel protein.**

**(A)** Lateral insertion (adapted from Fig. 8, Höhr et al., 2018) **(i)** VDAC precursors approach the OM from the IMS. **(ii)** The C-terminal  $\beta$ -signal of VDAC precursor interferes with the Sam50 structure by binding to the  $\beta 1$  strand of Sam50 and disrupting the  $\beta 1$ -  $\beta 16$  interactions within Sam50. This enforces opening of a lateral gate. **(iii)** The initial opening is followed by sequential insertion of additional precursor  $\beta$ -hairpins through the lateral gate of Sam50. **(iv)** The lateral gate of Sam50 re-closes to **(v)** release the fully formed  $\beta$ -barrel of VDAC into the MOM. **(B)** Barrel switching model (based on Takeda et al., 2021) **(i)** SAM complex consisting of Sam50, Sam35 and Sam37 switches to **(ii)** a SAM monomer (Sam50a+Sam35+Sam37) along with a second Sam50b barrel. **(iii)** The assembling VDAC precursor displaces Sam50b. **(iv)** Once fully assembled in the MOM, mature VDAC dissociates from the complex to be replaced by Sam50b [Figure from (Moitra and Rapaport 2021)].

## 1.4 Biogenesis of chloroplast $\beta$ -barrel proteins

Although, a plethora of details are available for the mitochondrial outer membrane  $\beta$ -barrel protein biogenesis, very little is known about the early cytosolic stages of biogenesis of chloroplast OM  $\beta$ -barrel proteins. Most chloroplast OM  $\beta$ -barrel proteins are hypothesised to be imported into chloroplasts with the help of translocase of the outer membrane of chloroplast (TOC) and translocase of the inner membrane of chloroplast (TIC) complexes and inserted into the OM potentially by OEP80, which is similar to BamA or Sam50 in bacteria and mitochondria, respectively (Figure 1.4) (Soll and Schleiff 2004; Jores and Rapaport 2017).

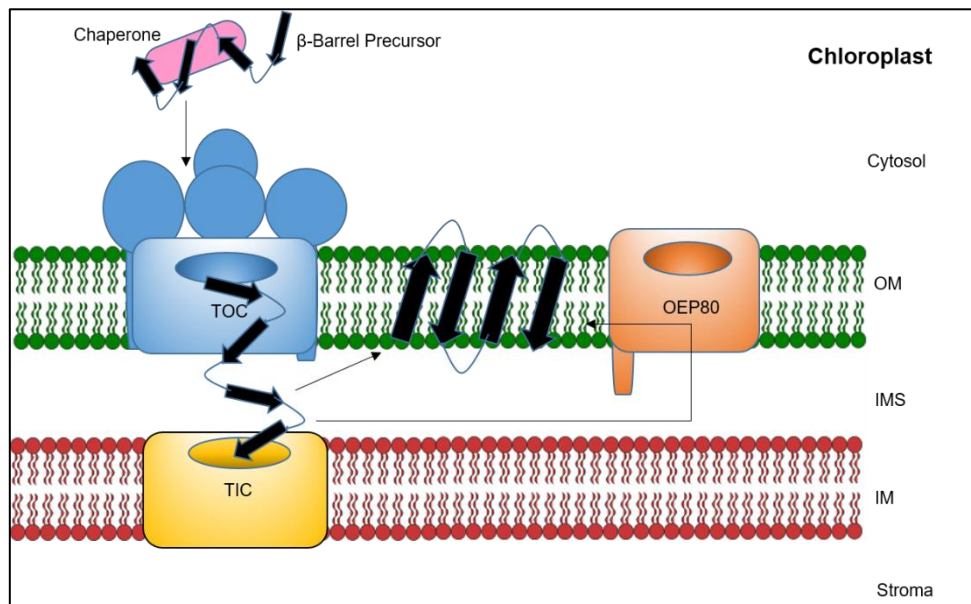


**Figure 1.4 – Biogenesis pathway of chloroplast  $\beta$ -barrel proteins.**

The chloroplast  $\beta$ -barrel proteins are imported into chloroplasts with the help of translocase of the outer membrane of chloroplast (TOC) and translocase of the inner membrane of chloroplast (TIC) (in case of Toc75-III) complexes and inserted into the outer membrane potentially by OEP80.

The chloroplast  $\beta$ -barrel protein Toc75-III contains a cleavable, bipartite targeting signal – N terminal transit peptide that is targeted to the stroma through the Toc75-III central pore, and a downstream polyglycine stretch that stops the translocation of Toc75-III across the inner membrane. The former signal is cleaved by stromal processing peptidase and the latter segment by the plastidic type I signal peptidase 1. Another central chloroplast OM  $\beta$ -barrel protein,

OEP80 itself, has been shown to contain a cleavable N-terminal signal that exposes its POTRA domains to the IMS of plastids, where it likely interacts with its substrates (Gross et al. 2020). One of the open questions in the field concerns the underlying mechanisms preventing mis-targeting of  $\beta$ -barrel precursors between mitochondria and chloroplasts in plant cells. The hydrophobicity itself is not the determinant that discriminates between mitochondrial and chloroplast targeting, but rather the profile of the hydrophobicity of the penultimate strand. While a hydrophilic patch exists at the N-terminus of the penultimate strand of plastidic  $\beta$ -barrel proteins, mitochondrial proteins contain such a patch at the C-terminus of this strand (Klinger et al. 2019). However, the defined signal for chloroplast targeting remains to be established.

## Chapter 2

### Research Objectives

Detailed studies have uncovered the cellular machinery involved in specifically targeting mitochondrial  $\beta$ -barrel proteins to the organelle surface in an import competent conformation. Ultimately, these  $\beta$ -barrel proteins are integrated into the organelle OM with the help of dedicated import machineries.

The biogenesis pathways for  $\beta$ -barrel proteins are quite conserved over the course of evolution due to the endosymbiotic origins of mitochondria and chloroplasts from ancient prokaryotes.

The broad aim of my thesis was to study the extent of such evolutionary conservation of  $\beta$ -barrel biogenesis pathways. In particular, my work aims to assess yeast as a model organism to study the evolutionarily conserved pathways and mechanisms of  $\beta$ -barrel protein biogenesis, for both natural and *de novo* designed substrates.

The specific objectives of my work are –

- (A) Investigating whether heterologous  $\beta$ -barrel proteins such as *de novo* designed synthetic  $\beta$ -barrel proteins and bacterial secretins, could be expressed in yeast cells and integrated into their mitochondria.
  
- (B) Exploring the role of components of the yeast mitochondrial import and assembly machinery, like subunits of the TOM and TOB complexes, in the proper biogenesis of such heterologous  $\beta$ -barrel proteins.



## Chapter 3

### Materials and Methods

The details of Materials and Methods related to Chapter 4 can be found in the Appendix A.2 containing the published manuscript entitled ‘**Yeast can express and assemble bacterial secretins in the mitochondrial outer membrane**’ (DOI: 10.15698/mic2020.01.703).

This chapter consists of details of Materials and Methods related to Chapter 5 and contains sections adapted from the following manuscript ready for submission:

#### **Yeast mitochondria can process *de novo* designed $\beta$ -barrel proteins**

**Anasuya Moitra<sup>1</sup>**, Vitasta Tiku<sup>1</sup> and Doron Rapaport<sup>1</sup>

<sup>1</sup>Interfaculty Institute of Biochemistry, University of Tuebingen, Tuebingen, Germany.

#### **Author Contributions**

I designed and performed the vast majority of the experiments, analysed the data, prepared the figures and wrote the manuscript. VT planned and performed the cloning experiments for the  $\beta$ -signal mutants. DR designed experiments, analysed the data, supervised the overall project, acquired funding and wrote the manuscript.

### 3.1 Yeast strains and growth conditions

Standard genetic techniques were used for the growth and manipulation of yeast strains. The *Saccharomyces cerevisiae* strains used in this study are listed in Table 3.1. Yeast cells were usually grown at 30°C on synthetic selective (S) medium (0.67% [w/v] yeast nitrogen base without amino acids) containing galactose (Gal, 2%) + glucose (D, 0.1%) as carbon source. A mixture of the required amino acids, omitted for Leu to select for transformants with the pYX142 plasmid, was added as well. Cells deleted for *MAS37* (*mas37Δ*) were grown at 24°C to avoid accumulation of suppressors (Habib et al. 2005). Transformation of yeast cells was performed by the lithium acetate method (Gietz and Woods 2006).

For experiments with cells depleted for *TOB55*, a strain where *TOB55* expression is under the control of the *GAL10* promoter was used (Paschen et al. 2003). Cells of this strain were initially grown at 30°C on synthetic depleted (S) medium containing lactate (Lac, 2%) + galactose (Gal, 0.1%) as carbon source and amino acid mixture as above. After a few days of growth on this medium, cells were shifted to S media containing 0.1% glucose instead of 0.1% galactose. Cells were harvested at the indicated time points after the shift from galactose- to glucose-containing medium.

### 3.2 Recombinant DNA techniques

The DNA sequences encoding Tmb2.3 and Tmb2.17 (Vorobieva et al. 2021) were synthesised by Eurofins Genomics (Germany) after optimisation for the codon usage of *S. cerevisiae*. These DNA segments were amplified by PCR with primers containing 5' EcoRI and 3' HindIII restriction sites, 5' yeast Kozak sequence, and a DNA sequence encoding C-terminal HA tag. Subsequently, the PCR products were subcloned into the yeast expression vector pYX142 where the expressed gene is under the control of the *TPI* promoter. To create single amino acid mutations in the  $\beta$ -signal motif of the TMBs, forward and reverse primers were used for site-directed mutagenesis by the standard whole plasmid mutagenesis method. The mutations Q115A and A115Q were introduced using as template pYX142-Tmb2.3-HA or pYX142-Tmb2.17-HA, respectively. Table 3.2 and Table 3.3 contain the lists of primers and plasmids used in this study, respectively.

### 3.3 Isolation of mitochondria

Mitochondrial fractions were obtained according to an established protocol (Daum, Böhni, and Schatz 1982). Yeast cells were grown in liquid media to logarithmic phase, harvested, and

resuspended in resuspension buffer (100 mM Tris, 10 mM DTT). Cells were harvested again and resuspended in spheroblasting buffer (1.2 M Sorbitol, 20 mM KPI, pH 7.2) without zymolyase, followed by harvesting. These pellets were gently dissolved in spheroblasting buffer with zymolyase (4.5 mg/g of cells) and incubated at 30°C for 1 h while shaking at 120 rpm. The obtained spheroblasts were dissolved in homogenisation buffer (0.6 M Sorbitol, 10 mM Tris, pH 7.4, 1 mM EDTA, 0.2% fatty acid free BSA) with 1 mM phenylmethylsulfonyl fluoride (PMSF) and homogenised with a douncer to obtain the whole cell lysate. Cell debris were removed by a clarifying spin (600xg, 5 min, 4°C), followed by isolation of crude mitochondria (18000xg, 10 min, 4°C). The supernatant obtained in this step represents the cytosolic fraction of this separation. Mitochondria were washed once in SEM buffer (250 mM Sucrose, 1 mM EDTA, 10 mM MOPS, pH 7.2) containing 2 mM PMSF and pelleted again (18000xg, 10 min, 4°C).

### **3.4 Subcellular fractionation**

Mitochondrial fraction and whole cell lysate were obtained as described above. To acquire the cytosolic fraction, the post mitochondrial fraction was clarified by spinning (18000xg, 15 min, 4°C) and the supernatant subjected to high speed centrifugation (200,000xg, 1h, 4°C). The resulting supernatant constituted the cytosolic fraction. The sticky, transparent pellet was resuspended in 3 mL SEM buffer containing 2 mM PMSF, homogenised with a douncer and centrifuged at 18000xg for 20 min at 4°C. The supernatant of this step constituted of the ER/microsomes fraction.

To obtain highly pure mitochondria, the mitochondrial fraction obtained as described above, was layered on a Percoll gradient and centrifuged (80000xg, 45 min, 4°C). Mitochondria in the brownish layer at the bottom interface were collected with a Pasteur pipette and washed once in SEM buffer containing 1 mM PMSF and pelleted again (18000xg, 10 min, 4°C). The whole cell lysate, ER, and cytosolic fractions were precipitated by using chloroform/methanol precipitation method and all samples including mitochondria were dissolved in 2X sample buffer (125 mM Tris pH 6.8, 4% SDS, 20% glycerol, 10% 2-mercapto-ethanol, 2 mg/mL bromophenol blue) to a concentration of 2 mg/mL. Samples were heated at 95°C for 10 min and further analysed by SDS-PAGE and immunoblotting.

### **3.5 Protease protection assay**

Mitochondria (100 µg) were resuspended in 200 µL of SEM buffer and incubated on ice for 30 min in the presence or absence of 1% Triton-X-100. This was followed by addition of either

10 or 50  $\mu\text{g}/\text{mL}$  of Proteinase K (PK) or Trypsin and further incubation on ice for 30 min. PK was then inhibited by supplementing the reaction with 2 mM PMSF, while trypsin was inhibited by addition of 1 mg/mL of soybean trypsin inhibitor (STI), followed by incubation on ice for 10 min. In the control samples (C), mitochondria were incubated on ice for 30 min with 50  $\mu\text{g}/\text{mL}$  of Trypsin (in the absence of 1% Triton-X-100), that had been pre-incubated (10 min) with STI, so as to block the proteolytic activity of trypsin and serve as an indicator of the inhibitor's efficacy. Samples without Triton were then centrifuged (18000xg, 15 min, 4°C), whereas the Triton solubilised samples were subjected to trichloroacetic acid (TCA) precipitation. The precipitated samples and the pellets from samples without Triton were resuspended in 40  $\mu\text{L}$  2X sample buffer, heated at 95°C for 10 min and subjected to SDS-PAGE and immunoblotting.

### **3.6 Alkaline (carbonate) extraction**

Isolated mitochondria (100  $\mu\text{g}$ ) were resuspended in 100  $\mu\text{L}$  of 100 mM  $\text{Na}_2\text{CO}_3$ , pH 11.5 and incubated on ice for 30 min. To separate the membranous pellet fraction and the soluble supernatant fraction, samples were centrifuged (76000xg, 30 min, 4°C). Soluble supernatant fractions were subjected to TCA precipitation and the precipitated samples as well as the original pellets were resuspended in 40  $\mu\text{L}$  2X sample buffer, heated at 95°C for 10 mins and subjected to SDS-PAGE and immunoblotting.

### **3.7 Western blotting and immunodecoration**

For analysis of steady state levels of various proteins, mitochondrial fractions were dissolved in 2X sample buffer to a concentration of 2 mg/mL. Whole cell lysate and cytosolic fractions were precipitated using chloroform/methanol and dissolved in 2X sample buffer to a concentration of 2 mg/mL. All samples were heated at 95°C for 10 mins and further analysed by SDS-PAGE and immunoblotting.

Samples were analysed on 12.5% SDS-PAGE and transferred onto nitrocellulose membranes via semi-dry Western blotting. Membranes were blocked with 5% skimmed milk (in 1xTBS buffer), incubated with primary antibodies, washed, and then incubated with horseradish peroxidase-conjugated goat anti-rabbit or goat anti-rat secondary antibodies. The antibodies used in this study are listed in Table 3.4.

### **3.8 Blue-native (BN) PAGE**

Isolated mitochondria (100  $\mu$ g) were washed with SEM buffer and spun (20000xg, 10 min, 4°C). The pellets were solubilised with a detergent-containing buffer (1% digitonin in 20 mM Tris, 0.1 mM EDTA, 50 mM NaCl, 10% glycerol, pH 7.4) for 30 min on ice, followed by a clarifying spin (13000xg, 10 min, 4°C). The supernatant was mixed with 10X sample buffer (5% [w/v] Coomassie brilliant blue G-250, 100 mM Bis-Tris, 500 mM 6-aminocaproic acid, pH 7.0) and analysed on a gel containing 6-14% gradient of acrylamide. Proteins were blotted onto polyvinylidene fluoride (PVDF) membrane and detected by immunodecoration. Native Mark Unstained Protein Standard (Thermo Scientific) was used as molecular weight markers.

### **3.9 Analysis of growth of yeast cells**

For drop dilution assay, cells were grown overnight in liquid cultures and then diluted and grown further on SD-Leu liquid media to an OD<sub>600nm</sub> of 1.0. Then, a serial dilution of the cultures in fivefold increments was performed, followed by spotting 5  $\mu$ L of each diluted culture on solid selective media plates and further growth at 24°C, 30°C, or 37°C for 2-5 days.

To analyse the growth of liquid cultures, cells were inoculated for overnight cultures in 3-5 mL of SD-Leu liquid media and 1 OD<sub>600nm</sub> unit of cells were harvested on the following day. The cells were resuspended in 1 mL sterile water. Then, to obtain a starting culture of 0.1 OD<sub>600nm</sub> of cells per well, 20  $\mu$ L of cell suspension and 180  $\mu$ L of the desired medium [SD-Leu or S(Gal+0.1%D)-Leu] were pipetted into each well of round-bottomed 96 wells plates. The plate was sealed with a semi-permeable membrane and placed in the SPECTROstar Nano microplate reader. Cells were allowed to grow at 30°C for 72 h, with the OD<sub>600nm</sub> measured every 10 mins after 30 secs double orbital shaking at 300 rpm. Data obtained were analysed by the MARS software and plotted by Excel.

### 3.10 Relevant tables

**Table 3.1. Yeast strains used in this study.**

<b>Name</b>	<b>Mating type</b>	<b>Genetic background</b>	<b>Reference</b>
<b>W303<math>\alpha</math></b>	MAT $\alpha$	<i>ade2-1 can1-100 his3-11 leu2 3_112 trp1<math>\Delta</math>2 ura3-52</i>	Lab stock
<b>W303<math>\alpha</math></b>	MAT $\alpha$	<i>ade2-1 can1-100 his3-11 leu2 3_112 trp1<math>\Delta</math>2 ura3-52</i>	Lab stock
<b><i>tom20<math>\Delta</math></i></b>	MAT $\alpha$	W303 $\alpha$ , <i>tom20<math>\Delta</math>::KanR</i>	Lab stock
<b><i>tom70<math>\Delta</math>/tom71<math>\Delta</math></i></b>	MAT $\alpha$	W303 $\alpha$ , <i>tom70<math>\Delta</math>::KanMX4; tom71<math>\Delta</math>::NatNT2</i>	(Jores et al. 2018)
<b>YPH499</b>	MAT $\alpha$	<i>ura3-52 lys2-801_amber ade2-101_ochre trp1-<math>\Delta</math>63 his3-<math>\Delta</math>200 leu2-<math>\Delta</math>1</i>	Lab stock
<b><i>mas37<math>\Delta</math></i></b>	MAT $\alpha$	YPH499, <i>mas37<math>\Delta</math>::HIS3</i>	(Habib et al. 2005)
<b><i>GAL10-TOB55</i></b>	MAT $\alpha$	YPH499, GAL10/His8-Tob55	(Paschen et al. 2003)

**Table 3.2. Primers used in this study.**

Primer name	Sequence (5'-3')	Note
tmb2-3 For	AAGCCGAGAATTC AAAAAATGCAAGAT GGACCAGGTAC	Forward primer for amplification of TMB2.3 gene with 5' <b>EcoRI</b> restriction site and 5' <b>yeast kozak sequence</b>
tmb2-3 Rev	TCGGCTTAAGCTTT ACGCATAGTCAGGA ACATCGTATGGGTAT GGATCCCCAGGTTGT ATTCTGTACGAT	Reverse primer for amplification of TMB2.3 gene with 3' <b>HindIII</b> restriction site, <b>stop codon</b> , C-terminal <b>HA-tag</b> and <b>linker</b>
tmb2-17 For	AAGCCGAGAATTC AAAAAATGGAACAA AAGCCAGGTAC	Forward primer for amplification of TMB2.17 gene with 5' <b>EcoRI</b> restriction site and 5' <b>yeast kozak sequence</b>
tmb2-17 Rev	TCGGCTTAAGCTTT ACGCATAGTCAGGA ACATCGTATGGGTAT GGATCCCCATCCTTG ACTTTATAGGCA	Reverse primer for amplification of TMB2.17 gene with 3' <b>HindIII</b> restriction site, <b>stop codon</b> , C-terminal <b>HA-tag</b> and <b>linker</b>
TMB2.3SDAfor	CTTACAGTTCCTTGC AGCCGGTTTATCG	Forward primer for site-directed mutagenesis ( <b>Q115A</b> ) in pYX142-Tmb2.3-HA
TMB2.3SDArev	CGATAAACCGGCTG CAAGGAACTGTAAG	Reverse primer for site-directed mutagenesis ( <b>Q115A</b> ) in pYX142-Tmb2.3-HA
TMB2.17SDAfor	ATTGCAGAAGGTTC AGATAGGGATTGCC	Forward primer for site-directed mutagenesis ( <b>A115Q</b> ) in pYX142-Tmb2.17-HA
TMB2.17SDArev	GGCAATCCCTATCTG AACCTTCTGCAAT	Reverse primer for site-directed mutagenesis ( <b>A115Q</b> ) in pYX142-Tmb2.17-HA

**Table 3.3. Plasmids used in this study.**

<b>Plasmid</b>	<b>Promoter</b>	<b>Coding sequence</b>	<b>Markers</b>	<b>Source</b>
<b>pYX142 <math>\phi</math></b>	TPI	Empty vector ( $\phi$ )	LEU2, Amp <sup>R</sup>	Lab stock
<b>pYX142-Tmb2.3-HA</b>	TPI	Tmb2.3 full length with C-terminal HA tag	LEU2, Amp <sup>R</sup>	This study
<b>pYX142-Tmb2.17-HA</b>	TPI	Tmb2.17 full length with C-terminal HA tag	LEU2, Amp <sup>R</sup>	This study
<b>pYX142-Tmb2.3<sub>Q115A</sub>-HA</b>	TPI	Tmb2.3 full length with the mutation Q115A and C-terminal HA tag	LEU2, Amp <sup>R</sup>	This study
<b>pYX142-Tmb2.17<sub>A115Q</sub>-HA</b>	TPI	Tmb2.17 full length with the mutation A115Q and C-terminal HA tag	LEU2, Amp <sup>R</sup>	This study

**Table 3.4. Antibodies used in this study.**

<b>Antibodies</b>	<b>Dilution</b>	<b>Source</b>
<b>Polyclonal rat anti-HA</b>	1:1000	11867423001 (Roche)
<b>Polyclonal rabbit anti-Porin</b>	1:2000	Lab stocks
<b>Polyclonal rabbit anti-Erv2</b>	1:1000	Lab of Roland Lill
<b>Polyclonal rabbit anti-Hexokinase</b>	1:2000	Bio-Trend (#100-4159)
<b>Polyclonal rabbit anti-Pic2</b>	1:10,000	Lab stocks
<b>Polyclonal rabbit anti-Hsp60</b>	1:10,000	Lab stocks
<b>Polyclonal rabbit anti-Tom20</b>	1:4000	Lab stocks
<b>Polyclonal rabbit anti-Tom40</b>	1:4000	Lab stocks
<b>Polyclonal rabbit anti-Tom70</b>	1:2000	Lab stocks
<b>Polyclonal rabbit anti-Tob55</b>	1:2000	Lab stocks
<b>Polyclonal rabbit anti-Aconitase1</b>	1:1000	Lab stocks
<b>Polyclonal rabbit anti-Hsp104</b>	1:25000	Lab stocks
<b>Horseradish peroxidase coupled goat anti-rabbit</b>	1:10,000	1721019 (Bio-rad)
<b>Horseradish peroxidase coupled goat anti-rat</b>	1:5000	ab6845 (Abcam)

# Chapter 4

## Yeast can express and assemble bacterial secretins in the mitochondrial outer membrane

This chapter consists of sections adapted from the following published article:

(DOI: 10.15698/mic2020.01.703)

### Yeast can express and assemble bacterial secretins in the mitochondrial outer membrane

Janani Natarajan<sup>1</sup>, **Anasuya Moitra**<sup>1</sup>, Sussanne Zabel<sup>1, §</sup>, Nidhi Singh<sup>2</sup>, Samuel Wagner<sup>2,3</sup> and Doron Rapaport<sup>1, \*</sup>

<sup>1</sup>Interfaculty Institute of Biochemistry, University of Tuebingen, Tuebingen, Germany.

<sup>2</sup>Interfaculty Institute of Microbiology and Infection Medicine (IMIT), University of Tuebingen, Tuebingen, Germany.

<sup>3</sup>German Center for Infection Research (DZIF), partner-site Tuebingen, Tuebingen, Germany.

<sup>§</sup>Current address: Center for Bioinformatics (ZBIT), University of Tuebingen, 72076 Tuebingen, Germany

<sup>\*</sup>Corresponding author

#### Author Contributions

I performed experiments for the revised version of this contribution. I analysed the whole cell extracts from the different strains expressing InvG-HA and SsaC-HA (Figure 6D and Figure 7C). I furthermore edited the final manuscript.

JN designed and performed all the experiments, analysed the data, prepared the figures and wrote the manuscript. SZ performed the cloning and initial biochemical experiments for the secretins. NS performed the experiments to obtain bacterial cultures expressing secretins. SW supervised the bacterial project, acquired funding and edited the manuscript. DR analysed the data, supervised the overall project, acquired funding, wrote and edited the manuscript.

## 4.1 Introduction

The OM of Gram-negative bacteria contains membrane embedded  $\beta$ -barrel proteins. One such class of proteins is called secretins. They are part of the secretory systems developed by bacteria to aid in the transport and secretion of substrates and toxins into the environment and/or host cells (Green and Mecsas 2016; Kubori and Nagai 2016). Type II and III secretion systems and type IV pili (T2SS, T3SS, and T4P, respectively) secrete toxins into the exoplasm (T2SS), directly into the cytosol of the host cells (T3SS), or build adhesion factors (T4P) (Alvarez-Martinez and Christie 2009; Galan and Wolf-Watz 2006; Korotkov, Sandkvist, and Hol 2012; Johnson et al. 2006). These three systems consist of a massive complex spanning both the inner and outer membrane of bacteria. Secretins form, as part of this complex, large multimeric pores in the OM of Gram-negative bacteria.

Recent studies have elucidated the structure of certain secretins as rich in  $\beta$ -strands. The C-terminus of secretins is conserved across different secretion systems and has a high tendency to form membrane-embedded  $\beta$ -sheets (Genin and Boucher 1994). Some secretins have a domain at their C-terminus called the S domain, which is required for the interaction with their corresponding specific assembly factor, lipoproteins called pilotins (Daefler and Russel 1998; Koo, Burrows, and Lynne Howell 2012). The most variable part of secretins is their periplasmic N-terminal domain that is proposed to have a system- and species-specific role rather than a universal function. The assembled secretin forms a gated pore in the OM, which is open only for the translocation of proteins through the channel. Figure 4.1B shows the cryo-EM structure of the *Salmonella* SPI-1 type III secretion injectisome secretin InvG along with its monomeric form (Figure 4.1A). This complex is composed of 15 monomers of InvG that form a symmetric ring structure with an unexpected double walled  $\beta$ -barrel architecture (Hu et al. 2018). SsaC is another secretin which is part of the T3SS in *Salmonella*, and is encoded by the SPI-2 (Ochman et al. 1996). Figure 4.2 shows the Alphafold predicted structure of the SsaC monomer (Jumper et al. 2021; Varadi et al. 2022).

Secretins are synthesized in the cytoplasm and are probably stabilized by cytoplasmic factors, followed by their transport through the inner membrane via the Sec translocon. This is followed by the transport of secretins across the periplasm to the OM via Lol-dependent (via pilotins), BAM-dependent, unassisted, or an accessory protein-assisted pathway. Despite our understanding of the structure and function of secretins, very little is known about the mechanism by which secretins assemble into the OM. Since, the biogenesis pathways of  $\beta$ -

barrel proteins are highly conserved in bacteria and mitochondria, we used yeast cells as a model system to study the assembly process of secretins. To that end, we analyzed the biogenesis of InvG and SsaC (both T3SS) in wild type cells or in cells mutated for known mitochondrial import and assembly factors.

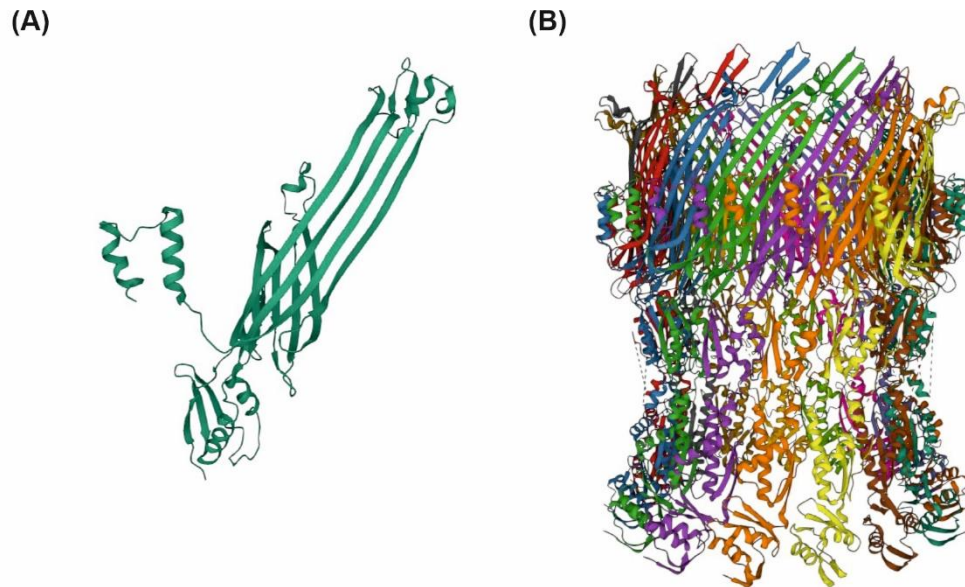
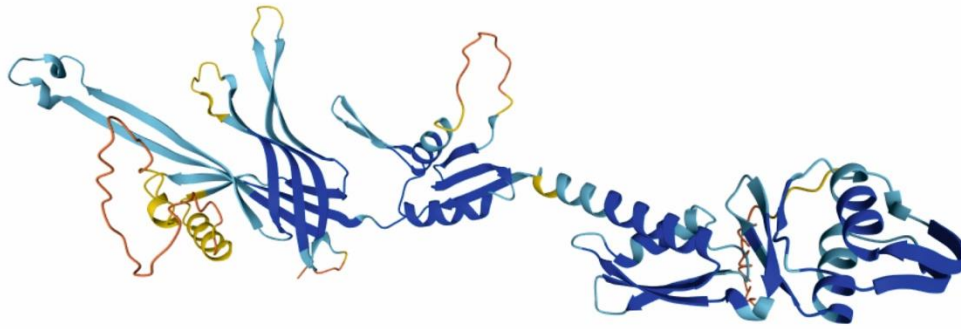


**Figure 4.1 - Structure of InvG.** (A) InvG secretin domain  $\beta$ -barrel monomer from *Salmonella* SPI-1 injectisome NC-base (PDB accession number 6PEE). (B) Structure of the *Salmonella* SPI-1 type III secretion injectisome secretin InvG in the open gate state (PDB accession number 6DV3).



Model Confidence:

- Very high (pLDDT > 90)
- Confident (90 > pLDDT > 70)
- Low (70 > pLDDT > 50)
- Very low (pLDDT < 50)

**Figure 4.2 – Predicted structure of SsaC.** AlphaFold structure prediction of SsaC from *Salmonella typhimurium* (strain SL1344) (UniProt accession number A0A0H3NG81).

## 4.2 Results

### 4.2.1 Assembly of the T3SS secretin InvG in yeast mitochondria

To study the biogenesis pathways of secretins, InvG and SsaC were expressed in yeast as C-terminally HA-tagged proteins under the *GAL* promoter. The transformed cells were grown on S(Gal+0.1%Glu)-Leu media to select for expressing transformants, while keeping the expression at moderate levels and to counteract toxic effects of overexpression. InvG-HA was shown to localise to both mitochondria and ER and could assemble into native-like higher oligomers in mitochondria. Alkaline extraction and protease protection assays revealed that the protein was embedded in the mitochondrial OM and exposed to the cytosol. The effect of the TOM complex on the assembly of InvG was investigated by expressing the protein in either *tom70/71Δ* or *tom20Δ* yeast deletion strains. Our results revealed that there was no significant change in the steady state levels of InvG in mitochondria isolated from *tom70/71Δ* cells in comparison to the amounts in control organelles (Figure 4.3A). In contrast, significantly elevated amounts of InvG were observed in mitochondria isolated from *tom20Δ* cells (Figure 4.3A). This suggests that the biogenesis of InvG-HA is independent of Tom70, while the presence of Tom20 has a potential inhibitory effect on its assembly in the mitochondrial OM.

We next asked whether the TOB complex is involved in InvG assembly. However, expression of InvG in cells lacking Mas37 did not result in any significant changes in the steady state levels of InvG (Figure 4.3A). These results are in line with previous observations that the BAM complex (the bacterial equivalent of the TOB complex) does not play a role in the assembly of this secretin.

Next, we wanted to better understand the involvement of Tom20 in the assembly of InvG. Thus, we expressed InvG in cells overexpressing *TOM20* (or lacking it, for comparison) and monitored its steady state levels in crude mitochondria isolated from these cells. Interestingly, the mitochondrial amounts of InvG were reduced when *TOM20* was overexpressed, while the deletion of *TOM20* resulted in elevated mitochondrial levels in comparison to the corresponding wild type cells (Figure 4.3A and B). When we then checked in a similar way the effect of Tom70 on the biogenesis of InvG, we observed no significant changes in the amount of InvG in the crude mitochondria from cells with altered expression of Tom70 (Figure 4.3C).

These results point to a specific effect of Tom20 on the biogenesis of InvG. To test whether the import components affect the total cellular levels of InvG, I analysed the steady-state amounts of the protein in whole cell lysates. Whereas we could not detect significant alterations upon deletions of either *TOM70/71* or *MAS37*, cells lacking Tom20 had overall reduced levels of InvG (Figure 4.3D). In line with the latter observation, overexpression of Tom20 resulted in slightly higher cellular amounts of InvG (Figure 4.3D). Hence, it seems that although the presence of Tom20 improves the overall stability of InvG, it does not have a positive effect on the assembly of InvG into the mitochondrial OM.

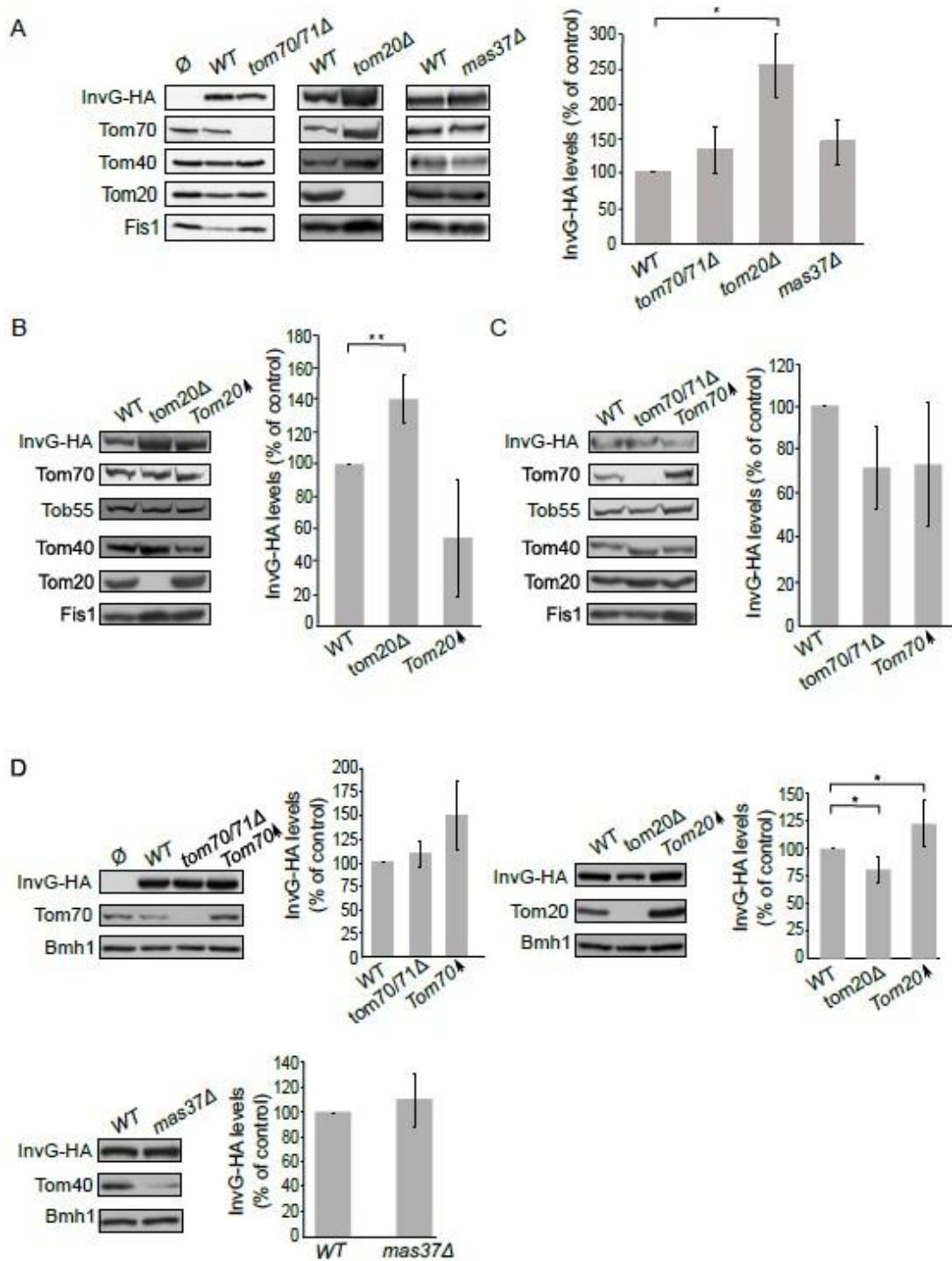


**Figure 4.3 - Improved assembly of InvG in mitochondria lacking Tom20.**

**(A) Left panels:** Mitochondria were isolated from the indicated strains transformed with either an empty vector ( $\emptyset$ ) or a plasmid encoding InvG-HA. Samples were analysed by SDS-PAGE and immunodecorated with the indicated antibodies. **Right panel:** The steady state levels of InvG-HA in at least three experiments as in the left panel were quantified. The signal of Fis1 was taken as a loading

control. Levels of InvG-HA in the corresponding wild type cells were set to 100%. The bar diagram shows the mean values  $\pm$  s.d. of at least three independent experiments (\*,  $P < 0.05$ ; \*\*,  $P < 0.01$ ; two-tailed Student's t-test). **(B)** Crude mitochondria were obtained from WT, *tom20 $\Delta$*  or a strain overexpressing *TOM20* (Tom20 $\uparrow$ ) harbouring a plasmid encoding InvG-HA. Further treatment and analysis were as described in the legend to part A. **(C)** Crude mitochondria were obtained from WT, *tom70/71 $\Delta$*  or a strain overexpressing *TOM70* (Tom70 $\uparrow$ ) harbouring a plasmid encoding InvG-HA. Further treatment and analysis were as described in the legend to part A. **(D)** Whole cell lysate was obtained from the indicated cells and was analysed by SDS-PAGE followed by immunodecoration with antibodies against the indicated proteins. The steady state levels of InvG-HA in at least three experiments for each strain were quantified. The signal of Bmh1 was taken as a loading control. Levels of InvG-HA in the corresponding wild type cells were set to 100%. The bar diagram shows the mean values  $\pm$  s.d. of at least three independent experiments. (\*,  $P < 0.05$ ; two-tailed Student's t-test). [This figure is equivalent to Figure 6 from (Natarajan et al. 2019)]

#### **4.2.2 Assembly of the T3SS secretin SsaC in yeast mitochondria**

Next, we investigated the biogenesis of SsaC, a secretin whose targeting and assembly pathways were not studied so far. SsaC-HA was shown to localise to mainly mitochondria with minor ER localisation and could not assemble into any detectable native-like higher oligomers. Alkaline extraction and protease protection assays revealed that SsaC was partially embedded in the mitochondrial OM, exposed to the cytosol, while the remaining fraction was present in the soluble fraction. To assess the involvement of the TOM complex receptors and the TOB complex in the biogenesis of SsaC, the protein was expressed in *tom70/71 $\Delta$* , *tom20 $\Delta$* , or *mas37 $\Delta$*  yeast cells and the steady state levels in isolated mitochondria were monitored. Interestingly, the absence of Tom70/71 resulted in a two-fold increase in the levels of SsaC whereas deletion of *TOM20* or *MAS37* led to a reduction in the mitochondrial levels of this secretin (Figure 4.4A). The reduction upon deletion of *MAS37* points to a requirement of the TOB complex in the biogenesis of SsaC in yeast cells, which could be extrapolated to a probable dependence on the BAM complex in bacteria.

The elevated levels of SsaC upon deletion of *TOM70/71* led us to check whether this increase was due to an unfavourable involvement of Tom70. To that aim, we expressed SsaC in cells either lacking or overexpressing Tom70. Indeed, we could observe that there was a significant decrease in the amounts of SsaC in crude mitochondria isolated from cells overexpressing *TOM70* in comparison to control organelles. Along the same line, we detected a significant

increase in the SsaC levels in mitochondria lacking Tom70 (Figure 4.4A and B). To verify that the changes in the levels of SsaC upon manipulating the Tom70/71 amounts is not the outcome of variations in the overall cellular amounts, I monitored the levels of SsaC in whole cell extracts. We observed that deletion of *TOM70/71* indeed resulted in moderately, but significantly, higher amounts of cellular SsaC (Figure 4.4C), suggesting that the absence of these import receptors increases the life-span of this secretin. In contrast, altered amounts of Tom20 or Mas37 did not affect the overall cellular levels of SsaC (Figure 4.4C). Taken together, these findings lead us to conclude that Tom70 inhibits, directly or indirectly, the mitochondrial assembly of SsaC.

### 4.3 Discussion

Secretins are homo-oligomers present in bacterial secretion systems that form pores in the bacterial OM. The integration of secretins into their target membrane is most probably a species-specific process. The exact mechanism of membrane insertion of the assembled oligomers and/or factors that assist the unassembled monomers to oligomerize and then insert correctly into the bacterial OM is still unknown.

In this study, we established yeast mitochondria as a model system to study the biogenesis of bacterial secretins. Even though *in vitro* systems based on artificial membranes have explored partially the requirements for secretin multimerization and insertion into membranes (Guilvout et al. 2006; Guilvout et al. 2011), mitochondria, due to their evolutionary relation to bacteria, may provide an improved model system. We could show that both InvG and SsaC could be expressed in yeast cells and were enriched in the mitochondrial fraction rather than in membranes of other organelle. For InvG, we could demonstrate the formation of oligomers in the mitochondrial OM and these oligomers behave like the InvG oligomers in bacteria, indicating a native-like structure and supporting the validity of the mitochondrial system. The presence of pore-forming native-like oligomers for InvG might explain their negative effect on the growth of yeast cells expressing them. Accordingly, SsaC, that appears to remain monomeric in yeast cells, is not toxic to these cells. The exact mechanism for the oligomerization initiation of SsaC is unknown and it might be that a crucial assembly factor is missing in the yeast system.

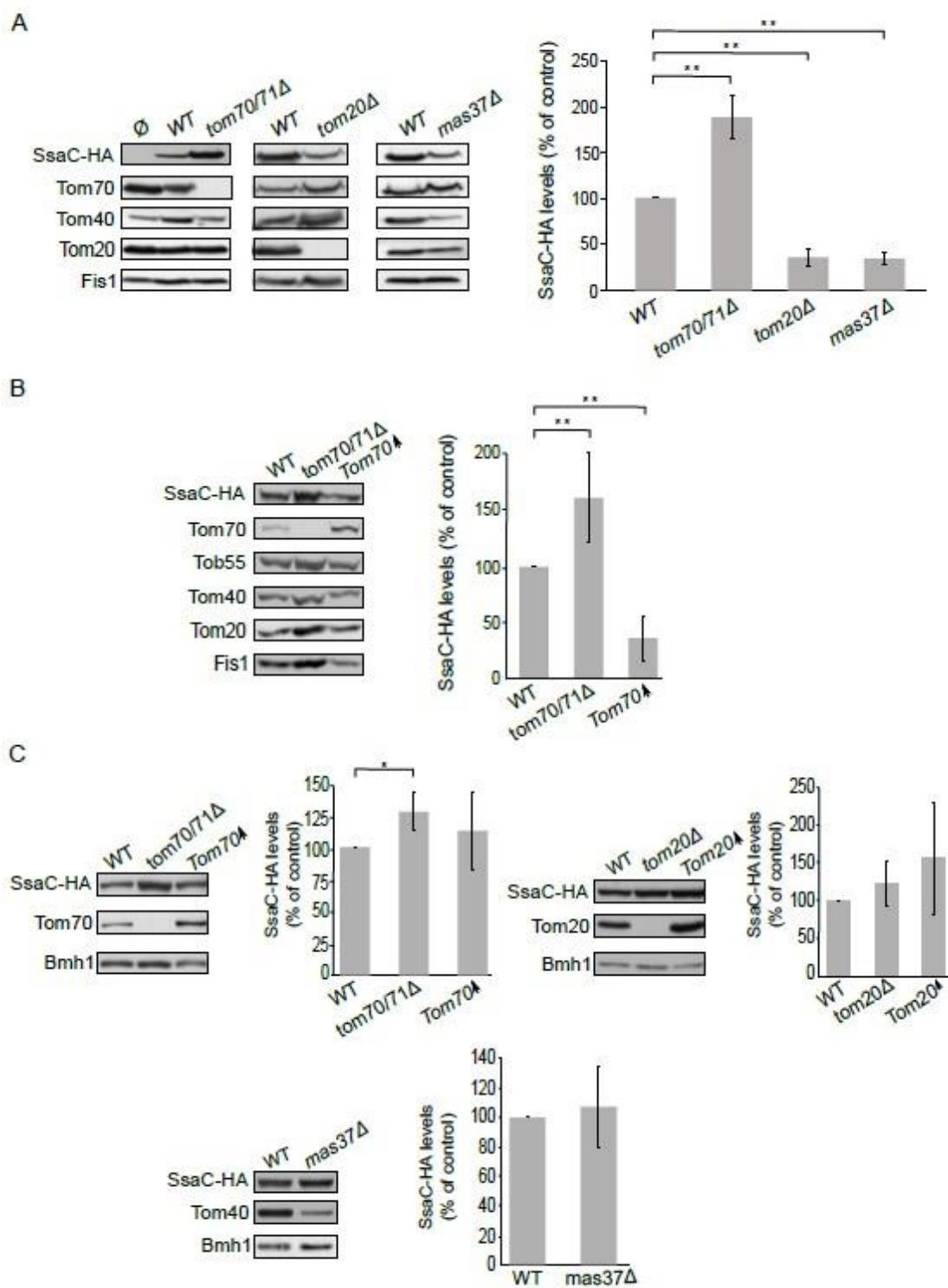


**Figure 4.4 - Lack of Tom70 improves the biogenesis of SsaC in mitochondria.**

(A) Isolated mitochondria were obtained from the indicated strains transformed with either an empty vector ( $\emptyset$ ) or a plasmid encoding SsaC-HA. Further treatment and analysis were as described in the legend to Figure 4.3A. (B) Crude mitochondria were obtained from WT, *tom70/71Δ*, or a strain

overexpressing *TOM70* (Tom70 $\uparrow$ ) harbouring a plasmid encoding SsaC-HA. Further treatment and analysis were as described in the legend to Figure 4.3A. (C) Whole cell lysate was obtained from the indicated cells and was analysed by SDS-PAGE followed by immunodecoration with antibodies against the specified proteins. The steady state levels of SsaC-HA in at least three experiments for each strain were quantified and further analysis was as described in the legend to Figure 4.3D. (\*\*,  $P < 0.01$ ; two-tailed Student's t-test). [This figure is equivalent to Figure 7 from (Natarajan et al. 2019)]

The biogenesis of secretin proteins in the mitochondrial OM can follow two distinct pathways: (1) After their synthesis in the cytosol, the secretin monomers are translocated across the mitochondrial OM into the IMS by the TOM complex and are inserted from the inside of the OM by either self-assembly or with the help of the TOB complex. (2) Upon synthesis in the cytosol, the secretin monomers assemble on the outside of the mitochondrial surface before integrating into the mitochondrial OM from the cytosolic side. The sensitivity to an externally added protease and our observations that no protease-resistant intermediates were formed in the mitochondrial IMS indicate that after the synthesis and oligomerization of both secretins, they insert into the mitochondrial OM from outside of the mitochondrial surface while their bulk is facing the cytosol. These differences are explained by the fact that in bacterial cells, the secretins are synthesized in the cytoplasm and cross the inner membrane before their assembly from the periplasm into the OM, whereas in yeast cells they are synthesized on cytosolic ribosomes and can directly assemble from this compartment onto the mitochondrial OM.

A differential dependence on import factors was observed for the T3SS secretins, InvG and SsaC. InvG does not require Tom20 for its assembly whereas, SsaC requires Tom20 and Mas37, a subunit of the TOB complex. SsaC also assembles more efficiently in the mitochondrial OM in the absence of Tom70. SsaC is the only bacterial secretin we observe that is influenced by the TOB complex. Since the TOB complex is homologous to the bacterial BAM complex, we propose that the BAM complex is probably involved in the membrane assembly of SsaC. In the case of InvG, the subcellular fractionation indicates enrichment of the secretin also in the microsomal fraction where it can form native like oligomers. Thus, it seems that InvG can oligomerise and insert spontaneously into membranes.

Collectively, our findings indicate that the secretins require different factors for assembly into the mitochondrial OM. This variable dependency might be extrapolated to the bacterial system and suggest that different secretins might follow different pathways and interact with various assembly factors. Future studies can shed more light on these mechanisms.

# Chapter 5

## Yeast mitochondria can process *de novo* designed $\beta$ -barrel proteins

This chapter consists of sections adapted from the following manuscript ready for submission:

### Yeast mitochondria can process *de novo* designed $\beta$ -barrel proteins

Anasuya Moitra<sup>1</sup>, Vitasta Tiku<sup>1</sup> and Doron Rapaport<sup>1</sup>

<sup>1</sup>Interfaculty Institute of Biochemistry, University of Tuebingen, Tuebingen, Germany.

#### Author Contributions

I designed and performed the vast majority of the experiments, analysed the data, prepared the figures and wrote the manuscript. VT planned and performed the cloning for the  $\beta$ -signal mutants. DR designed experiments, analysed the data, supervised the overall project, acquired funding and wrote the manuscript.

## 5.1 Introduction

$\beta$ -barrel proteins are found in the OM of Gram-negative bacteria along with the OM of mitochondria and chloroplasts (Hill et al. 1998; Gray, Burger, and Lang 1999; Schleiff et al. 2003; Young et al. 2007). This relationship matches the evolutionary origins of mitochondria and chloroplasts from ancient Gram-negative bacterial endosymbionts. Over the course of this evolution, most of the organellar genes, were transferred to the nucleus, with the mitochondrial and chloroplast genome retaining the codes for only a few key components like that of the respiratory chain complexes and the Rubisco subunit, respectively (Gray, Burger, and Lang 1999; Soll and Schleiff 2004). Thus, the mitochondrial and chloroplast  $\beta$ -barrel proteins are transcribed in the nucleus and translated on cytosolic ribosomes. Then, they need to be targeted to the correct subcellular organelle and ultimately integrated with the help of dedicated import machineries into the respective outer membranes.

The biogenesis pathways for  $\beta$ -barrel proteins have been quite conserved during evolution (Diederichs et al. 2020). Such conserved mechanisms prompted studies to investigate the evolutionary lineage of these pathways. Bacterial and chloroplast  $\beta$ -barrel proteins have been shown to be targeted and integrated into mitochondria upon expression in yeast cells (Walther et al. 2009; Ulrich et al. 2012; Ulrich et al. 2014; Jores et al. 2016; Natarajan et al. 2019). This opened the realm of possibilities for the potential of yeast cells to assemble and integrate novel  $\beta$ -barrel proteins. A recent study from the Baker lab showed that *de novo* designed synthetic eight stranded  $\beta$ -barrel proteins (Tmb2.3 and Tmb2.17) could fold and assemble into synthetic lipid membranes (Vorobieva et al. 2021). To better understand the basic principles of the biogenesis of  $\beta$ -barrel proteins, we investigated whether such synthetic  $\beta$ -barrel proteins could also be expressed in yeast cells and integrated into their mitochondria. We further explored the role of yeast mitochondrial import and assembly machinery components in the proper biogenesis of such  $\beta$ -barrel proteins.

## 5.2 Results

### 5.2.1 TMBs can localise to and integrate into the mitochondrial outer membrane

To better understand the biogenesis process of  $\beta$ -barrel proteins, we aimed to study the targeting and assembly of *de novo* designed members of this family. To this end, we utilized recently reported two artificial  $\beta$ -barrel proteins that were named TMB2.3 and TMB2.17

(Vorobieva et al. 2021). To facilitate their expression in yeast (*S. cerevisiae*), we created artificial genes with codon usage optimized to that of *S. cerevisiae*. Both DNA segments included at their 3' end a sequence encoding a HA-tag to allow detection with the corresponding antibody. The resulting coding sequences were cloned into the yeast expression vector pYX142 under the control of the *TPI* (triosephosphate isomerase, a housekeeping enzyme) promoter.

Next, wild type (WT) yeast cells were transformed with either the empty vector or the vector coding for either Tmb2.3-HA or Tmb2.17-HA. Importantly, analysis of proteins from whole cell lysates of cells transformed with the coding plasmids showed a specific HA-containing band migrating at an apparent mass of 14 kDa (data not shown). To test whether the expression of these  $\beta$ -barrel proteins affects the growth of the corresponding cells, growth curves of liquid cultures were obtained and drop dilution assays were performed. Both approaches showed that the expression of these TMBs does not have any influence on the growth of yeast cells (Figure 5.1).

Confirming the proper expression and the lack of a toxic effect, we next aimed to ascertain the subcellular location to which these proteins are targeted. To address this question, we performed subcellular fractionation of the above cells. Interestingly, while Tmb2.3-HA was predominantly localised to mitochondria, Tmb2.17-HA was found in both the ER and mitochondrial fractions (Figure 5.2). As a confirmation of the successful separation of the different fractions, the mitochondrial OM protein Porin, the ER protein Erv2, and the cytosolic protein Hexokinase were detected in their respective fractions. These findings demonstrate that at least one of the TMBs behaved similar to bacterial and chloroplasts  $\beta$ -barrel proteins that were also targeted to mitochondria upon their expression in yeast cells (Walther et al. 2009; Ulrich et al. 2012).

The hydrophobicity of the different  $\beta$ -hairpins has been shown to dictate the efficiency of mitochondrial localisation of  $\beta$ -barrel proteins (Jores et al. 2016). Hence, we analysed the hydrophobicity patterns of the eight  $\beta$ -strands of both TMBs (Figure 5.3). The higher hydrophobicity of the two strands of Tmb2.3 facing the lipid phase (face B of strands 4 and 8) could potentially explain its greater mitochondrial localisation efficiency (Figure 5.3B). Whereas the overall higher hydrophobicity of the individual  $\beta$ -hairpins of Tmb2.17 (Figure 5.3C) could be hypothesized to account for its partial ER localisation (Chio, Cho, and Shan 2017).

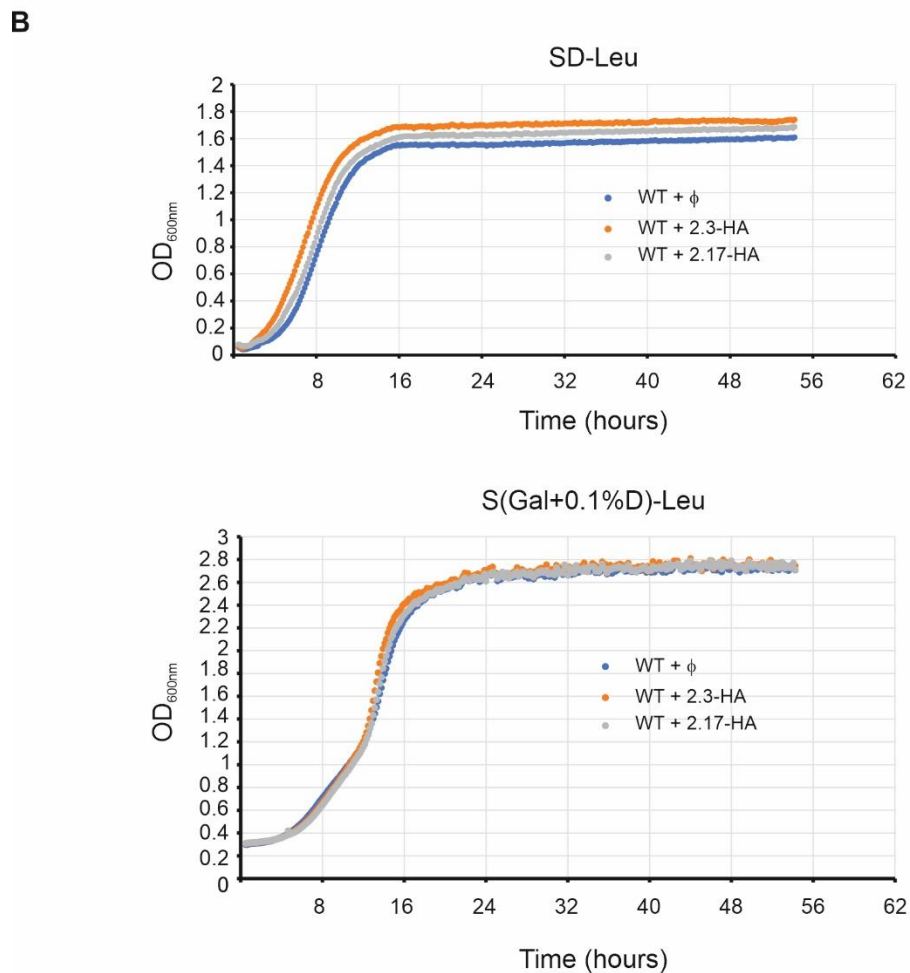
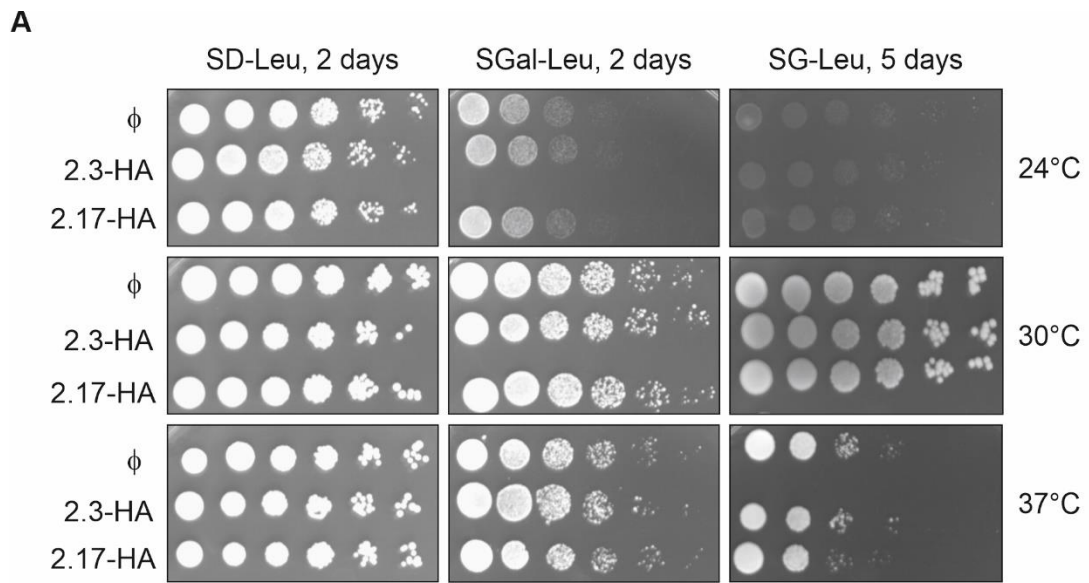


**Figure 5.1 – Expression of both TMBs does not affect the growth of yeast cells. (A)** WT yeast cells were transformed with an empty plasmid ( $\phi$ ) or with a plasmid encoding for either Tmb2.3-HA (2.3-

HA) or Tmb2.17-HA (2.17-HA). The growth of the cells was analysed by drop-dilution assay on the indicated media for the mentioned days at 24°C, 30°C and 37°C. **(B)** WT yeast cells transformed as in A were allowed to grow in SD-Leu (upper panel) or S(Gal+0.1%D)-Leu (lower panel) liquid media at 30°C for 72 h in a 96 well plate and growth was monitored by SPECTROstar Nano microplate reader. Data obtained were analysed by the MARS software and plotted by Excel. The plot shows the mean values of OD<sub>600nm</sub> of three technical replicates for each strain till 56 h.

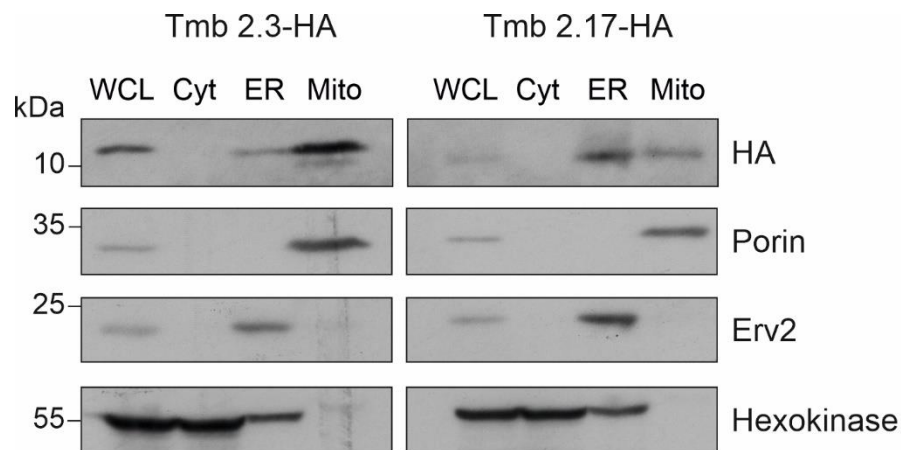


**Figure 5.2 – Tmb2.3 and Tmb2.17 are targeted mainly to mitochondria upon expression in yeast cells.** WT yeast cells expressing either Tmb2.3-HA (left panel) or Tmb2.17-HA (right panel) were subjected to subcellular fractionation, followed by analysis of the whole cell lysate (WCL), cytosol (Cyt), endoplasmic reticulum (ER)/microsomes and mitochondria (Mito) fractions by SDS-PAGE and immunodecoration with the indicated antibodies. Erv2 and Porin/VDAC are ER and mitochondrial marker proteins, respectively, while Hexokinase is used as a cytosolic marker.

Next, we investigated the membranal integration capability of these TMBs by subjecting mitochondria isolated from WT cells, expressing either Tmb2.3-HA or Tmb2.17-HA, to alkaline extraction. *Bona fide* membrane proteins like the OM proteins Tom20 and Tom40 and mitochondrial inner membrane (IM) protein Pic2 were found in the pellet (P) fraction, whereas soluble matrix protein Hsp60 was detected in the supernatant (S). Both Tmb2.3-HA and Tmb2.17-HA were found in the pellet fraction indicating that they are membrane embedded proteins (Figure 5.4).

**A**

Tmb2.3 (13541 Da) (NMR PDB 6X1K)  $\beta$  strand 

MQDGPGTLDVFVAAGWNTDNTIEITGGATYQLSPYIMVKAGYGWNNSSLNRFEEFGGG  
LQYKVTPDLEPYAWAGATYNTDNTLVPAAGAGFRYKVSPEVKLVVEYGWNNSSLQFL  
QAGLSYRIQP

Tmb2.17 (13415 Da) (Crystal Structure PDB 6X9Z)  $\beta$  strand 

MEQKPGTLMVYVVVGYNVDVVGGAQYAVSPYLFLDVGYGWNNSSLNFLEVGG  
GVSYKVSPLPYVKAGFEYNTDNTIKPTAGAGALYRVSPNLALMVEYGWNNSSLQK  
VAIGIAYKVKD

**B**

	Tmb 2.3	Tmb 2.17
Strand 1 face A	-0.58	0.18
face B	2.62	3.02
Strand 2 face A	-1.58	-0.28
face B	1.82	1.70
Strand 3 face A	-0.70	-1.00
face B	1.66	1.92
Strand 4 face A	-2.20	0.25
face B	2.25	1.66
Strand 5 face A	1.72	-2.68
face B	0.50	1.61
Strand 6 face A	0.56	-1.01
face B	1.22	1.16
Strand 7 face A	-0.90	-0.05
face B	1.45	1.92
Strand 8 face A	-1.28	-0.92
face B	2.03	1.68

**C**

Hairpin	Tmb 2.3	Tmb 2.17
hp1	2.22	2.36
hp2	1.74	1.81
hp3	1.92	1.79
hp4	1.28	1.64
hp5	0.89	1.39
hp6	1.31	1.51
hp7	1.74	1.80

**Figure 5.3 – Analysis of the amino acid sequence and hydrophobicity patterns of the TMBs. (A)**

The amino acid sequence of the two TMBs along with the annotation of the eight  $\beta$ -strands according

to the published structures from Vorobieva et al. 2021. **(B)** The average hydrophobicity of the hydrophilic face (face A) and the hydrophobic face (face B) of each of the eight  $\beta$ -strands of Tmb2.3 and Tmb2.17 was calculated by summing up the hydropathy values of the residues either facing the lipid environment (face B) or the  $\beta$ -barrel lumen (face A) and dividing it by the number of the residues in that strand. The values are colour coded, with blue, white and red representing the highest, median and the lowest hydropathy values, respectively. **(C)** The average hydrophobicity of the hydrophobic face of the  $\beta$ -hairpins of Tmb2.3 and Tmb2.17 was calculated by summing up the hydropathy values of the residues facing the lipid environment from both  $\beta$ -strands that form each  $\beta$ -hairpin (hp) and dividing it by the number of the residues. The values are colour coded as in B.

To assess the topology of the TMBs and determine in which mitochondrial membrane they reside, mitochondria expressing these TMBs were subjected to treatment with the proteases Proteinase K (PK) or trypsin. OM proteins with an exposed cytosolic domain like Tom20 were completely digested by these proteases, whereas IM and matrix proteins like Pic2 and Hsp60, respectively, were protected from the protease. Both TMBs were partially susceptible to PK and better protected from trypsin (Figure 5.4). As a control, addition of 1% Triton-X-100 to the reaction, which leads to the solubilisation of the mitochondrial membranes, resulted in complete exposure of the proteins to the protease (Figure 5.4). Thus, we can conclude that the TMBs are embedded into the mitochondrial OM with a topology that exposes part of them to the cytosol.

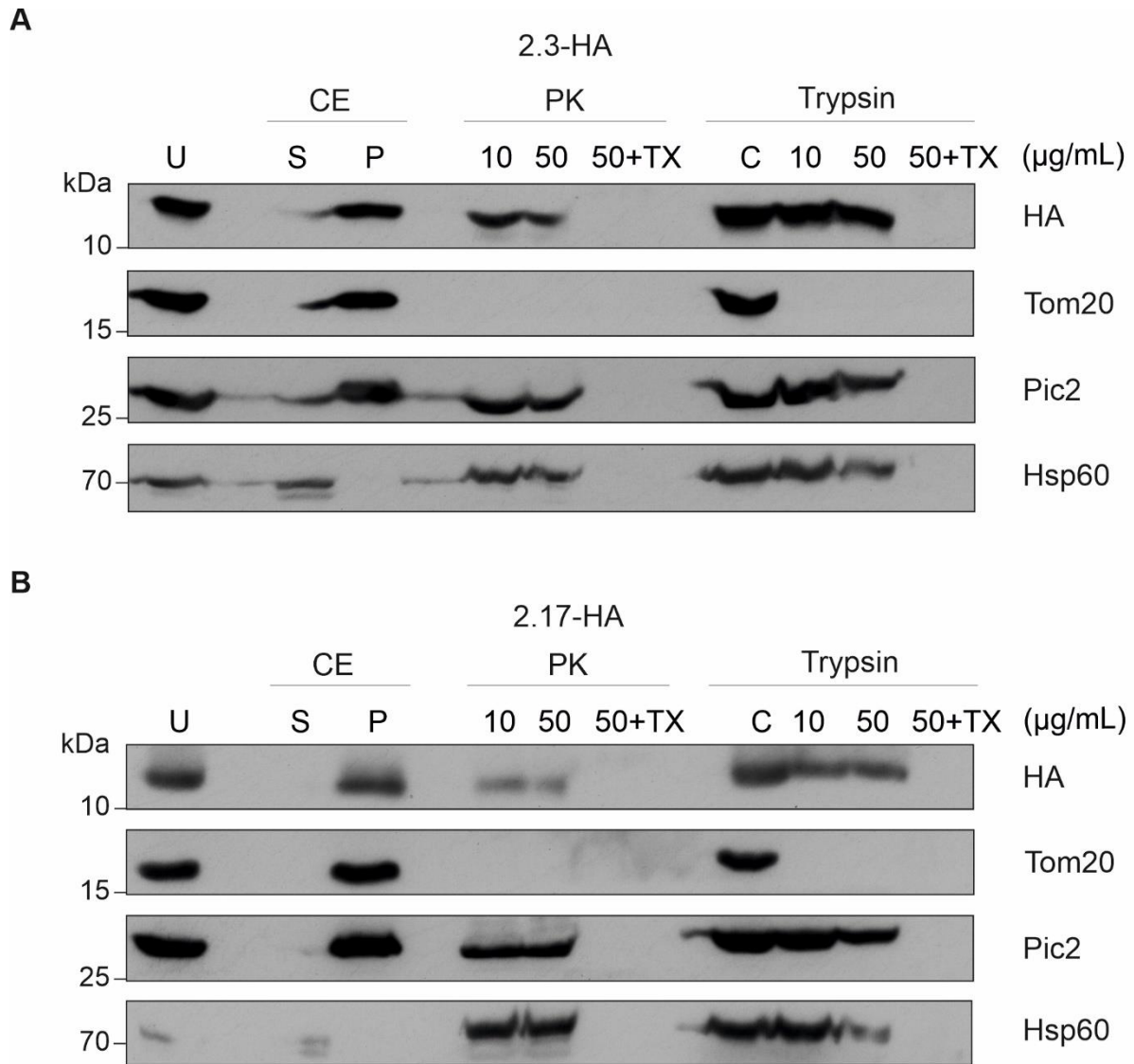


**Figure 5.4 – Both TMBs are embedded in the mitochondrial outer membrane.** (A, B) Mitochondria isolated from WT yeast cells expressing either Tmb2.3-HA (A) or Tmb2.17-HA (B) were left untreated (U), subjected to carbonate extraction (CE) to obtain supernatant (S) and pellet (P) fractions, or were treated with either 10 or 50 µg/ml of Proteinase K (PK) or Trypsin in the presence or absence of 1% Triton-X-100 (TX). In the control lane (C), mitochondria were treated with 50 µg/ml of Trypsin, that had been pre-incubated with the trypsin inhibitor, STI, so as to block the proteolytic activity of trypsin and serve as an indicator of the inhibitor’s efficacy. Samples were finally analysed by SDS-PAGE and immunoblotting. Tom20 is a mitochondrial OM protein exposed to the cytosol; Pic2 is embedded in the mitochondrial IM; Hsp60 is a soluble mitochondrial matrix protein.

### 5.2.2 The biogenesis of the synthetic TMBs does not depend on the import receptors Tom20 and Tom70

We established that TMBs can be targeted to the mitochondria upon expression in yeast cells. Next, we wanted to examine the possible import machineries that these proteins may utilise to arrive and thrive in the mitochondria.  $\beta$ -barrel proteins have been shown to interact with the TOM complex receptors (Wiedemann and Pfanner 2017). Recently, it was shown that the  $\beta$ -hairpin element could interact with Tom20 and the chaperone bound precursor could bind to Tom70 to enable the precursor to enter via the Tom40 pore (Jores et al. 2016; Jores et al. 2018). Hence, we wanted to check if the rather small TMBs also depend on these receptors for their entry into the mitochondria. To address this issue, WT, *tom20 $\Delta$* , and *tom70/71 $\Delta$*  yeast cells were transformed with an empty vector ( $\phi$ ) or a vector encoding either Tmb2.3-HA or Tmb2.17-HA. This was followed by isolation of the corresponding mitochondrial fraction (Mito), along with the whole cell lysate (WCL) and cytosol (Cyt) and subsequent analysis of the proteins of these fractions via SDS-PAGE and immunoblotting.

Surprisingly, the steady state levels of both Tmb2.3-HA and Tmb2.17-HA seem to be even higher in the mitochondrial fraction of cells lacking the Tom20 receptor (Figure 5.5A and 5.5B, respectively). Tom40 and Hexokinase are used as mitochondrial and cytosolic controls, respectively and their levels remain unchanged. Of note, the levels of the Tom70 receptor, which might compensate for the loss of Tom20, are also unaltered in cells deleted for Tom20 (Figure 5.5). Hence, it appears that Tom20 is not required for the proper import of the TMBs to mitochondria.

Similar observations were made when the other import receptors Tom70 and its paralog Tom71 were deleted. The levels of both the TMBs were somewhat higher in the *tom70/71 $\Delta$*  yeast cells (Figure 5.6). The steady state levels of Tom20 were slightly higher in the mutated organelles and this could potentially compensate for the loss of Tom70. Thus, we can conclude that the TMBs can be targeted to the mitochondria in the absence of either Tom20 or the Tom70/71 receptors.

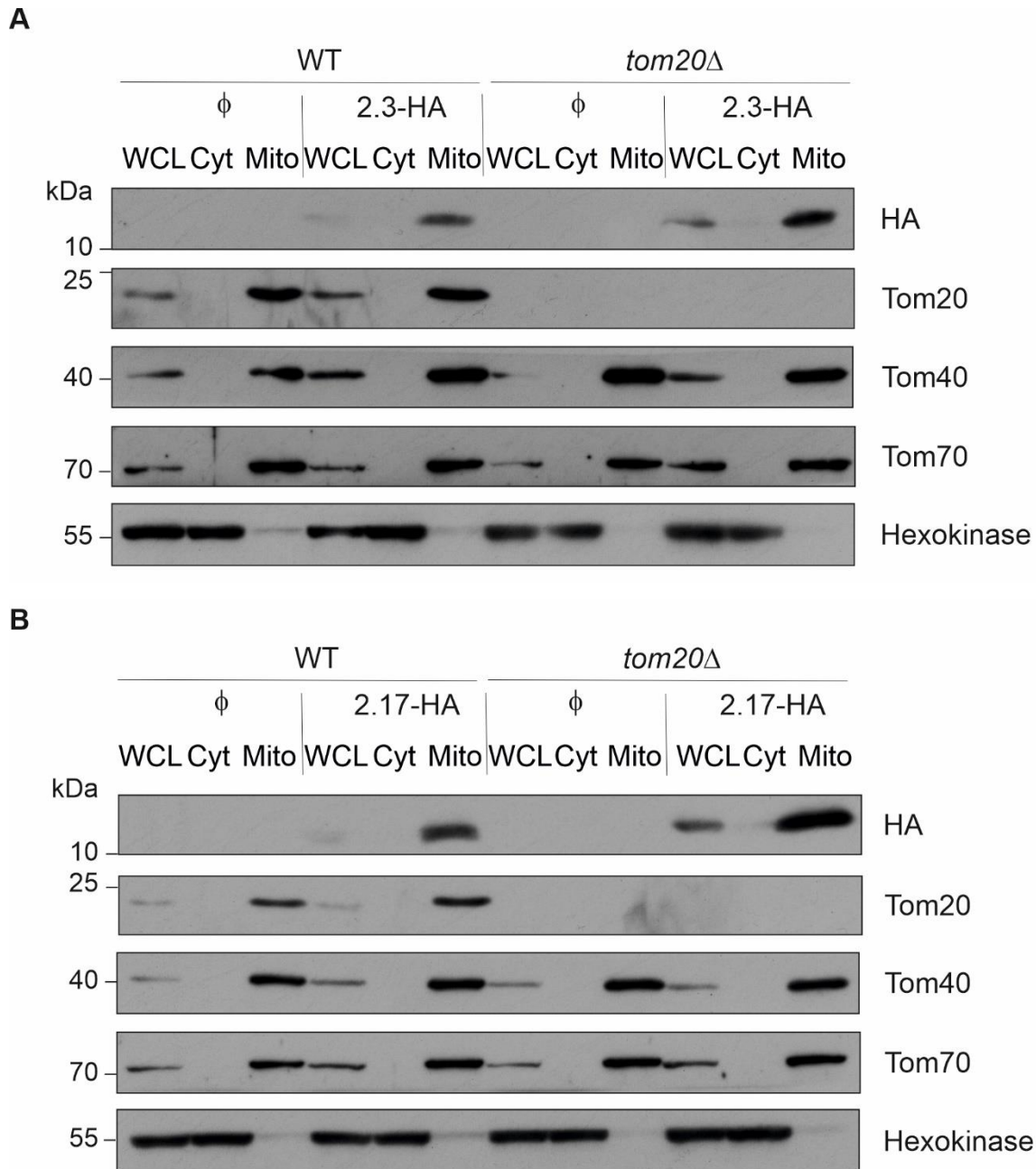


**Figure 5.5 – The steady state levels of both TMBs in yeast cells do not depend on Tom20. (A, B)** WT and *tom20Δ* yeast cells were transformed with an empty plasmid ( $\phi$ ) or with a plasmid encoding for either Tmb2.3-HA (A) or Tmb2.17-HA (B). Whole cell lysate (WCL), cytosol (Cyt), and mitochondrial (Mito) fractions isolated from the transformed cells were subjected to SDS-PAGE and immunoblotting with the indicated antibodies. Tom40 and Tom70 are mitochondrial OM proteins, while Hexokinase is used as a cytosolic marker.

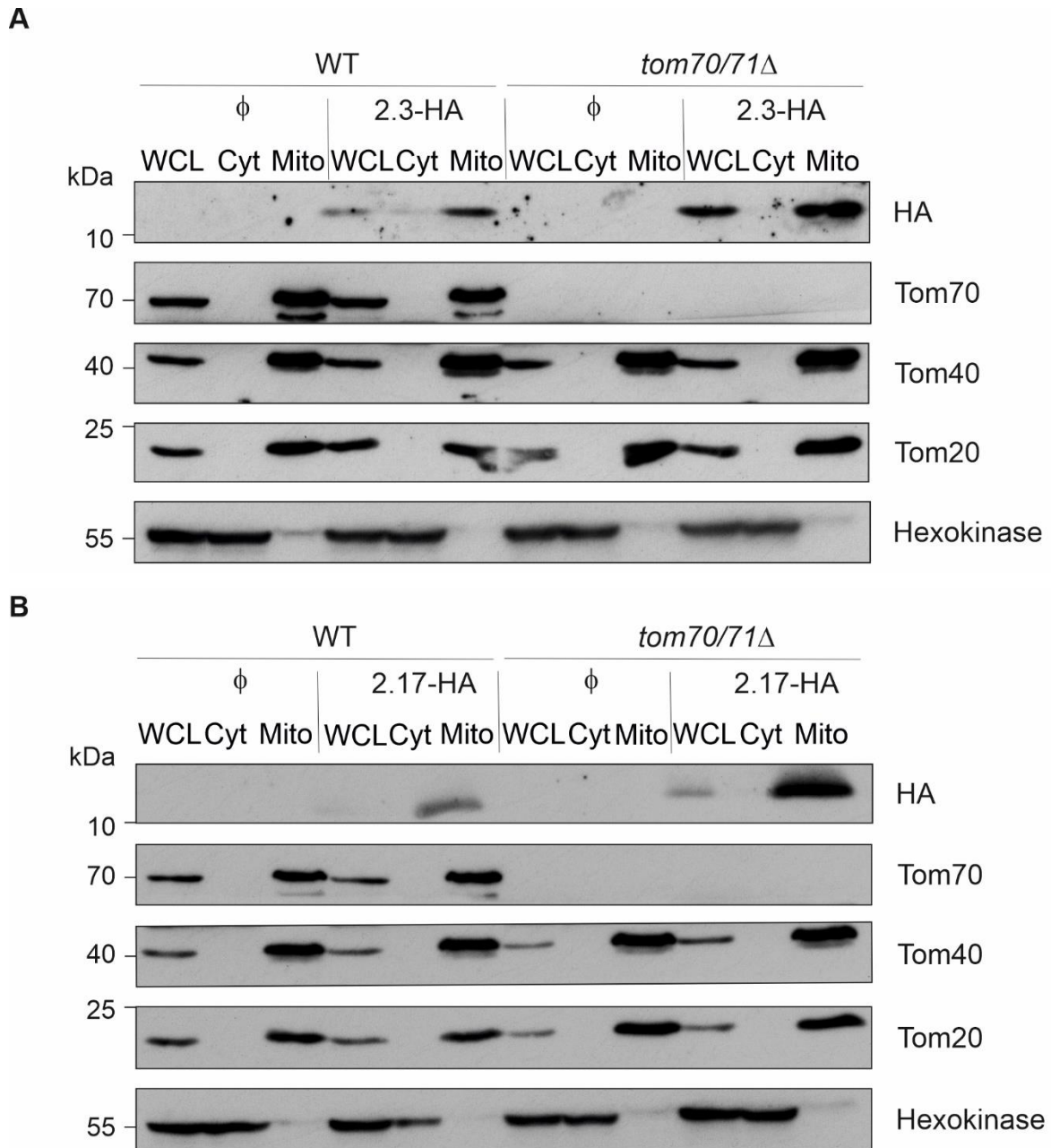


**Figure 5.6 – Tom70 is not involved in the biogenesis of both TMBs. (A, B)** WT and *tom70/tom71Δ* yeast cells were transformed with an empty plasmid ( $\phi$ ) or with a plasmid encoding for either Tmb2.3-HA (A) or Tmb2.17-HA (B). Whole cell lysate (WCL), cytosol (Cyt), and mitochondrial (Mito) fractions isolated from the transformed cells were subjected to SDS-PAGE and immunoblotting with the indicated antibodies.

### 5.2.3 The assembly of the TMBs depends to a variable extent on the TOB complex

Once the  $\beta$ -barrel protein precursors reach the mitochondrial surface, they are initially processed by the TOM complex (Neupert and Herrmann 2007). Then, they reach the IMS where they are bound by the sTIM chaperones to prevent aggregation (Weinhäupl et al. 2018). Finally, the  $\beta$ -barrel precursors are assembled in the mitochondrial OM via the TOB complex consisting of Mas37, Mas35 and Tob55 (Wiedemann et al. 2003; Kozjak et al. 2003; Habib et al. 2005; Habib et al. 2006; Kutik et al. 2008; Höhr et al. 2018; Takeda et al. 2021). Thus, we wanted to assess whether the absence of certain critical components of the TOB complex could affect also the assembly of these synthetic TMBs.

To that goal, we transformed an empty plasmid ( $\phi$ ) or plasmids encoding either Tmb2.3-HA or Tmb2.17-HA into WT or cells lacking Mas37. The cells were grown at 24°C to avoid accumulation of suppressors at elevated temperatures as Mas37 is crucial for the proper function of the TOB complex. Subcellular fractions were isolated and the steady state levels of both TMBs analysed by SDS-PAGE and immunoblotting. We observed that the mitochondrial levels of both Tmb2.3-HA and Tmb2.17-HA were significantly lower in *mas37 $\Delta$*  cells as compared to those in control cells (Figure 5.7A and 5.7B, respectively). This behaviour is similar to that of a canonical mitochondrial  $\beta$ -barrel protein like Tom40. As expected, the levels of Tom20, a mitochondrial signal-anchored protein, were unaffected as its biogenesis is known to be independent of the TOB complex. Similarly, the levels of the cytosolic chaperone Hsp104 were also unaltered (Figure 5.7A, B).

Next, we wanted to examine the role of Mas37 in the assembly of these TMBs in the mitochondrial OM. Therefore, mitochondria isolated from WT or *mas37 $\Delta$*  cells expressing the TMBs were subjected to BN-PAGE followed by immunoblotting. In the control organelles, Tmb2.3-HA could form high molecular weight oligomers, while Tmb2.17-HA was mostly present as monomers. Interestingly, in the organelles lacking Mas37, Tmb2.3-HA could no longer assemble into higher oligomers and was found to exist, similar to Tmb2.17-HA, only as monomers (Figure 5.7C, left panel). As a control, the TOM complex which was immunodecorated at about 400 kDa with antibodies against Tom40, was also detected in lower levels upon deletion of *MAS37* (Figure 5.7C, right panel). These findings suggest that Tmb2.3-HA can assemble into higher oligomers in a TOB complex dependent manner.

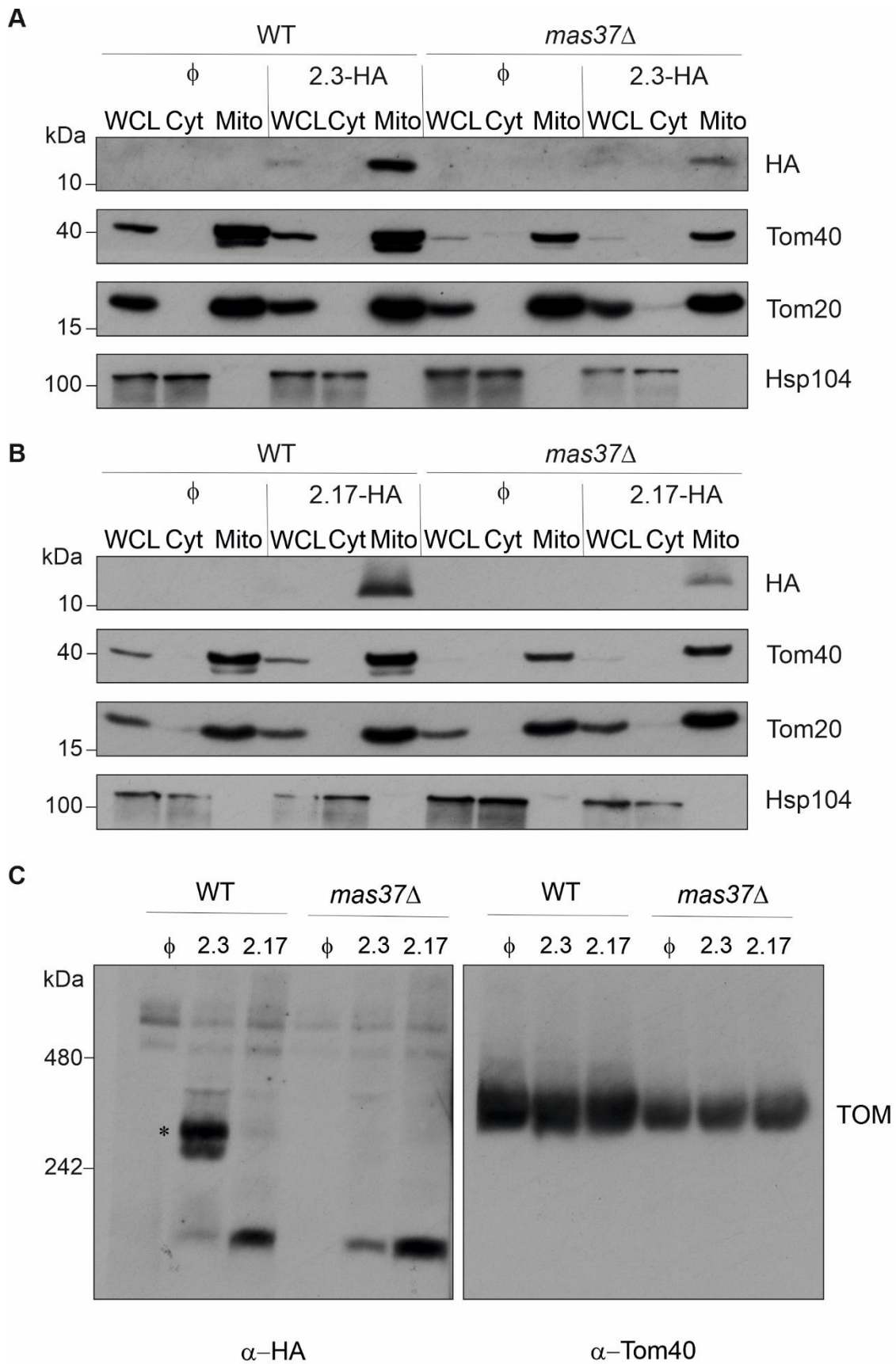


**Figure 5.7 – The membrane integration of both TMBs requires Mas37.** (A, B) WT and *mas37* $\Delta$  yeast cells were transformed with an empty plasmid ( $\phi$ ) or with a plasmid encoding for either Tmb2.3-

HA (A) or Tmb2.17-HA (B). Whole cell lysate (WCL), cytosol (Cyt), and mitochondrial (Mito) fractions isolated from the transformed cells were subjected to SDS-PAGE and immunoblotting with the indicated antibodies. (C) Mitochondria isolated as in A and B were analysed by BN-PAGE and immunoblotting with antibodies against either the HA tag (left panel) or Tom40 (right panel). Tom40 is a known substrate of Mas37. A high molecular weight form of Tmb2.3-HA and the TOM complex are indicated by an asterisk or 'TOM', respectively.

Observing this effect of Mas37, we wanted to assess the importance of Tob55, the central component of the TOB complex, for the biogenesis of the TMBs. A complete knockdown of Tob55 is detrimental for the yeast cells. Hence, we transformed an empty vector ( $\phi$ ) or vector encoding either Tmb2.3-HA or Tmb2.17-HA into cells expressing Tob55 under the control of the inducible *GALI0* promoter. To ensure the expression of Tob55, the cells were initially grown at 30°C in selective lactate medium with galactose. Then, to deplete Tob55, the cells were harvested and re-suspended in glucose containing medium. Cells were then harvested at the indicated time points after a shift from galactose- to glucose-containing medium, mitochondria were isolated, and the steady state levels of the TMBs analysed by SDS-PAGE and immunoblotting.

We observed that the levels of Tob55 were depleted after 51 hours on glucose containing medium (Figure 5.8A, B). As a consequence, Porin/VDAC, a quintessential mitochondrial OM  $\beta$ -barrel protein, that depends on Tob55 for optimum assembly, was depleted after 71 hours while steady state levels of the matrix protein Aconitase, whose biogenesis is independent of Tob55, remained unaffected (Figure 5.8A, B). Similar to Porin, Tmb2.3-HA levels decreased upon Tob55 depletion (Figure 5.8A). Unexpectedly, Tmb2.17-HA levels slightly increased in the mitochondria from Tob55-depleted cells (Figure 5.8B).

These observations led us to ask whether Tob55 was crucial also for the assembly of the higher oligomers of Tmb2.3-HA. As we observed before, BN-PAGE analysis revealed that Tmb2.3-HA could form higher oligomers in the presence of Tob55, while Tmb2.17-HA was mostly present as monomers (Figure 5.8C, left panel). Of note, upon depletion of Tob55, Tmb2.3-HA could no longer assemble into higher oligomers and was found to exist only as monomers. In agreement with the analysis by SDS-PAGE, Tmb2.17-HA monomers were detected in increased amounts in the organelles depleted for Tob55 (Figure 5.8C, left panel). As expected, Porin also formed higher oligomers in the presence of Tob55, but their levels were substantially decreased upon Tob55 depletion (Figure 5.8C, right panel). Taken together, these data indicate

the differential involvement of the TOB complex in the biogenesis and assembly of the artificial TMBs. Whereas the complex facilitates the membrane integration and oligomerization of Tmb2.3-HA, it is dispensable for the biogenesis of Tmb2.17-HA.

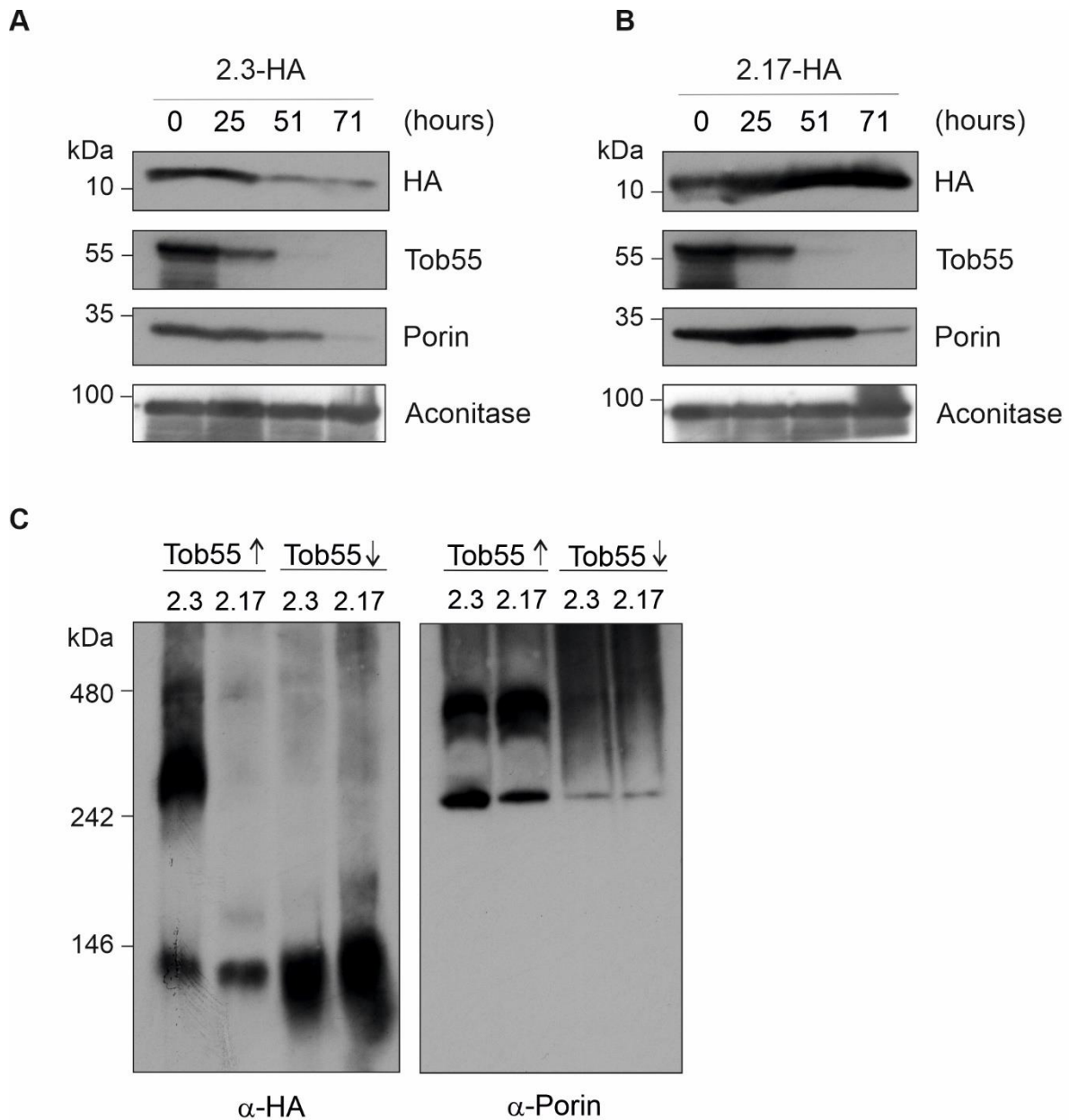


**Figure 5.8 – Depletion of Tob55 affects the assembly of Tmb2.3 but not that of Tmb2.17.** (A, B) Plasmids encoding Tmb2.3-HA and Tmb2.17-HA were transformed into yeast cells expressing Tob55 under the control of the inducible *GAL10* promoter. To induce the depletion of Tob55, cells were shifted at t=0 from galactose- to glucose-containing medium and harvested at the indicated time points after this shift. Mitochondria were isolated and proteins were analysed by SDS-PAGE and immunoblotting with antibodies against the indicated proteins. Aconitase is a mitochondrial matrix protein. (C)

Mitochondria were isolated from cells described above grown on galactose (Tob55 $\uparrow$ ) or depleted for Tob55 by growth for 71 hrs on glucose containing medium (Tob55 $\downarrow$ ). Samples were analysed by BN-PAGE and immunodecoration with antibodies against either the HA tag (left panel) or Porin/VDAC (right panel). Porin/VDAC is a  $\beta$ -barrel protein embedded in the mitochondrial OM and a known substrate of Tob55.

#### **5.2.4 Single amino acid mutation in the $\beta$ -signal does not significantly alter the biogenesis of both TMBs**

Previous studies showed that the last C-terminal  $\beta$ -strand of mitochondrial  $\beta$ -barrel proteins contains a stretch of amino acids that facilitate their interaction with the TOB complex (Kutik et al. 2008). These residues were called the  $\beta$ -signal and comprised of the following motif: Po-X-G-X-X-Hy-X-Hy-X, where Po stands for a polar residue, G for Glycine and Hy represents a hydrophobic residue. Deletion or mutation of the  $\beta$ -signal did not interfere with the initial targeting of newly synthesized  $\beta$ -barrel proteins to mitochondria.

We wanted to investigate whether sequences similar to such a  $\beta$ -signal present within the TMBs, could explain their differential dependence on the TOB complex. To this end, we analysed the amino acid sequence of both TMBs. They showed a 60% sequence identity [using Clustal Omega (Madeira et al. 2022), data not shown]. The amino acid sequence and the annotation of the eight  $\beta$ -strands are shown in Figure 5.3A (adapted from Vorobieva et al., 2021). The analysis revealed that Tmb2.3 indeed contained the canonical  $\beta$ -signal, whereas Tmb2.17 had only a partial consensus sequence. Tmb2.17 lacked the polar residue at the N-terminus of the  $\beta$ -signal (Q115 in Tmb2.3, A115 in Tmb2.17) (Figure 5.9A, wild type TMBs).

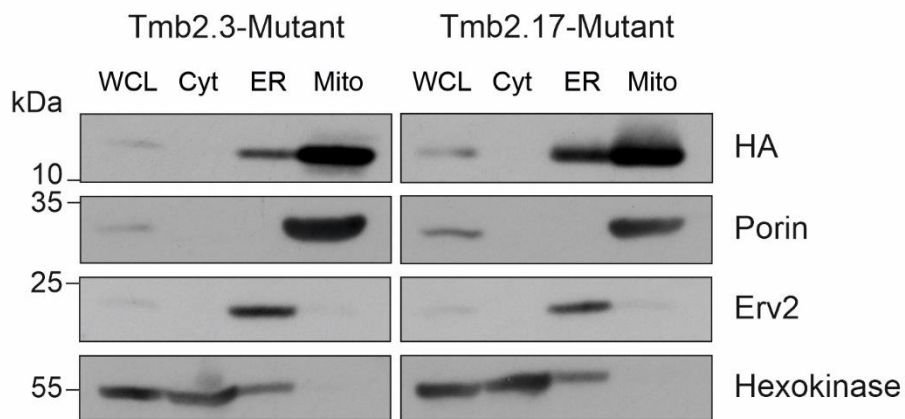
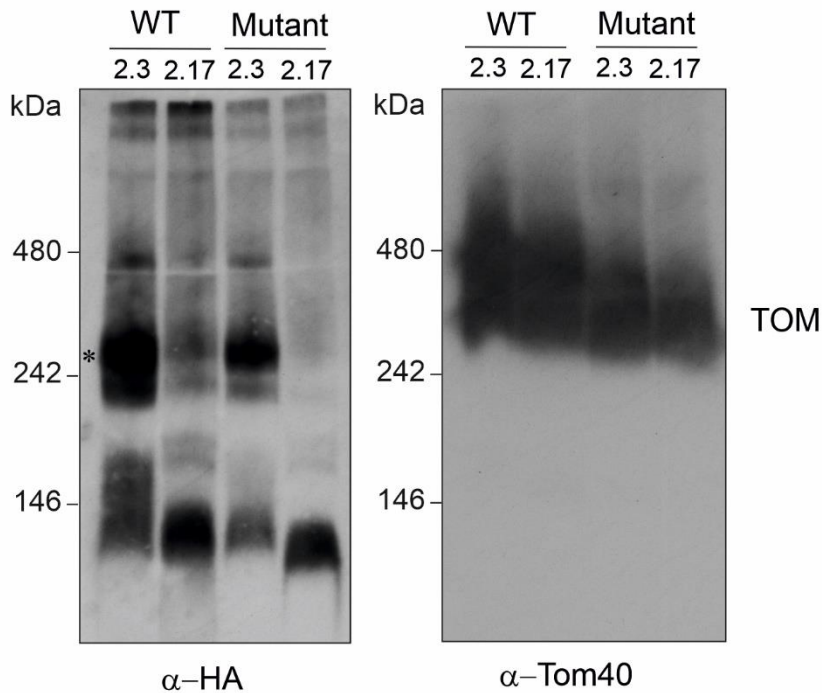
Hence, we wanted to assess whether this residue (Q115) of the  $\beta$ -signal was crucial for the assembly of the TMBs into higher oligomeric forms. Thus, Vitasta Tiku performed site-directed mutagenesis to generate the following C-terminal HA-tagged mutants of the TMBs: Tmb2.3<sub>Q115A</sub>-HA and Tmb2.17<sub>A115Q</sub>-HA (Figure 5.9A, mutant TMBs). WT yeast cells were transformed with vectors encoding these mutant TMBs, grown on S(Gal+0.1%D)-Leu media and subjected to subcellular fractionation. The results revealed that the mutation did not interfere with the initial targeting of the TMBs. Tmb2.3<sub>Q115A</sub>-HA was still predominantly mitochondrial, while Tmb2.17<sub>A115Q</sub>-HA was distributed between the ER and mitochondria (Figure 5.9B). However, BN-PAGE analysis followed by immunoblotting of mitochondria isolated from cells expressing either the WT or mutant TMBs showed that loss of Q115 led to

a minor decrease in the higher oligomeric forms of Tmb2.3<sup>Q115A</sup>-HA compared to wild type Tmb2.3-HA, while both the WT and mutant Tmb2.17 were predominantly present as lower monomeric forms (Figure 5.9C, left panel). However, the TOM complex, which was immunodecorated at about 400 kDa with antibodies against Tom40, was also detected in lower levels for the mutants (Figure 5.9C, right panel). Hence, further experiments with uniform loading controls are required to make the final conclusion. Also, the role of the most C-terminal amino acid residue in the  $\beta$ -signal motif, which is different for the two TMBs (Q123 for Tmb2.3 and K123 for Tmb2.17), needs to be investigated. Overall, it seems that a single amino acid mutation in the  $\beta$ -signal motif of the TMBs does not have any significant effect on their overall biogenesis.

**A****β-signal residue**

β-signal motif

Po-X-G-X-X-Hy-X-Hy-X

**wildtype**Tmb 2.3    115 **Q** A G L S Y R I Q 123Tmb 2.17   115 **A** I G I A Y K V K 123**mutant**Tmb 2.3    115 **A** A G L S Y R I Q 123Tmb 2.17   115 **Q** I G I A Y K V K 123**B****C**

**Figure 9 – Single amino acid mutation in the β-signal does not significantly alter the mitochondrial localisation or assembly of Tmb2.3 and Tmb2.17 (A) Conserved mitochondrial β-signal motif (top)**

and the corresponding  $\beta$ -signal motif in the TMBs (bottom). The  $\beta$ -signal residues are in red and the mutated residues in bold. Po, polar; Hy, hydrophobic. **(B)** WT yeast cells expressing either Tmb2.3<sub>Q115A</sub>-HA or Tmb2.17<sub>A115Q</sub>-HA (mutants) were subjected to subcellular fractionation, followed by analysis of the whole cell lysate (WCL), cytosol (Cyt), endoplasmic reticulum (ER)/microsomes and mitochondria (Mito) fractions by SDS-PAGE and immunodecoration with the indicated antibodies. Erv2 and Porin/VDAC are ER and mitochondrial marker proteins, respectively, while Hexokinase is used as a cytosolic marker. **(C)** Mitochondria isolated from WT cells expressing either wild type or mutant TMBs were subjected to BN-PAGE and immunoblotting with antibodies against either the HA tag (left panel) or Tom40 (right panel).

### 5.3 Discussion

The evolutionary conservation of the biogenesis pathways of  $\beta$ -barrel proteins allowed us in the past to express and target bacterial and chloroplast  $\beta$ -barrel proteins into yeast mitochondria (Walther et al. 2009; Ulrich et al. 2012; Ulrich et al. 2014; Jores et al. 2016; Natarajan et al. 2019). Recently, Vorobieva et al. designed synthetic eight stranded  $\beta$ -barrel proteins, namely Tmb2.3 and Tmb2.17, that could be assembled into a barrel structure in liposome (Vorobieva et al. 2021). To better understand the general principles of the biogenesis of  $\beta$ -barrel proteins, we wanted to test whether such artificially designed proteins could also be recognized by and assembled into yeast mitochondria. Subcellular fractionation experiments revealed that both TMBs could be targeted to the mitochondria, with partial ER localisation as well. Similar observations were also made when bacterial secretins like PulD, InvG or SsaC were expressed in yeast cells (Natarajan et al. 2019). Of note, Tmb2.3-HA was more efficiently localised to the mitochondria in comparison to Tmb2.17-HA.  $\beta$ -barrel proteins are targeted and assembled into the mitochondria based on the hydrophobicity and the sequence of the last few  $\beta$ -hairpins (Kutik et al. 2008; Jores et al. 2016; Klinger et al. 2019). The differential localisation efficiency could potentially be attributed to the difference in the sequence and hydrophobicity of the last few  $\beta$ -hairpins of the two different proteins, thus indicating that conserved structural features of  $\beta$ -barrel proteins may be recognised by the yeast cell machinery and dictate the mitochondrial localisation of even synthetic  $\beta$ -barrel proteins. It is interesting to note that both TMBs, although they contain only 8  $\beta$ -strands, were integrated properly into the mitochondrial OM demonstrating the capacity of the organelle to deal with any type of membrane embedded  $\beta$ -barrel proteins. These observations are in line with our previous findings that yeast

mitochondria can deal with the bacterial  $\beta$ -barrel protein OmpA, which also contains only 8  $\beta$ -strands (Walther et al. 2009).

Interestingly, when we assessed the role of the TOM complex receptors in the biogenesis of the TMBs, we observed that in the absence of either one of the receptors (Tom20 or Tom70), the mitochondrial steady state levels of the TMBs were enhanced. Similar observations were made for the secretins InvG-HA and SsaC-HA where absence of Tom20 or Tom70 led to increased amounts of the protein in the mitochondria respectively (Natarajan et al. 2019). This behaviour might be explained by the small size of the artificial TMBs that have only 8  $\beta$ -strands as compared to the 16 or 19 strands of *bona fide* mitochondrial  $\beta$ -barrel proteins. As Tom70, in addition to its receptor function, is also the docking site for cytosolic chaperones that escort the newly synthesized  $\beta$ -barrel substrates, the smaller size of the substrates might reduce the need for such an escort and hence also the relevance of the chaperone docking site. An alternative, but not mutually exclusive, option is a compensating function of the remaining receptor in the absence of its counterpart. Also, a possible role of Tom22 in the absence of either Tom20 or Tom70 remains to be investigated. Thus, we can conclude that the absence of a single receptor does not impair the biogenesis of the TMBs.

After the initial recognition at the mitochondrial surface by the TOM complex receptors, followed by the actual translocation through the Tom40 pore,  $\beta$ -barrel proteins are assembled into the mitochondrial OM with the help of sTIM chaperones and the TOB complex (Weinhäupl et al. 2018; Wiedemann et al. 2004; Wiedemann et al. 2003; Kozjak et al. 2003; Habib et al. 2005; Habib et al. 2006; Kutik et al. 2008; Höhr et al. 2018; Takeda et al. 2021). We investigated the role of the TOB complex in the assembly of the synthetic TMBs. In the absence of Mas37, the mitochondrial steady state levels of the TMBs decreased, similar to *bona fide* mitochondrial  $\beta$ -barrel protein Tom40. It is known that absence of Mas37 decreases the stability of the TOB complex, thus affecting the efficiency of integration of the TMBs into the mitochondrial OM. Additional decrease in Tom40 levels, which by itself is a substrate of the TOB complex, may also contribute to the lower steady state levels of the TMBs. BN-PAGE analysis of mitochondria from *mas37 $\Delta$*  cells demonstrated the importance of Mas37 and the TOB complex not only for the general import of Tmb2.3, but also for its optimal assembly. Tmb2.17-HA always existed as lower monomeric forms and absence of Mas37 had no impact on its integration into the mitochondrial OM. The inability of Tmb2.17-HA to form higher oligomers could be attributed to the absence of a *bona fide* mitochondrial  $\beta$ -signal in its sequence.

Besides Mas37, our findings also indicate an involvement of Tob55 in the biogenesis and assembly of Tmb2.3-HA. In contrast, Tmb2.17-HA levels were even slightly increased upon Tob55 depletion. Hence, it seems that different  $\beta$ -barrel proteins can be dependent to a variable extent on the proper function of the TOB complex. Such distinctions could be hypothesised to be mapped to the dissimilarities in their sequence (60% identity), hydrophobicity patterns of the  $\beta$ -strands, and/or different sequence of the classical  $\beta$ -signal at the last  $\beta$ -strand. This variability also raises the question that how Tmb2.17 can integrate into the mitochondrial OM in the absence of a functional TOB complex and future studies should address such apparent TOB-independent membrane integration.

Collectively, our study demonstrates that synthetic TMBs can be targeted to mitochondria upon their expression in yeast cells. Their biogenesis is independent of the TOM receptors and differentially dependent on the TOB complex. These findings shed new light on the general principles of the biogenesis of  $\beta$ -barrel proteins.

## References

- Alvarez-Martinez, C. E., and P. J. Christie. 2009. 'Biological diversity of prokaryotic type IV secretion systems', *Microbiol Mol Biol Rev*, 73: 775-808.
- Araiso, Yuhei, Akihisa Tsutsumi, Jian Qiu, Kenichiro Imai, Takuya Shiota, Jiyao Song, Caroline Lindau, Lena-Sophie Wenz, Haruka Sakaue, Kaori Yunoki, Shin Kawano, Junko Suzuki, Marilena Wischnewski, Conny Schütze, Hirotaka Ariyama, Toshio Ando, Thomas Becker, Trevor Lithgow, Nils Wiedemann, Nikolaus Pfanner, Masahide Kikkawa, and Toshiya Endo. 2019. 'Structure of the mitochondrial import gate reveals distinct preprotein paths', *Nature*, 575: 395-401.
- Bausewein, T., D. J. Mills, J. D. Langer, B. Nitschke, S. Nussberger, and W. Kühlbrandt. 2017. 'Cryo-EM Structure of the TOM Core Complex from *Neurospora crassa*', *Cell*, 170: 693-700.e7.
- Benz, Roland. 1989. "Porins from Mitochondrial and Bacterial Outer Membranes: Structural and Functional Aspects." In *Anion Carriers of Mitochondrial Membranes*, edited by Angelo Azzi, Katarzyna A. Nałęcz, Maciej J. Nałęcz and Lech Wojtczak, 199-214. Berlin, Heidelberg: Springer Berlin Heidelberg.
- Beverly, Kristen N., Michael R. Sawaya, Einhard Schmid, and Carla M. Koehler. 2008. 'The Tim8-Tim13 complex has multiple substrate binding sites and binds cooperatively to Tim23', *Journal of Molecular Biology*, 382: 1144-56.
- Bölter, B., J. Soll, K. Hill, R. Hemmler, and R. Wagner. 1999. 'A rectifying ATP-regulated solute channel in the chloroplastic outer envelope from pea', *EMBO J*, 18: 5505-16.
- Chio, U. S., H. Cho, and S. O. Shan. 2017. 'Mechanisms of Tail-Anchored Membrane Protein Targeting and Insertion', *Annu Rev Cell Dev Biol*, 33: 417-38.
- Daefler, Simon, and Marjorie Russel. 1998. 'The *Salmonella typhimurium* InvH protein is an outer membrane lipoprotein required for the proper localization of InvG', *Molecular Microbiology*, 28: 1367-80.
- Daum, G., P. C. Böhni, and G. Schatz. 1982. 'Import of proteins into mitochondria. Cytochrome b2 and cytochrome c peroxidase are located in the intermembrane space of yeast mitochondria', *Journal of Biological Chemistry*, 257: 13028-33.
- Diederichs, Kathryn A., Xiaodan Ni, Sarah E. Rollauer, Istvan Botos, Xiaofeng Tan, Martin S. King, Edmund R. S. Kunji, Jiansen Jiang, and Susan K. Buchanan. 2020. 'Structural

- insight into mitochondrial  $\beta$ -barrel outer membrane protein biogenesis', *Nature Communications*, 11: 3290.
- Freitag, Helmut, Walter Neupert, and Roland Benz. 1982. 'Purification and Characterisation of a Pore Protein of the Outer Mitochondrial Membrane from *Neurospora crassa*', *Eur. J. Biochem.*, 123: 629-36.
- Galan, J. E., and H. Wolf-Watz. 2006. 'Protein delivery into eukaryotic cells by type III secretion machines', *Nature*, 444: 567-73.
- Genin, S., and C. A. Boucher. 1994. 'A superfamily of proteins involved in different secretion pathways in gram-negative bacteria: modular structure and specificity of the N-terminal domain', *Mol Gen Genet*, 243: 112-8.
- Gentle, Ian E., Lena Burri, and Trevor Lithgow. 2005. 'Molecular architecture and function of the Omp85 family of proteins', *Molecular Microbiology*, 58: 1216-25.
- Gentle, Ian, Kipros Gabriel, Peter Beech, Ross Waller, and Trevor Lithgow. 2003. 'The Omp85 family of proteins is essential for outer membrane biogenesis in mitochondria and bacteria', *Journal of Cell Biology*, 164: 19-24.
- Gietz, R. D., and R. A. Woods. 2006. 'Yeast transformation by the LiAc/SS Carrier DNA/PEG method', *Methods Mol Biol*, 313: 107-20.
- Goetze, Tom Alexander, Katrin Philippar, Irina Ilkavets, Jürgen Soll, and Richard Wagner. 2006. 'OEP37 Is a New Member of the Chloroplast Outer Membrane Ion Channels', *Journal of Biological Chemistry*, 281: 17989-98.
- Gray, Michael W. 1999. 'Evolution of organellar genomes', *Current Opinion in Genetics & Development*, 9: 678-87.
- Gray, Michael W., Gertraud Burger, and B. Franz Lang. 1999. 'Mitochondrial Evolution', *Science*, 283: 1476-81.
- Green, E. R., and J. Meccas. 2016. 'Bacterial Secretion Systems: An Overview', *Microbiol Spectr*, 4.
- Gross, Lucia E, Anna Klingler, Nicole Spies, Theresa Ernst, Nadine Flinner, Stefan Simm, Roman Ladig, Uwe Bodensohn, and Enrico Schleiff. 2021. 'Insertion of plastidic  $\beta$ -barrel proteins into the outer envelopes of plastids involves an intermembrane space intermediate formed with Toc75-V/OEP80', *The Plant Cell*, 33: 1657-81.
- Gross, Lucia E., Nicole Spies, Stefan Simm, and Enrico Schleiff. 2020. 'Toc75-V/OEP80 is processed during translocation into chloroplasts, and the membrane-embedded form exposes its POTRA domain to the intermembrane space', *FEBS OpenBio*, 10: 444-54.

- Guilvout, Ingrid, Mohamed Chami, Andreas Engel, Anthony P. Pugsley, and Nicolas Bayan. 2006. 'Bacterial outer membrane secretin PulD assembles and inserts into the inner membrane in the absence of its pilotin', *The EMBO Journal*, 25: 5241-49.
- Guilvout, Ingrid, Nicholas N. Nickerson, Mohamed Chami, and Anthony P. Pugsley. 2011. 'Multimerization-defective variants of dodecameric secretin PulD', *Research in Microbiology*, 162: 180-90.
- Habib, Shukry J., Thomas Waizenegger, Maciej Lech, Walter Neupert, and Doron Rapaport. 2005. 'Assembly of the TOB Complex of Mitochondria', *Journal of Biological Chemistry*, 280: 6434-40.
- Habib , Shukry J., Thomas Waizenegger , Agathe Niewienda , Stefan A. Paschen , Walter Neupert , and Doron Rapaport 2006. 'The N-terminal domain of Tob55 has a receptor-like function in the biogenesis of mitochondrial  $\beta$ -barrel proteins', *Journal of Cell Biology*, 176: 77-88.
- Harsman, Anke, Annette Schock, Birgit Hemmis, Vanessa Wahl, Ingrid Jeshen, Philipp Bartsch, Armin Schlereth, Heidi Pertl-Obermeyer, Tom Alexander Goetze, Jürgen Soll, Katrin Philippar, and Richard Wagner. 2016. 'OEP40, a Regulated Glucose-permeable  $\beta$ -Barrel Solute Channel in the Chloroplast Outer Envelope Membrane', *The Journal of Biological Chemistry*, 291: 17848-60.
- Hemmler, Roland, Thomas Becker, Enrico Schleiff, Bettina Bölter, Tanja Stahl, Jürgen Soll, Tom A. Götze, Simona Braams, and Richard Wagner. 2006. 'Molecular Properties of Oep21, an ATP-regulated Anion-selective Solute Channel from the Outer Chloroplast Membrane', *Journal of Biological Chemistry*, 281: 12020-29.
- Hill, Kerstin, Kirstin Model, Michael T. Ryan, Klaus Dietmeier, Falk Martin, Richard Wagner, and Nikolaus Pfanner. 1998. 'Tom40 forms the hydrophilic channel of the mitochondrial import pore for preproteins', *Nature*, 395: 516-21.
- Höhr, Alexandra I. C., Caroline Lindau, Christophe Wirth, Jian Qiu, David A. Stroud, Stephan Kutik, Bernard Guiard, Carola Hunte, Thomas Becker, Nikolaus Pfanner, and Nils Wiedemann. 2018. 'Membrane protein insertion through a mitochondrial  $\beta$ -barrel gate', *Science*, 359: eaah6834.
- Hoppins, S. C., and F. E. Nargang. 2004. 'The Tim8-Tim13 complex of *Neurospora crassa* functions in the assembly of proteins into both mitochondrial membranes', *The Journal of Biological Chemistry*, 279: 12396-405.
- Hsueh, Yi-Ching, Nadine Flinner, Lucia E. Gross, Raimund Haarmann, Oliver Mirus, Maik S. Sommer, and Enrico Schleiff. 2017. 'Chloroplast outer envelope protein P39 in

- Arabidopsis thaliana belongs to the Omp85 protein family', *Proteins: Structure, Function, and Bioinformatics*, 85: 1391-401.
- Hu, J., L. J. Worrall, C. Hong, M. Vuckovic, C. E. Atkinson, N. Caveney, Z. Yu, and N. C. J. Strynadka. 2018. 'Cryo-EM analysis of the T3S injectisome reveals the structure of the needle and open secretin', *Nature Communications*, 9: 3840.
- Johnson, T. L., J. Abendroth, W. G. Hol, and M. Sandkvist. 2006. 'Type II secretion: from structure to function', *FEMS Microbiol Lett*, 255: 175-86.
- Jores, Tobias, Anna Klinger, Lucia E. Groß, Shin Kawano, Nadine Flinner, Elke Duchardt-Ferner, Jens Wöhnert, Hubert Kalbacher, Toshiya Endo, Enrico Schleiff, and Doron Rapaport. 2016. 'Characterization of the targeting signal in mitochondrial  $\beta$ -barrel proteins', *Nature Communications*, 7: 12036.
- Jores, Tobias, Jannis Lawatscheck, Viktor Beke, Mirita Franz-Wachtel, Kaori Yunoki, Julia C. Fitzgerald, Boris Macek, Toshiya Endo, Hubert Kalbacher, Johannes Buchner, and Doron Rapaport. 2018. 'Cytosolic Hsp70 and Hsp40 chaperones enable the biogenesis of mitochondrial  $\beta$ -barrel proteins', *The Journal of Cell Biology*, 217: 3091.
- Jores, Tobias, and Doron Rapaport. 2017. 'Early stages in the biogenesis of eukaryotic  $\beta$ -barrel proteins', *FEBS Letters*, 591: 2671-81.
- Jumper, John, Richard Evans, Alexander Pritzel, Tim Green, Michael Figurnov, Olaf Ronneberger, Kathryn Tunyasuvunakool, Russ Bates, Augustin Žídek, Anna Potapenko, Alex Bridgland, Clemens Meyer, Simon A. A. Kohl, Andrew J. Ballard, Andrew Cowie, Bernardino Romera-Paredes, Stanislav Nikolov, Rishub Jain, Jonas Adler, Trevor Back, Stig Petersen, David Reiman, Ellen Clancy, Michal Zielinski, Martin Steinegger, Michalina Pacholska, Tamas Berghammer, Sebastian Bodenstern, David Silver, Oriol Vinyals, Andrew W. Senior, Koray Kavukcuoglu, Pushmeet Kohli, and Demis Hassabis. 2021. 'Highly accurate protein structure prediction with AlphaFold', *Nature*, 596: 583-89.
- Kim, Y. E., M. S. Hipp, A. Bracher, M. Hayer-Hartl, and F. U. Hartl. 2013. 'Molecular chaperone functions in protein folding and proteostasis', *Annu Rev Biochem*, 82: 323-55.
- Klinger, Anna, Victoria Gosch, Uwe Bodensohn, Roman Ladig, and Enrico Schleiff. 2019. 'The signal distinguishing between targeting of outer membrane  $\beta$ -barrel protein to plastids and mitochondria in plants', *Biochimica et Biophysica Acta (BBA) - Molecular Cell Research*, 1866: 663-72.

- Koehler, C. M., E. Jarosch, K. Tokatlidis, K. Schmid, R. J. Schweyen, and G. Schatz. 1998. 'Import of mitochondrial carriers mediated by essential proteins of the intermembrane space', *Science*, 279: 369-73.
- Koo, Jason, Lori L. Burrows, and P. Lynne Howell. 2012. 'Decoding the roles of pilotins and accessory proteins in secretin escort services', *FEMS Microbiology Letters*, 328: 1-12.
- Korotkov, K. V., M. Sandkvist, and W. G. Hol. 2012. 'The type II secretion system: biogenesis, molecular architecture and mechanism', *Nat Rev Microbiol*, 10: 336-51.
- Kozjak, V., N. Wiedemann, D. Milenkovic, C. Lohaus, H. E. Meyer, B. Guiard, C. Meisinger, and N. Pfanner. 2003. 'An essential role of Sam50 in the protein sorting and assembly machinery of the mitochondrial outer membrane', *The Journal of Biological Chemistry*, 278: 48520-3.
- Krimmer, T., D. Rapaport, M. T. Ryan, C. Meisinger, C. K. Kassenbrock, E. Blachly-Dyson, M. Forte, M. G. Douglas, W. Neupert, F. E. Nargang, and N. Pfanner. 2001. 'Biogenesis of porin of the outer mitochondrial membrane involves an import pathway via receptors and the general import pore of the TOM complex', *The Journal of Cell Biology*, 152: 289-300.
- Krishnan, S., and N. V. Prasadarao. 2012. 'Outer membrane protein A and OprF: versatile roles in Gram-negative bacterial infections', *FEBS J*, 279: 919-31.
- Kubori, Tomoko, and Hiroki Nagai. 2016. 'The Type IVB secretion system: an enigmatic chimera', *Current Opinion in Microbiology*, 29: 22-29.
- Kutik, Stephan, Diana Stojanovski, Lars Becker, Thomas Becker, Michael Meinecke, Vivien Krüger, Claudia Prinz, Chris Meisinger, Bernard Guiard, Richard Wagner, Nikolaus Pfanner, and Nils Wiedemann. 2008. 'Dissecting Membrane Insertion of Mitochondrial  $\beta$ -Barrel Proteins', *Cell*, 132: 1011-24.
- Madeira, F., M. Pearce, A. R. N. Tivey, P. Basutkar, J. Lee, O. Edbali, N. Madhusoodanan, A. Kolesnikov, and R. Lopez. 2022. 'Search and sequence analysis tools services from EMBL-EBI in 2022', *Nucleic Acids Res*, 50: W276-9.
- Michel, A. H., and B. Kornmann. 2012. 'The ERMES complex and ER-mitochondria connections', *Biochem Soc Trans*, 40: 445-50.
- Moitra, Anasuya, and Doron Rapaport. 2021. 'The Biogenesis Process of VDAC – From Early Cytosolic Events to Its Final Membrane Integration', *Frontiers in Physiology*, 12.
- Müller, J. E., D. Papic, T. Ulrich, I. Grin, M. Schütz, P. Oberhettinger, J. Tommassen, D. Linke, K. S. Dimmer, I. B. Autenrieth, and D. Rapaport. 2011. 'Mitochondria can recognize and assemble fragments of a beta-barrel structure', *Mol Biol Cell*, 22: 1638-47.

- Natarajan, J., A. Moitra, S. Zabel, N. Singh, S. Wagner, and D. Rapaport. 2019. 'Yeast can express and assemble bacterial secretins in the mitochondrial outer membrane', *Microbial Cell*, 7: 15-27.
- Natarajan, J., N. Singh, and D. Rapaport. 2019. 'Assembly and targeting of secretins in the bacterial outer membrane', *Int J Med Microbiol*, 309: 151322.
- Neupert, W., and J. M. Herrmann. 2007. 'Translocation of proteins into mitochondria', *Annu Rev Biochem*, 76: 723-49.
- Nicolaisen, K., S. Missbach, Y. C. Hsueh, F. Ertel, H. Fulgosi, M. S. Sommer, and E. Schleiff. 2015. 'The Omp85-type outer membrane protein p36 of *Arabidopsis thaliana* evolved by recent gene duplication', *J Plant Res*, 128: 317-25.
- Noinaj, Nicholas, Adam J. Kuszak, Curtis Balusek, James C. Gumbart, and Susan K. Buchanan. 2014. 'Lateral opening and exit pore formation are required for Bama function', *Structure (London, England : 1993)*, 22: 1055-62.
- Nunnari, J., and A. Suomalainen. 2012. 'Mitochondria: in sickness and in health', *Cell*, 148: 1145-59.
- Ochman, H., F. C. Soncini, F. Solomon, and E. A. Groisman. 1996. 'Identification of a pathogenicity island required for *Salmonella* survival in host cells', *Proceedings of the National Academy of Sciences of the United States of America*, 93: 7800-4.
- Papanikou, E., S. Karamanou, and A. Economou. 2007. 'Bacterial protein secretion through the translocase nanomachine', *Nat Rev Microbiol*, 5: 839-51.
- Paschen, S. A., T. Waizenegger, T. Stan, M. Preuss, M. Cyrklaff, K. Hell, D. Rapaport, and W. Neupert. 2003. 'Evolutionary conservation of biogenesis of beta-barrel membrane proteins', *Nature*, 426: 862-6.
- Paschen, Stefan A., Walter Neupert, and Doron Rapaport. 2005. 'Biogenesis of  $\beta$ -barrel membrane proteins of mitochondria', *Trends in Biochemical Sciences*, 30: 575-82.
- Pauptit, Richard A., Tilman Schirmer, Johan N. Jansonius, Arg P. Rosenbusch, Michael W. Parker, Alec D. Tucker, Demetrius Tsernoglou, Manfred S. Weiss, and Georg E. Schulz. 1991. 'A common channel-forming motif in evolutionarily distant porins', *Journal of Structural Biology*, 107: 136-45.
- Pohlmeier, K., J. Soll, R. Grimm, K. Hill, and R. Wagner. 1998. 'A high-conductance solute channel in the chloroplastic outer envelope from Pea', *Plant Cell*, 10: 1207-16.
- Qiu, J., L. S. Wenz, R. M. Zerbes, S. Oeljeklaus, M. Bohnert, D. A. Stroud, C. Wirth, L. Ellenrieder, N. Thornton, S. Kutik, S. Wiese, A. Schulze-Specking, N. Zufall, A. Chacinska, B. Guiard, C. Hunte, B. Warscheid, M. van der Laan, N. Pfanner, N.

- Wiedemann, and T. Becker. 2013. 'Coupling of mitochondrial import and export translocases by receptor-mediated supercomplex formation', *Cell*, 154: 596-608.
- Raghavan, Adithya, Tatiana Sheiko, Brett H. Graham, and William J. Craigen. 2012. 'Voltage-dependant anion channels: Novel insights into isoform function through genetic models', *Biochimica et Biophysica Acta (BBA) - Biomembranes*, 1818: 1477-85.
- Rapaport, D., and W. Neupert. 1999. 'Biogenesis of Tom40, core component of the TOM complex of mitochondria', *J Cell Biol*, 146: 321-31.
- Schleiff, E., and T. Becker. 2011. 'Common ground for protein translocation: access control for mitochondria and chloroplasts', *Nat Rev Mol Cell Biol*, 12: 48-59.
- Schleiff, E., J. R. Silvius, and G. C. Shore. 1999. 'Direct membrane insertion of voltage-dependent anion-selective channel protein catalyzed by mitochondrial Tom20', *The Journal of Cell Biology*, 145: 973-78.
- Schleiff, Enrico, Lutz Andreas Eichacker, Kerstin Eckart, Thomas Becker, Oliver Mirus, Tanja Stahl, and Jürgen Soll. 2003. 'Prediction of the plant  $\beta$ -barrel proteome: A case study of the chloroplast outer envelope', *Protein Science*, 12: 748-59.
- Shiota, T., K. Imai, J. Qiu, V. L. Hewitt, K. Tan, H. H. Shen, N. Sakiyama, Y. Fukasawa, S. Hayat, M. Kamiya, A. Elofsson, K. Tomii, P. Horton, N. Wiedemann, N. Pfanner, T. Lithgow, and T. Endo. 2015. 'Molecular architecture of the active mitochondrial protein gate', *Science*, 349: 1544-8.
- Soll, Jürgen, and Enrico Schleiff. 2004. 'Protein import into chloroplasts', *Nature Reviews Molecular Cell Biology*, 5: 198.
- Struyvé, M., M. Moons, and J. Tommassen. 1991. 'Carboxy-terminal phenylalanine is essential for the correct assembly of a bacterial outer membrane protein', *Journal of Molecular Biology*, 218: 141-8.
- Takeda, Hironori, Akihisa Tsutsumi, Tomohiro Nishizawa, Caroline Lindau, Jon V. Busto, Lena-Sophie Wenz, Lars Ellenrieder, Kenichiro Imai, Sebastian P. Straub, Waltraut Mossmann, Jian Qiu, Yu Yamamori, Kentaro Tomii, Junko Suzuki, Takeshi Murata, Satoshi Ogasawara, Osamu Nureki, Thomas Becker, Nikolaus Pfanner, Nils Wiedemann, Masahide Kikkawa, and Toshiya Endo. 2021. 'Mitochondrial sorting and assembly machinery operates by  $\beta$ -barrel switching', *Nature*, 590: 163-69.
- Tucker, Kyle, and Eunyong Park. 2019. 'Cryo-EM structure of the mitochondrial protein-import channel TOM complex at near-atomic resolution', *Nature Structural & Molecular Biology*, 26: 1158-66.

- Ulrich, Thomas, Lucia E. Gross, Maik S. Sommer, Enrico Schleiff, and Doron Rapaport. 2012. 'Chloroplast  $\beta$ -Barrel Proteins Are Assembled into the Mitochondrial Outer Membrane in a Process That Depends on the TOM and TOB Complexes', *Journal of Biological Chemistry*, 287: 27467-79.
- Ulrich, Thomas, Philipp Oberhettinger, Monika Schütz, Katharina Holzer, Anne S. Ramms, Dirk Linke, Ingo B. Autenrieth, and Doron Rapaport. 2014. 'Evolutionary Conservation in Biogenesis of  $\beta$ -Barrel Proteins Allows Mitochondria to Assemble a Functional Bacterial Trimeric Autotransporter Protein\*', *Journal of Biological Chemistry*, 289: 29457-70.
- Ulrich, Thomas, and Doron Rapaport. 2015. 'Biogenesis of beta-barrel proteins in evolutionary context', *International Journal of Medical Microbiology*, 305: 259-64.
- Varadi, M., S. Anyango, M. Deshpande, S. Nair, C. Natassia, G. Yordanova, D. Yuan, O. Stroe, G. Wood, A. Laydon, A. Židek, T. Green, K. Tunyasuvunakool, S. Petersen, J. Jumper, E. Clancy, R. Green, A. Vora, M. Lutfi, M. Figurnov, A. Cowie, N. Hobbs, P. Kohli, G. Kleywegt, E. Birney, D. Hassabis, and S. Velankar. 2022. 'AlphaFold Protein Structure Database: massively expanding the structural coverage of protein-sequence space with high-accuracy models', *Nucleic Acids Res*, 50: D439-d44.
- Vorobieva, Anastassia A., Paul White, Binyong Liang, Jim E. Horne, Asim K. Bera, Cameron M. Chow, Stacey Gerben, Sinduja Marx, Alex Kang, Alyssa Q. Stiving, Sophie R. Harvey, Dagan C. Marx, G. Nasir Khan, Karen G. Fleming, Vicki H. Wysocki, David J. Brockwell, Lukas K. Tamm, Sheena E. Radford, and David Baker. 2021. 'De novo design of transmembrane  $\beta$  barrels', *Science*, 371: eabc8182.
- Walther, Dirk M., Martine P. Bos, Doron Rapaport, and Jan Tommassen. 2010. 'The Mitochondrial Porin, VDAC, Has Retained the Ability to Be Assembled in the Bacterial Outer Membrane', *Molecular Biology and Evolution*, 27: 887-95.
- Walther, Dirk M., Drazen Papic, Martine P. Bos, Jan Tommassen, and Doron Rapaport. 2009. 'Signals in bacterial beta-barrel proteins are functional in eukaryotic cells for targeting to and assembly in mitochondria', *Proceedings of the National Academy of Sciences of the United States of America*, 106: 2531-36.
- Walther, Dirk M., Doron Rapaport, and Jan Tommassen. 2009. 'Biogenesis of beta-barrel membrane proteins in bacteria and eukaryotes: evolutionary conservation and divergence', *Cellular and Molecular Life Sciences : CMLS*, 66: 2789-804.

- Wang, Wenhe, Xudong Chen, Laixing Zhang, Jingbo Yi, Qingxi Ma, Jian Yin, Wei Zhuo, Jinke Gu, and Maojun Yang. 2020. 'Atomic structure of human TOM core complex', *Cell Discovery*, 6: 67.
- Webb, Chaille T., Michael A. Gorman, Michael Lazarou, Michael T. Ryan, and Jacqueline M. Gulbis. 2006. 'Crystal Structure of the Mitochondrial Chaperone TIM9•10 Reveals a Six-Bladed  $\alpha$ -Propeller', *Molecular Cell*, 21: 123-33.
- Weinhäupl, K., C. Lindau, A. Hessel, Y. Wang, C. Schütze, T. Jores, L. Melchionda, B. Schönfisch, H. Kalbacher, B. Bersch, D. Rapaport, M. Brennich, K. Lindorff-Larsen, N. Wiedemann, and P. Schanda. 2018. 'Structural Basis of Membrane Protein Chaperoning through the Mitochondrial Intermembrane Space', *Cell*, 175: 1365-79.e25.
- Wiedemann, N., V. Kozjak, A. Chacinska, B. Schönfisch, S. Rospert, M. T. Ryan, N. Pfanner, and C. Meisinger. 2003. 'Machinery for protein sorting and assembly in the mitochondrial outer membrane', *Nature*, 424: 565-71.
- Wiedemann, Nils, and Nikolaus Pfanner. 2017. 'Mitochondrial Machineries for Protein Import and Assembly', *Annual Review of Biochemistry*, 86: 685-714.
- Wiedemann, Nils, Kaye N. Truscott, Sylvia Pfannschmidt, Bernard Guiard, Chris Meisinger, and Nikolaus Pfanner. 2004. 'Biogenesis of the Protein Import Channel Tom40 of the Mitochondrial Outer Membrane: INTERMEMBRANE SPACE COMPONENTS ARE INVOLVED IN AN EARLY STAGE OF THE ASSEMBLY PATHWAY\*', *Journal of Biological Chemistry*, 279: 18188-94.
- Wimley, William C. 2003. 'The versatile  $\beta$ -barrel membrane protein', *Current Opinion in Structural Biology*, 13: 404-11.
- Yamano, K., Y. Yatsukawa, M. Esaki, A. E. Hobbs, R. E. Jensen, and T. Endo. 2008. 'Tom20 and Tom22 share the common signal recognition pathway in mitochondrial protein import', *The Journal of Biological Chemistry*, 283: 3799-807.
- Young, Matthew J., Denice C. Bay, Georg Hausner, and Deborah A. Court. 2007. 'The evolutionary history of mitochondrial porins', *BMC Evolutionary Biology*, 7: 31.

## Acknowledgements

Firstly, I would like to thank Prof. Dr. Doron Rapaport, for choosing me to be a part of his wonderful lab and introducing me to the intriguing world of  $\beta$ -barrel proteins. I would like to thank him for providing me with interesting projects, exciting scientific opportunities, constant motivation and invaluable supervision. I am very grateful for his unwavering support and guidance, particularly during tumultuous times and I thank him for his infinite patience with my odd working times.

Next, I would like to thank Prof. Dr. Ralf-Peter Jansen, for being my second supervisor and reviewing this thesis in spite of the tight timeline. I am also grateful to him and Prof. Dr. Andrei Lupas for being a part of my thesis advisory committee over the last 4 years and for their continuous guidance, critical inputs and sage advice. I also thank Prof. Dr. Gabriele Dodt and Prof. Dr. Samuel Wagner for kindly being in my thesis examining committee.

My gratitude to the Max Planck Society, University of Tuebingen and the Deutsche Forschungsgemeinschaft (DFG) for funding my doctoral research.

I am grateful to the IMPRS 'From Molecules to Organisms' and the Max Planck Institute of Biology, Tuebingen for providing the framework for my graduate study through enriching courses, workshops, career seminars and Deutschkurse. Heartfelt thanks to Sibylle Patheiger, Jeanette Mueller, Sarah Danes, George Deffner, Tina Peart and Susan Jones for their unending support and guidance as I navigated through all the administrative and immigration-related matters and for all the fun events they organized to keep our spirits high, especially through the pandemic years. I would like to thank the IFIB administrative staff particularly, Dr. Klaus Möschel, Claudia Heberle, Birgit Sailer and Luis Hartmann for ensuring the smooth functioning of our life at the institute.

I thank Dr. Janani Natarajan and Vitasta Tiku for their contributions to my doctoral projects. Special thanks to our collaborators in Frankfurt (Prof. Dr. Enrico Schleiff) and Tuebingen (University Proteome Center) for their contributions to the earlier projects of my tenure.

I would like to thank my amazing lab members who made the lab environment fun, supportive and productive! They were my home away from home! Firstly, I would like to thank Dr. Tobias Jores, for introducing me to all the cool techniques in the lab, and for letting me inherit his projects, materials and protocols. To Dr. Janani Natarajan, for instilling her faith in me for the secretin project and for her immense patience and guidance. To the Double Ds – Diana, for

providing me my wonderful home and her fun energy, and Daniela for her calmness and wisdom. To Moni, for always being a trailblazer. To Elena, our superwoman technician, for keeping the lab up and running, for her amazing sense of humor and for tolerating my broken Deutsch. I am particularly indebted to her for doing countless schnellpreps and mitopreps that were instrumental in the completion of my projects. To Dr. Kai Dimmer, for his immense scientific expertise, for numerous fun chats related to Marvel and for sharing my enthusiasm for movies and the latest pop culture.

To Dr. Layla Drwesh, fellow IMPRS, Mensa and Praktikum partner, yeast extractor and importer of radioactive proteins, for her enlightening scientific discussions, help with trouble shooting, sharing materials and protocols and for always being very ‘cool’. To Dr. Jialin Zhou, for being cute, for her constant encouragement, for the tequila shots and delicious snacks, and her ever-smiling visage. To Fenja Vaas, for being the backbone of the lab, for bringing her artistic magic, for ordering the most elegant cocktails always, and for saving me from embarrassing situations. To Dr. Klaudia Maruszczak, for being my first friend in the lab and dorm and for being my partying Guru, for her infectious enthusiasm and laughter, fiery spirit, and scientific brilliance. I am particularly indebted to you for your technical help, critical inputs and insightful discussions to push my doctoral project to completion. To Nitya Aravindan, for your quiet strength, chai-samosa and coffee-bruschetta chats, mind-bending TV reels, having my back in troubled times, and for being a fellow dog-lover. To Vitasta Tiku, for taking charge of lab activities, literally having my back, for your empathy and hugs, for your bibliophilia and for Todd. To Zacharias Fakihi, for being the fellow lab weekender, happy hour and fume enthusiast, for listening to my rants and for being my Deutsch ambassador. To Roza Dimogkioka, for ‘white water rafting’, literally saving my life, for being the global ‘Jimmy’ citizen, and for the memes. To Jiaxin ‘John’ Qian, for the fun Tiktoks, yeast extract queries, for being the fellow foodie and for your positive outlook.

My gratitude to all the past and present PhD reps, for your enthusiasm and dedication, and for providing a sounding board to my ideas and opinions.

To fellow IFIB graduates, especially Saira, for being my fellow night-shifter and cheerleader. To the Max Planckians, especially Minakshi, Devansh, Hadeer, Alejandra, Marco and Saskia, for the intellectual conversations and for your warmth and friendship. To Amit and Anupam, for being fierce and loyal friends. To Alexandros for being your unique self. To Xi, for being my first friend, emergency contact and for being the boss lady. To Joe, for being the

‘urlaubmeister’, salsa and coffee partner, and for your British accent. To Mikel, for being the meme lord and fun Österberger, for your wisdom and your candour. And to you all three, for being my family in Tuebingen.

My deepest thanks to my friends and family back home and all over the world for standing by me in the darkest of times. Special thanks to my Bros, Suranjana, Rinita and Divya, for your everlasting friendship and sisterhood.

Finally, I dedicate this thesis to my parents. To Maa, for being my rock and strength, and for ensuring I stand up after every fall. And to Baba, for being the wind beneath my wings, for your goodness, and pearls of wisdom, and for inspiring me to never stop learning.



# Appendix

## A.1 Author Contributions

### Author abbreviations

AM	Anasuya Moitra
VT	Vitasta Tiku
JN	Janani Natarajan
SZ	Sussanne Zabel
NS	Nidhi Singh
SW	Samuel Wagner
DR	Doron Rapaport

### Author contributions

#### Chapter 1

AM wrote the original draft, made all the figures and edited the final manuscript. DR co-wrote and edited the final manuscript.

#### Chapter 3 and 5

AM designed and performed the vast majority of the experiments, analysed the data, prepared the figures and wrote the manuscript. VT planned and performed the cloning experiments for the  $\beta$ -signal mutants. DR designed experiments, analysed the data, supervised the overall project, acquired funding and wrote the manuscript.

#### Chapter 4

AM performed experiments for the revised version of this contribution. AM analysed the whole cell extracts from the different strains expressing InvG-HA and SsaC-HA (Figure 6D and Figure 7C). AM furthermore edited the final manuscript.

JN designed and performed all the experiments, analysed the data, prepared the figures and wrote the manuscript. SZ performed the cloning and initial biochemical experiments for the secretins. NS performed the experiments to obtain bacterial cultures expressing secretins. SW supervised the bacterial project, acquired funding and edited the manuscript. DR analysed the data, supervised the overall project, acquired funding, wrote and edited the manuscript.

## A.2 Accepted publications

1. Natarajan, J., **Moitra, A.**, Zabel, S., Singh, N., Wagner, S., & Rapaport, D. (2019). Yeast can express and assemble bacterial secretins in the mitochondrial outer membrane. *Microbial Cell*, 7(1), 15–27. <https://doi.org/10.15698/mic2020.01.703>
2. **Moitra, A.**, & Rapaport, D. (2021). The Biogenesis Process of VDAC - From Early Cytosolic Events to Its Final Membrane Integration. *Frontiers in Physiology*, 12, 732742. <https://doi.org/10.3389/fphys.2021.732742>

# Yeast can express and assemble bacterial secretins in the mitochondrial outer membrane

Janani Natarajan<sup>1</sup>, Anasuya Moitra<sup>1</sup>, Sussanne Zabel<sup>1,§</sup>, Nidhi Singh<sup>2</sup>, Samuel Wagner<sup>2,3</sup> and Doron Rapaport<sup>1,\*</sup>

<sup>1</sup> Interfaculty Institute of Biochemistry, University of Tübingen, Tübingen, Germany.

<sup>2</sup> Interfaculty Institute of Microbiology and Infection Medicine (IMIT), University of Tübingen, Tübingen, Germany.

<sup>3</sup> German Center for Infection Research (DZIF), partner-site Tübingen, Tübingen, Germany.

<sup>§</sup> Current address: Center for Bioinformatics (ZBIT), University of Tübingen, Tübingen, Germany.

\* Corresponding Author:

Doron Rapaport, Interfaculty Institute of Biochemistry, University of Tübingen, Hoppe-Seyler-Str. 4, 72076 Tübingen, Germany. Tel.: 49-7071-2974184; E-mail: doron.rapaport@uni-tuebingen.de

**ABSTRACT** Secretins form large multimeric pores in the outer membrane (OM) of Gram-negative bacteria. These pores are part of type II and III secretion systems (T2SS and T3SS, respectively) and are crucial for pathogenicity. Recent structural studies indicate that secretins form a structure rich in  $\beta$ -strands. However, little is known about the mechanism by which secretins assemble into the OM. Based on the conservation of the biogenesis of  $\beta$ -barrel proteins in bacteria and mitochondria, we used yeast cells as a model system to study the assembly process of secretins. To that end, we analyzed the biogenesis of PulD (T2SS), SsaC (T3SS) and InvG (T3SS) in wild type cells or in cells mutated for known mitochondrial import and assembly factors. Our results suggest that secretins can be expressed in yeast cells, where they are enriched in the mitochondrial fraction. Interestingly, deletion of mitochondrial import receptors like Tom20 and Tom70 reduces the mitochondrial association of PulD but does not affect that of InvG. SsaC shows another dependency pattern and its membrane assembly is enhanced by the absence of Tom70 and compromised in cells lacking Tom20 or the topogenesis of outer membrane  $\beta$ -barrel proteins (TOB) complex component, Mas37. Collectively, these findings suggest that various secretins can follow different pathways to assemble into the bacterial OM.

doi: 10.15698/mic2020.01.703

Received originally: 03.05.2019;

in revised form: 31.10.2019,

Accepted 04.11.2019,

Published 19.11.2019.

**Keywords:** *InvG, mitochondria, outer membrane, protein sorting, PulD, Secretins, SsaC.*

**Abbreviations:**

*BAM* –  $\beta$ -barrel assembly machinery,

*IMS* – intermembrane space,

*OM* – outer membrane,

*PulD-FL* – full length PulD,

*PulD-T* – truncated PulD,

*T2SS* – type II secretion system,

*T3SS* – type III secretion system,

*T4P* – type IV pili,

*TOM* – translocase of the outer membrane.

## INTRODUCTION

To aid their survival, Gram-negative bacteria have developed several secretory systems that are involved in transport and secretion of substrates and toxins through their outer membrane (OM) [1, 2]. Type II and III secretion systems as well as type IV pili (T2SS, T3SS, and T4P, respectively) secrete toxins into the exoplasm (T2SS), directly into the cytosol of the host cells (T3SS), or build adhesion factors (T4P) [3-6]. These three systems consist of a massive complex spanning both the inner and outer membrane. The most conserved part among these secretion systems are the components of the OM structure, called secretins [7, 8].

Secretins form highly stable homooligomeric rings in the OM, which consist of 12-15 copies and are usually resistant against detergents, higher temperatures and dena-

turing agents [9-14]. The aforementioned ring is actually a gated pore, which is open only when required for translocation of proteins [7, 15]. All secretins consist of a highly conserved protease-resistant, membrane-embedded C-domain and a less conserved periplasmic N-terminal part composed of two to four small domains (named N<sub>0</sub> to N<sub>3</sub>) (see Fig. 1A) [10, 12]. For their correct assembly, some secretins require small chaperone-like lipoproteins, called pilotins, which help in targeting their cognate secretins to the OM and are proposed to stabilize the secretin multimer [8, 16, 17]. Accordingly, such secretins harbour at their very C-terminal region, an additional domain (S domain) that mediates the interaction with their corresponding pilotins.

PulD from *Klebsiella oxytoca*, one of the most extensively studied secretins, belongs to the T2SS subfamily and

was reported to assemble *in vivo* and *in vitro* spontaneously into membranes [18, 19]. *In vivo*, PulD is targeted to the OM by its dedicated pilotin PulS and does not need other factors for multimerization [19–22]. In *Salmonella*, secretins are part of both T3SS encoded by the pathogenicity island 1 and 2 (SPI-1 and SPI-2) [23]. InvG, the secretin encoded by SPI-1, is well studied, whereas little is known about SsaC, a secretin encoded by SPI-2. Of note, for its correct localization in the OM, InvG requires its dedicated pilotin, InvH [24]. Cryo-EM (electron microscopy) studies revealed a pore structure with a 15-fold symmetry for the secretin InvG and its ring structure showed an unexpected double walled  $\beta$ -barrel architecture [8, 25, 26].

Despite this recent progress in our understanding of the structure and function of secretins, the mechanism by which they assemble in the OM is still an enigma. Secretins are synthesized in the cytoplasm and, similarly to other OM proteins, are probably stabilized there by cytoplasmic factors. Then, they are transported through the inner membrane by the Sec translocon. The transport of secretins from the periplasm to the OM can follow different pathways like Lol-dependent, BAM ( $\beta$ -barrel assembly machinery)-dependent, unassisted, or an accessory protein-assisted pathway. It is anticipated that for secretins with known pilotin, the pilotin transport via the Lol pathway guides the secretin monomers from the periplasm to the OM [20, 21, 27].

In the case of PulD, the pilotin PulS assists the initial assembly process of the secretin by the transport of the monomer units to the OM. After this transfer, the secretin monomers form a pre-pore in a process that is independent of PulS [10, 17, 19, 20, 22, 28]. The pre-pore then inserts into the membrane in a manner that was suggested to be unassisted [29]. The only region of the protein identified so far as critical for formation of the pre-pore is the N<sub>3</sub> domain, which is just upstream of the secretin barrel domain [22].

To shed more light on the biogenesis process of PulD and other secretins, we used yeast cells as a model system. This choice of experimental system is based on our previous observations that the evolutionary conservation of the  $\beta$ -barrel assembly machineries between bacteria and yeast mitochondria allows the successful usage of yeast mitochondria as a model system to study basic features of the assembly process of bacterial  $\beta$ -barrel proteins [30–32]. In addition, assembly of secretins into native-like oligomers at the mitochondrial OM can demonstrate that specific bacterial factors are not absolutely required for this process. Our experiments suggest that secretins can indeed be successfully expressed in yeast cells and their proper membrane assembly depends to a variable extent on additional biogenesis factors.

## RESULTS

### Establishing yeast cells as a model system to study secretins biogenesis

To study the assembly and biogenesis of bacterial secretins in yeast, four secretin proteins, the full-length T2SS secre-

tin, PulD (PulD-FL), its truncated version (PulD<sub>28-42/259-660</sub>, named PulD-T; comprising primarily the N<sub>0</sub>, N<sub>3</sub>, C, and S domains), and two T3SS secretins, InvG and SsaC (both containing a C-terminally HA-tag) were selected (see Fig. 1A for a scheme of these proteins). The DNA sequences encoding these proteins were cloned into a yeast expression vector in which their expression is under the control of the inducible galactose (*GAL*) promoter. First, we investigated whether the expression of secretins affects the growth of yeast cells. To this end, we expressed all four secretins in yeast cells and the growth of the transformed cells at various temperatures and on different carbon sources was monitored. As expected, growth assessment of the transformed yeast cells under fermentable/non-inducible conditions (S-Glu) showed no growth retardation of these cells (Fig. 1B). In contrast, the transformed yeast cells grew slower on an inducible carbon source (S-Gal), conditions that favour strong expression of the bacterial secretins (Fig. 1B). Expression of InvG-HA was highly toxic, expression of PulD and its truncated variant were moderately inhibitory, while expression of SsaC-HA had only a minor effect on the growth of the yeast cells.

To avoid very high expression levels of the secretins and thus to counteract potential toxic effects, the cells were grown with galactose together with 0.1% of glucose, which represses the *GAL* promoter (S-Gal + 0.1% Glu). Under these conditions, the expression of none of the secretin proteins resulted in slower growth of the cells (Fig. 1B). To verify that the lack of an inhibitory effect under these conditions did not result from deficiency of secretins expression, the cells were grown in liquid culture supplemented with Gal + 0.1% Glu for few hours and then lysed to test expression. We observed expression of all secretin proteins under these conditions, whereas, as expected for a repressor, growth on glucose alone (S-Glu) did not result in any detection of the proteins (Fig. 1C). The absence of toxic effects combined with reasonable expression levels lead us to use these conditions (S-Gal + 0.1% Glu) for all further experiments.

### Secretins can assemble in yeast mitochondria

To study the sub-cellular localization of the secretins in the transformed yeast cells, subcellular fractionation was performed. The results revealed that, similar to the mitochondrial marker proteins (Tom20, Fis1, or Tom70) PulD-FL, PulD-T and SsaC were located mainly in the mitochondrial fraction. In contrast, InvG was enriched in the ER fraction (Fig. 2A). The purity of the mitochondrial fraction was confirmed by the absence of a noteworthy signal for ER (Sec61 or Erv2) and cytosolic (Hexokinase or Bmh1) marker proteins in these samples (Fig. 2A). It has been reported that PulD oligomers are heat- and SDS-resistant [10]. Indeed, we observed that also in our system PulD proteins expressed in yeast are heat and SDS-resistant and they have to be boiled in 8 M urea in Laemmli buffer in order to dissociate their oligomers before analysis by SDS-PAGE (data not shown).

Since the ER/microsomes fraction was isolated by high speed centrifugation, it is possible that this fraction contained also aggregated material. This might explain the residual amounts of PulD-FL, PulD-T and SsaC in this fraction. Notably, in contrast to the other three constructs, although SsaC was clearly enriched in the mitochondrial fraction, a certain amount was also found in the cytosolic fraction suggesting that not all SsaC molecules were assembled into cellular membranes.

It has been previously reported that PulD and InvG form oligomers consisting of 12 and 15 copies, respectively [12, 13]. To investigate whether PulD and its truncated variant expressed in yeast cells had the ability to form native-like oligomers, we solubilized the mitochondrial fraction with various detergents and analysed oligomeric structures by blue native (BN)-PAGE. Of note, both PulD-FL and even more so PulD-T were detected in oligomeric structures (Fig. 2B). The size of the observed oligomer corresponds to what has been previously reported in bacterial membranes [22]. The presence of oligomers of the truncated version indicates that the N-terminal region does not play an important role in the oligomerization of PulD.

Remarkably, the migration of the InvG oligomer from either ER or mitochondria fraction was similar to that of InvG in bacterial membranes (Fig. 2C), supporting a native-like oligomerization of this secretin. Of note, although the steady state levels of InvG in the microsomes fraction were higher than those in mitochondria (Fig. 2A), the latter fraction contained more native-like oligomers (Fig. 2C). This observation supports our assumption that, at least, part of the apparent signal in the ER fraction actually represents aggregated material. Interestingly, SsaC did not form oligomers that could be detected by BN-PAGE (data not shown). The absence of detected oligomeric pore structures might explain why higher levels of this secretin were not toxic for yeast cells (Fig. 1B).

Next, we aimed to test whether the secretins were indeed inserted into a mitochondrial membrane or were only associated with the organelle. To that goal, isolated mitochondria harbouring the various secretins were subjected to alkaline extraction. PulD-FL, PulD-T and InvG were found solely in the pellet fraction together with other membrane-embedded mitochondrial proteins like Tom20 (Fig. 3A). In contrast, SsaC was present in both the pellet (like membrane-embedded proteins) and in the supernatant fraction (similarly to the soluble protein Hep1; Fig. 3A). These findings indicate that PulD-FL, PulD-T and InvG are fully embedded within mitochondrial membranes whereas SsaC is only partially membrane-embedded.

To investigate into which of the mitochondrial membranes the secretins were integrated, mitochondria con-

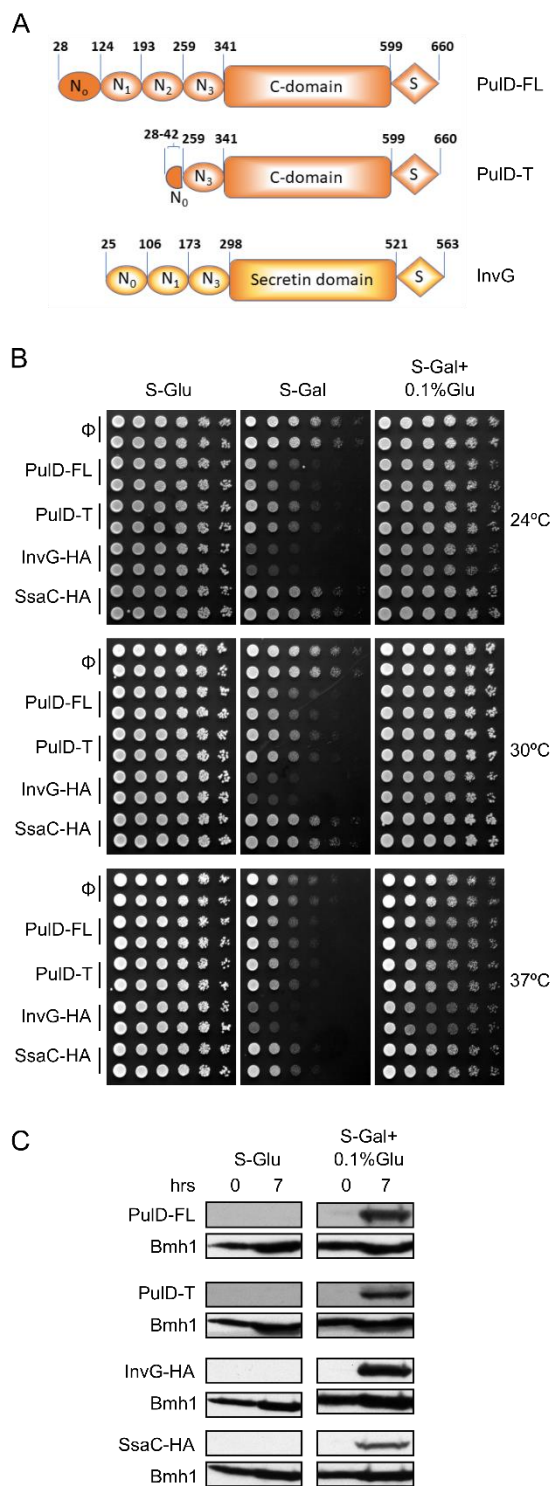


**FIGURE 1: Moderate expression of secretins is not toxic to yeast cells.** (A) Schematic representation of the PulD and InvG constructs used in this study. The numbering of the amino acid residues starts at the start codon and includes the processed signal sequence. Currently, there is no information on the various domains of SsaC. (B) Wild type yeast cells were transformed with a plasmid encoding the indicated bacterial secretins under the control of the inducible *GAL* promoter. Cells were grown in synthetic glucose-containing (S-Glu) medium to an OD<sub>600</sub> of 1.0 and spotted in a 1:5 dilution series on synthetic medium plates containing Glucose (S-Glu), Galactose (S-Gal), or Galactose + 0.1% Glucose (SGal + 0.1% Glu). Plates were then incubated at the indicated temperatures. Two colonies for each strain were analysed. (C) Wild type yeast cells transformed with a plasmid encoding the indicated secretins were grown in the indicated liquid media until logarithmic phase and then lysed. The cell lysates were analysed by SDS-PAGE and immunodecoration with antibodies against PulD or the HA-tag. The cytosolic protein Bmh1 was used as a loading control.

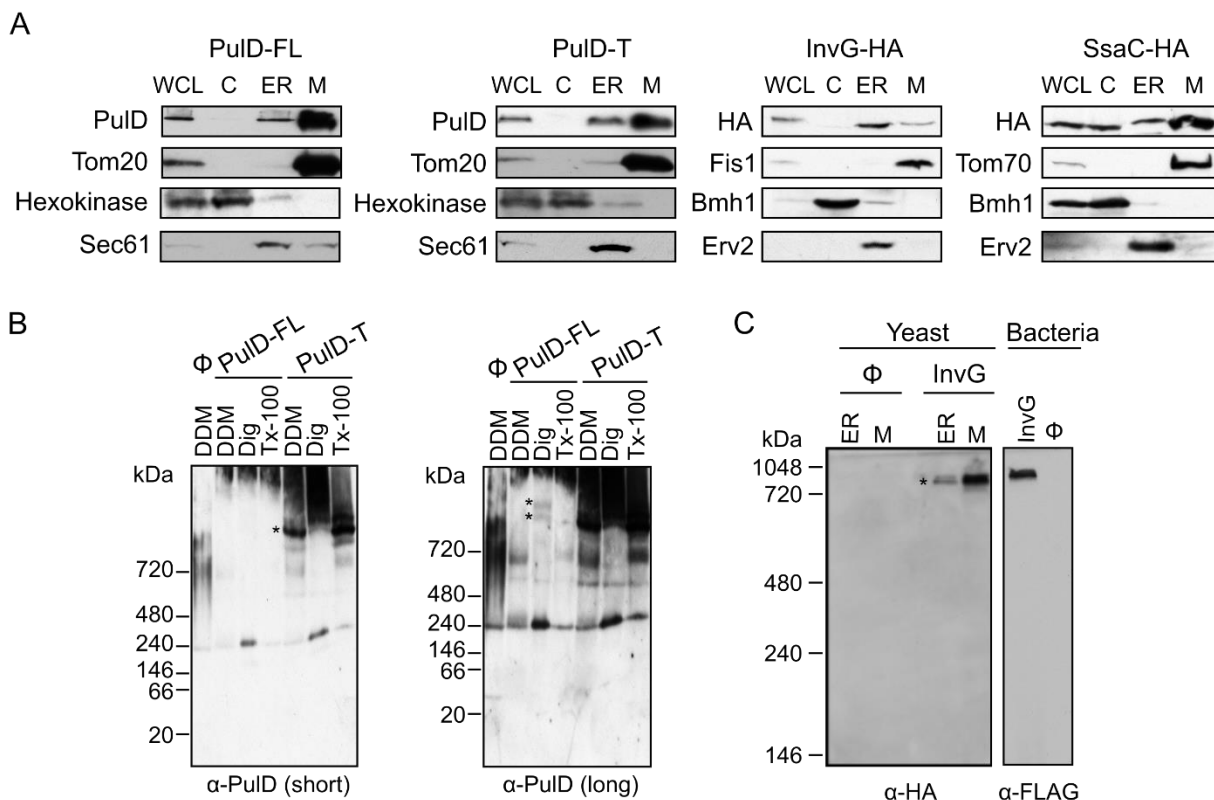


**FIGURE 2: Bacterial secretins are targeted within yeast cells mainly to mitochondria and form native-like complexes. (A)** Whole cell lysate (WCL) and fractions corresponding to cytosol (C), light microsomes (ER) and mitochondria (M) were obtained from wild type yeast cells transformed with a plasmid encoding the indicated secretin. Samples were analysed by SDS-PAGE and immunodecoration with antibodies against PuID, HA tag, and the marker proteins Tom20, Tom70 or Fis1 for the mitochondrial fraction, Bmh1 or Hexokinase for the cytosol, and Erv2 or Sec61 for the microsomal/ER fraction. **(B)** Mitochondria were isolated from wild type yeast cells transformed with the indicated PuID variant. The isolated organelles were solubilized with 1% digitonin, 1% DDM, or 0.5% Triton X-100 and analysed on a 6-13% BN-PAGE followed by immunodecoration with antibodies against PuID. Short and long exposures are presented. High molecular weight oligomers are indicated by asterisks. **(C)** Microsomal (ER) or mitochondria (M) fraction isolated from wild type cells transformed with an empty plasmid ( $\emptyset$ ) or a plasmid encoding HA-tagged InvG were lysed with 1% DDM and further analysed as described in part (B). Membranes of bacterial cells transformed with an empty plasmid ( $\emptyset$ ) or a plasmid encoding FLAG-tagged InvG were treated and analysed in parallel in the same way. High molecular weight oligomers are indicated by asterisks.

taining the bacterial secretins were treated with increasing amounts of externally added proteinase K (PK). Loss of signal was observed for all secretins, similar to the surface exposed Tom20. As expected, matrix proteins like Aco1 or Hep1 were resistant to the protease treatment indicating the intactness of the organelle (Fig. 3B). Collectively, these results indicate that the secretins are embedded in the mitochondrial OM and are exposed to the cytosol.

**Factors involved in the assembly of secretins into the mitochondrial OM**

The factors required for assembly of secretins in the bacterial OM are mostly unknown. Moreover, basically nothing is known about the biogenesis of SsaC. Using yeast as a model system, we investigated whether known mitochondrial import factors might be involved in the transport and/or assembly of the bacterial secretins into the OM. To this end, we monitored the steady state levels of the vari-

ous secretins upon their expression in yeast cells lacking one or more mitochondrial import components.

Mitochondrial  $\beta$ -barrel proteins are assembled into the mitochondrial OM by the coordinated action of the translocase of the outer (mitochondrial) membrane (TOM) and topogenesis of mitochondrial outer membrane  $\beta$ -barrel proteins (TOB) complexes, the latter also known as the sorting and assembly machinery (SAM) complex. To investigate whether the TOM complex plays a role in the assembly of PuID-FL in the mitochondrial membrane, we expressed the secretin in yeast cells deleted for either *TOM20* or *TOM70* and its paralogue *TOM71*. Tom71 can partially complement the loss of Tom70 [33]. Hence, to avoid any compensatory effects by Tom71, the double deletion strain *tom70/71* $\Delta$  was used for the analysis [34].

The absence of either Tom70/71 or Tom20 resulted in significantly lower amounts of PuID-FL in isolated mitochondria in comparison to its levels in wild type organelles (Fig. 4A). The dependency on the TOM receptor compo-



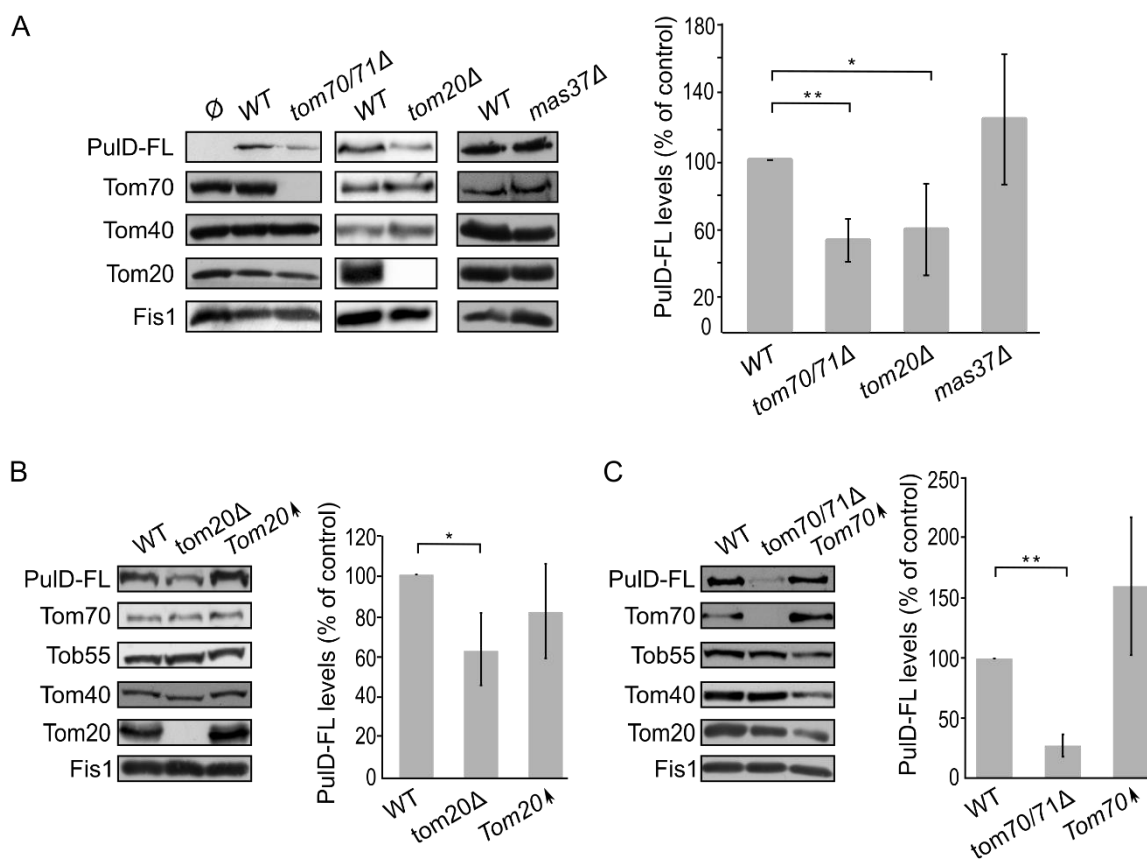


**FIGURE 4: The assembly of PuID-FL in mitochondria depends on import receptors. (A) Left panel:** Isolated mitochondria were obtained from the indicated strains transformed with either an empty vector ( $\emptyset$ ) or a plasmid encoding PuID-FL. Samples were analysed by SDS-PAGE and immunodecoration with the indicated antibodies. **Right panel:** the steady state levels of PuID-FL in at least three experiments as in the left panel were quantified. The signal of Fis1 was taken as a loading control. Levels of PuID-FL in the corresponding wild type (WT) cells were set to 100%. The bar diagram shows the mean values  $\pm$  s.d. of at least three independent experiments. (\*,  $P < 0.05$ ; \*\*,  $P < 0.01$ ; two tailed Student's t-test). **(B) Left panel:** Crude mitochondria were obtained from WT, *tom20Δ*, or a strain overexpressing *TOM20* (*Tom20* $\uparrow$ ) harbouring a plasmid expressing PuID-FL. Samples were analysed by SDS-PAGE and immunodecoration with the indicated antibodies. **Right panel:** the steady state levels of the PuID-FL secretin were quantified and further analysed as described for part (A). (\*,  $P < 0.05$ ; two-tailed Student's t-test). **(C)** Crude mitochondria were obtained from WT, *tom70/71Δ*, or a strain overexpressing *TOM70* (*Tom70* $\uparrow$ ) harbouring a plasmid expressing PuID-FL. Further treatment and analysis were as described in the legend of part (B).

of PuID-T were even moderately, but significantly, elevated when PuID-T was expressed in *tom20Δ* cells (Fig. 5A). In contrast, PuID-T expression in *mas37Δ* cells did not lead to a significant difference in the steady state levels of the secretin (Fig. 5A).

The observed elevated mitochondrial amounts of PuID-T in the absence of Tom20 might suggest that Tom20 has a negative effect on the biogenesis of this variant. To test this point, we expressed PuID-T in yeast cells, which either lack or overexpress *TOM20*, and compared the mitochondrial levels in the mutated cells to those in the control cells. Western blotting analysis verified that indeed the steady state levels of PuID-T in the crude mitochondria fraction were enhanced upon the absence of Tom20. However, overexpression of Tom20 did not change the detected amounts of PuID-T (Fig. 5B). In contrast to the effect of Tom20, the absence or the overexpression of Tom70 did not affect the levels of PuID-T (Fig. 5C). Collectively, Tom20

seems to be involved in the assembly of PuID-FL and PuID-T secretin in different ways. Whereas the former protein requires Tom20 for optimal biogenesis, the absence of the N-terminal domain removes this dependency and even reverses it. This difference might suggest an important role of the N-terminal region in regulation of the assembly of PuID.

#### Assembly of the T3SS secretins InvG and SsaC in yeast mitochondria

Next, we expanded our analysis to the secretins of T3SS. To that end, we investigated the effect of the TOM complex on the assembly of InvG by expressing the protein in either *tom70/71Δ* or *tom20Δ* yeast strains. Our results revealed that there was no significant change in the steady state levels of InvG in mitochondria isolated from *tom70/71Δ* cells in comparison to the amounts in control organelles (Fig. 6A). In contrast, significantly elevated amounts of

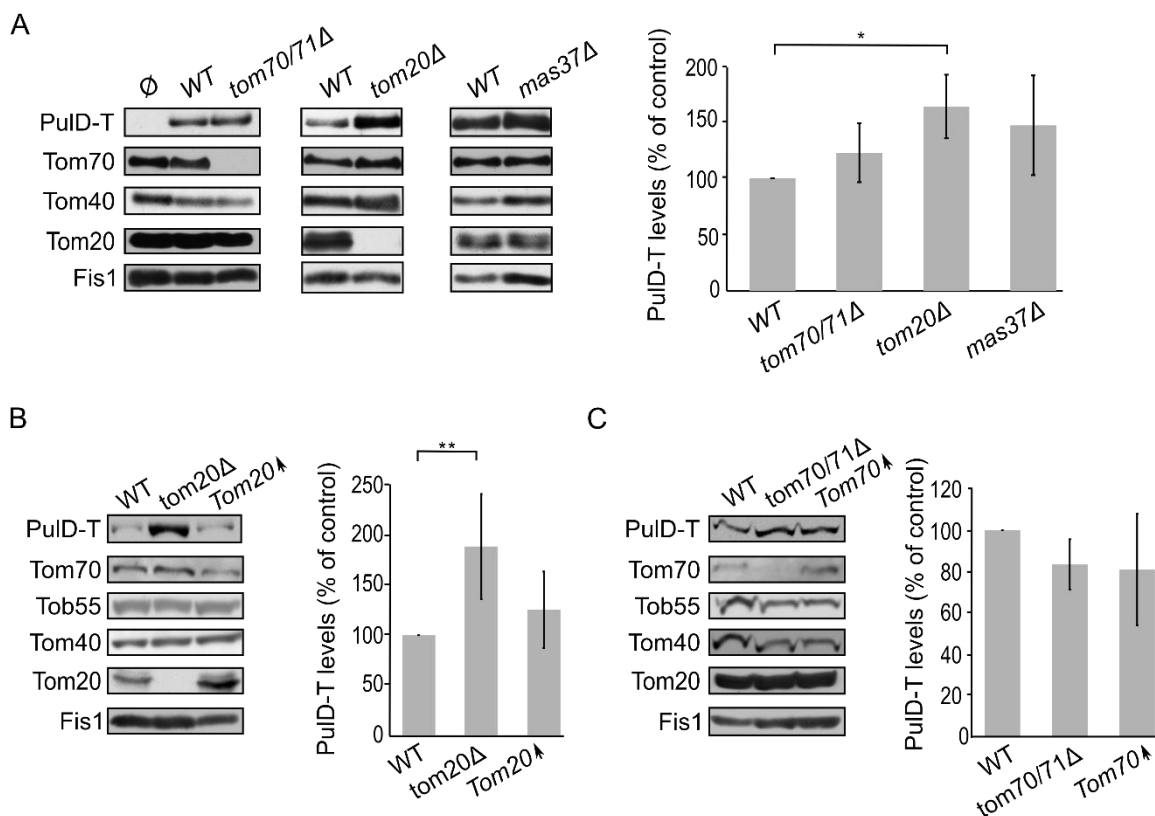


**FIGURE 5: The assembly of PuID-T in mitochondria is enhanced in the absence of Tom20. (A)** Mitochondria were isolated from the indicated strains transformed with either an empty vector ( $\emptyset$ ) or a plasmid encoding PuID-T. Further treatment and analysis were as described in the legend of Fig. 4A. **(B)** Crude mitochondria were obtained from wild type (WT), *tom20Δ* or a strain overexpressing *TOM20* (Tom20↑) harbouring a plasmid encoding PuID-T. Further treatment and analysis were as described in the legend of Fig. 4B. **(C)** Crude mitochondria were obtained from WT, *tom70/71Δ* or a strain overexpressing *TOM70* (Tom70↑) harbouring a plasmid encoding PuID-T. Further treatment and analysis were as described in the legend of Fig. 4B.

InvG were observed in mitochondria isolated from *tom20Δ* cells (Fig. 6A). We next asked whether the TOB is involved in InvG assembly. However, expression of InvG in cells lacking Mas37 did not result in any significant changes in the steady state levels of InvG (Fig. 6A). These results are in line with previous observations that the BAM complex does not play a role in the assembly of this secretin [27].

Next, we wanted to better understand the involvement of Tom20 in the assembly of InvG. Thus, we expressed InvG in cells overexpressing *TOM20* (or lacking it, for comparison) and monitored the steady state levels in crude mitochondria isolated from these cells. Interestingly, the mitochondrial amounts of InvG were reduced when *TOM20* was overexpressed, while the deletion of *TOM20* resulted in elevated mitochondrial levels in comparison to the corresponding wild type cells (Fig. 6A and B). When we then checked in a similar way the effect of Tom70 on the biogenesis of InvG, we observed no significant changes in the amount of InvG in the crude mitochondria from cells with altered expression of Tom70 (Fig. 6C). These results point to a specific effect of Tom20 on the biogenesis of InvG. To test whether the import components affect the total cellular levels of InvG, we analysed the steady-state amounts of

the protein in whole cell lysates. Whereas we could not detect significant alterations upon changes in the levels of either Tom70/71 or Mas37, cells lacking Tom20 had overall reduced levels of InvG (Fig. 6D). In line with the latter observation, overexpression of Tom20 resulted in slightly higher cellular amounts of InvG (Fig. 6D). Hence, it seems that although the presence of Tom20 improves the overall stability of InvG, it does not have a positive effect on the assembly of InvG into the mitochondrial OM.

Finally, we turned to investigate the biogenesis of SsaC, a secretin whose targeting and assembly pathways were not studied so far. SsaC was expressed in *tom70/71Δ*, *tom20Δ*, or *mas37Δ* yeast cells and the steady state levels in isolated mitochondria were monitored. Interestingly, the absence of Tom70/71 resulted in a two-fold increase in the levels of SsaC whereas deletion of *TOM20* or *MAS37* led to a reduction in the levels of this secretin (Fig. 7A). The reduction upon deletion of *MAS37* points to a requirement of the TOB complex in the biogenesis of SsaC in yeast cells, which could be extrapolated to a probable dependence on the BAM complex in bacteria.

The elevated levels of SsaC upon deletion of *TOM70/71* led us to check whether this increase was due to an unfa-

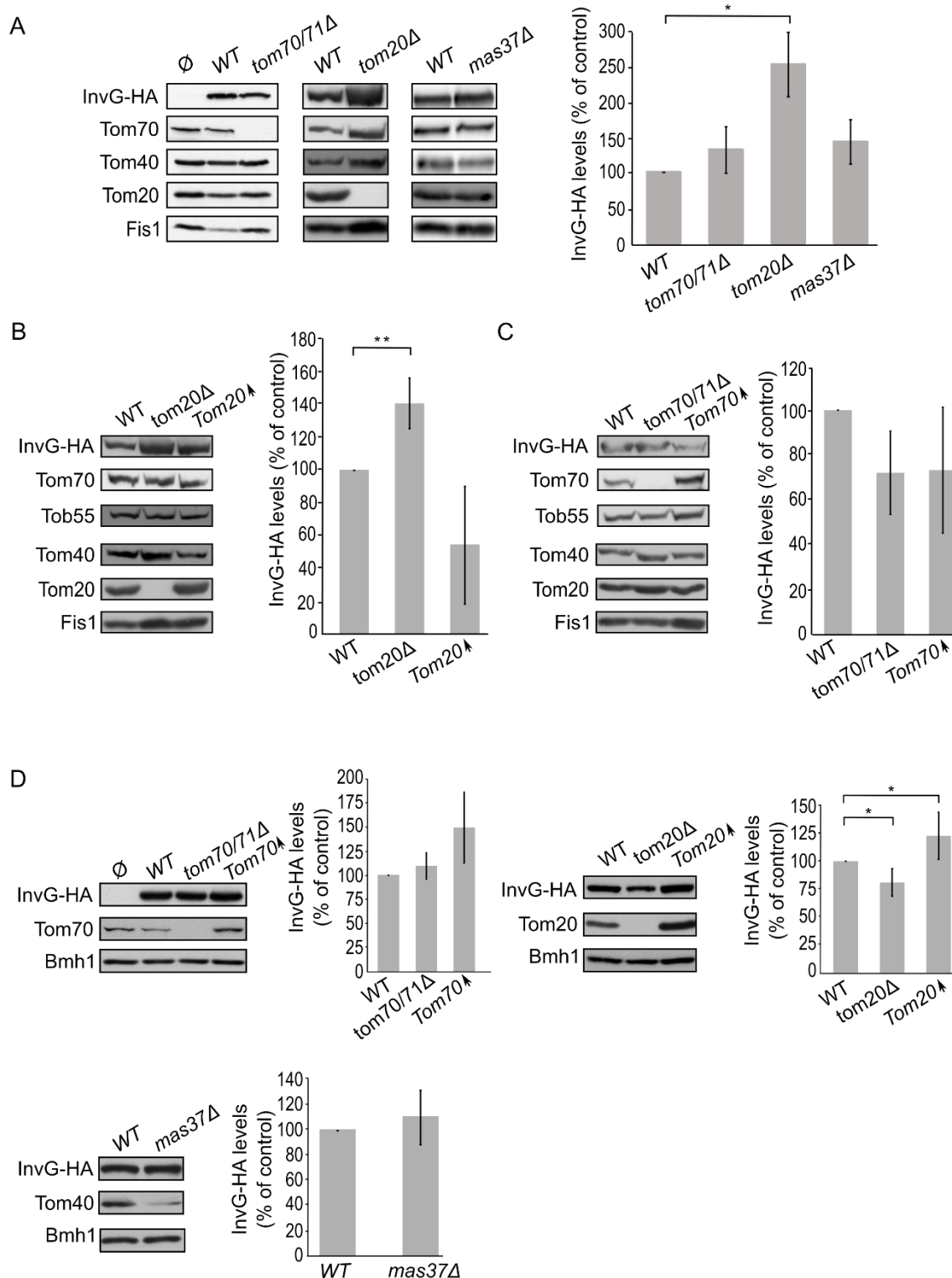


**Figure 6. Improved assembly of InvG in mitochondria lacking Tom20. (A)** Mitochondria were isolated from the indicated strains transformed with either an empty vector ( $\emptyset$ ) or a plasmid encoding InvG-HA. Further treatment and analysis were done as described in the legend of Fig. 4A. **(B)** Crude mitochondria were obtained from wild type (WT), *tom20Δ* or a strain overexpressing *TOM20* (Tom20 $\uparrow$ ) harbouring a plasmid encoding InvG-HA. Further treatment and analysis were as described in the legend of Fig. 4B. **(C)** Crude mitochondria were obtained from WT, *tom70/71Δ* or a strain overexpressing *TOM70* (Tom70 $\uparrow$ ) harbouring a plasmid encoding InvG-HA. Further treatment and analysis were done as described in the legend of Fig. 4B. **(D)** Whole cell lysate was obtained from the indicated cells and was analysed by SDS-PAGE followed by immunodecoration with antibodies against the indicated proteins. The steady state levels of InvG-HA in at least three experiments for each strain were quantified. The signal of Bmh1 was taken as a loading control. Levels of InvG-HA in the corresponding wild type cells were set to 100%. The bar diagram shows the mean values  $\pm$  s.d. of at least three independent experiments. (\*,  $P < 0.05$ ; two tailed Student's t-test).

avourable involvement of Tom70. To that aim, we expressed SsaC in cells either lacking or overexpressing Tom70. Indeed, we could observe that there was a significant decrease in the amounts of SsaC in crude mitochondria isolated from cells overexpressing Tom70 in comparison to control organelles. Along the same line, we detected a significant increase in the SsaC levels in mitochondria lacking Tom70 (Fig. 7A and B). To verify that the changes in the levels of SsaC upon manipulating the Tom70/71 amounts is not the outcome of variations in the overall cellular amounts, we monitored the levels of SsaC in whole cell extracts. We observed that deletion of *TOM70/71* indeed resulted in moderately, but significantly, higher amounts of cellular SsaC (Fig. 7C), suggesting that the absence of these import receptors increases the life-span of this secretin. In contrast, altered amounts of Tom20 or Mas37 did not affect the overall cellular levels of SsaC (Fig. 7C). Taken together, these findings lead us to conclude that Tom70 inhibits, directly or indirectly, the mitochondrial assembly of SsaC.

## DISCUSSION

Secretins are homo-oligomers present in bacterial secretion systems that form pores in the bacterial OM. The assembly of secretins in their target membrane is most probably a species-specific process. The exact mechanism of membrane insertion of the assembled oligomers and/or factors that assist the unassembled monomers to oligomerize and then insert correctly into the bacterial OM is still unknown.

In this study, we established yeast cells as a model system to study the biogenesis of bacterial secretins. Even though *in vitro* systems based on artificial membranes have explored partially the requirements for secretin multimerization and insertion into membranes [18, 28], mitochondria, due to their evolutionary relation to bacteria, may provide an improved model system [30]. We could show that all four tested secretins could be expressed in yeast and were enriched in the mitochondrial fraction. In the case of InvG, the subcellular fractionation indicates enrichment of the secretin also in the microsomal fraction where it can form native-like oligomers. Thus, it seems that InvG can oligomerize and insert spontaneously into different membrane types.

PuID-FL, PuID-T and InvG formed oligomers in the mitochondrial membrane. For InvG, we could demonstrate that these oligomers behave like the InvG oligomers in bacteria, indicating a native-like structure and supporting the validity of the mitochondrial system. It has been reported that the PuID pore allows efflux of small molecules [7]. Thus, the presence of pore-forming native-like oligomers of PuID and InvG in mitochondrial membranes might explain their negative effect on the growth of yeast cells expressing them. Along this line, SsaC that appears to remain monomeric in yeast cells is not toxic when expressed in yeast. The exact mechanism for the oligomerization initiation of SsaC is unknown and it might be that a crucial assembly factor is missing in the yeast system. Similar to what has

been reported for bacterial cells [10], we also observed that oligomers of PuID expressed in yeast are heat and SDS-resistant. This similarity further supports the native-like structure of the secretin oligomers upon their expression in yeast cells.

In bacteria, PuID and InvG require pilotins; the lipoprotein chaperones PuIS and InvH, respectively, that mediate correct localization of the secretins to the OM and protection against proteolysis [16]. In our system, we observe that PuID and InvG can assemble in the mitochondrial OM despite the absence of their cognate pilotins. Thus, we conclude that pilotins are not absolutely required for targeting and membrane integration.

The biogenesis of secretin proteins in the mitochondrial OM can follow two distinct pathways: (1) After their synthesis in the cytosol, the secretin monomers are translocated across the mitochondrial OM into the intermembrane space (IMS) by the TOM complex and are then inserted from the internal surface of the OM by either self-assembly or with the help of the TOB complex. (2) Upon synthesis in the cytosol, the secretin monomers assemble on the outside of the mitochondrial surface before integrating into the mitochondrial OM from the cytosolic side. The sensitivity to an externally added protease and our observations that no protease-resistant intermediates were formed in the mitochondrial IMS indicate that all four secretins, after synthesis and oligomerization, insert into the mitochondrial OM from the mitochondrial surface with the bulk facing the cytosol. This is in contrast to native PuID dodecamers consisting of a protease-resistant core (C domain) including the outer chamber, the central disc, and the plug [10, 12]. These differences might be explained by the fact that in bacterial cells the secretins are synthesized in the cytoplasm and cross the inner membrane before their assembly from the periplasm into the OM, whereas in yeast cells they are synthesized on cytosolic ribosomes and can directly assemble from this compartment onto the mitochondrial OM.

The insertion of bacterial secretins into the OM is still an enigma. To study potential dependence on accessory proteins, secretins were expressed in yeast cells deleted for specific import factors. Both variants, PuID-FL and PuID-T seem to be unaffected by the TOB complex, the yeast homolog of the bacterial BAM complex. This is in line with previous observations that T2SS secretins do not need the BAM complex for their assembly [27]. However, the absence of import components of the TOM complex, another central assembly factor in yeast mitochondria, resulted in different behaviour of PuID-FL and PuID-T. The former requires both Tom70 and Tom20 for its assembly in the mitochondrial OM whereas PuID-T assembles even more efficiently in the absence of Tom20. Since the only difference between the two secretins is their N-terminal domain, we hypothesize that this domain plays a role in the assembly of the secretin in the OM.

A differential dependence on import factors was observed also for the T3SS secretins, InvG and SsaC. InvG does not require Tom20 for its assembly whereas SsaC

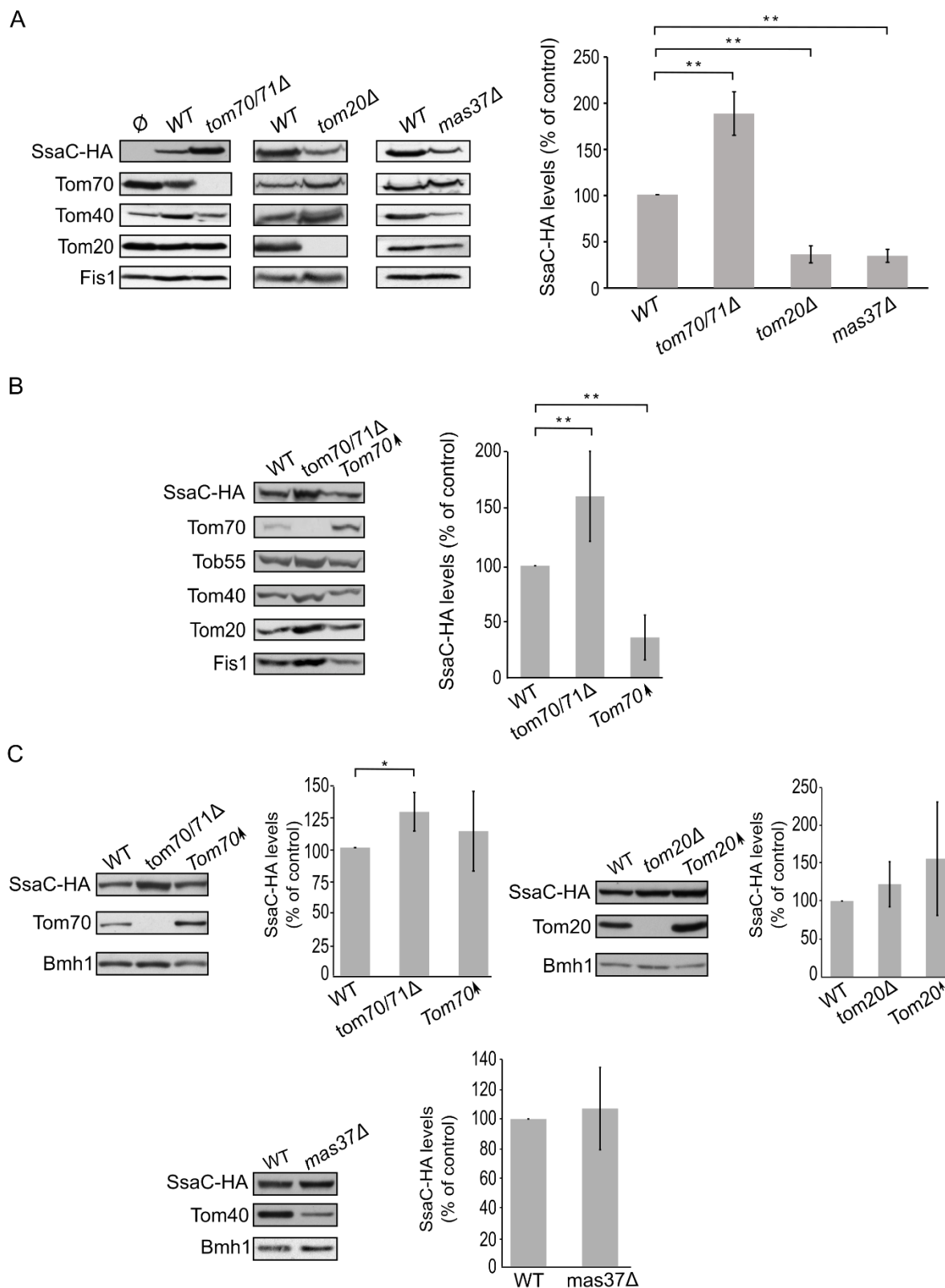


**FIGURE 7: Lack of Tom70 improves the biogenesis of SsaC in mitochondria. (A)** Isolated mitochondria were obtained from the indicated strains transformed with either an empty vector ( $\emptyset$ ) or a plasmid encoding SsaC-HA. Further treatment and analysis were done as described in the legend of Fig. 4A. **(B)** Crude mitochondria were obtained from wild type (WT), *tom70/71Δ* or a strain overexpressing *TOM70* (Tom70↑) harbouring a plasmid encoding SsaC-HA. Further treatment and analysis were done as described in the legend of Fig. 4B. **(C)** Whole cell lysate was obtained from the indicated cells and was analysed by SDS-PAGE followed by immunodecoration with antibodies against the indicated proteins. The steady state levels of SsaC-HA in at least three experiments for each strain were quantified and further analysis was as described in the legend of Fig. 6D. (\*,  $P < 0.05$ ; two tailed Student's t-test).

requires Tom20 and Mas37, a subunit of the TOB complex. SsaC also assembles more efficiently in the absence of Tom70. SsaC is the only bacterial secretin that we observed to be influenced by the TOB complex. Since TOB complex is the equivalent of the bacterial BAM complex, we propose that the BAM complex is probably involved in the membrane assembly of SsaC.

Collectively, our findings indicate that the secretins require different factors for assembly into mitochondrial OM. This variable dependency might be extrapolated to the bacterial system and suggests that different secretins might follow different pathways and interact with various assembly factors. Future studies will shed light onto these fascinating processes.

## MATERIALS AND METHODS

### Yeast strains and growth conditions

Standard genetic techniques were used for growth and manipulation of yeast strains. In this study, the wild-type yeast *S. cerevisiae* strains, JSY7452, YPH499 and W303 were utilized. The *tom20Δ* and *mas37Δ* strains were described before ([31, 35], respectively). The *tom70/71Δ* double-deletion strain was a kind gift of Dr. Okamoto [34]. See **Table 1** for a list of the yeast strains used in this study. Unless otherwise specified, cells were grown on synthetic depleted (S) medium (0.67% [w/v] bacto-yeast nitrogen base without amino acids) containing galactose (2%, [w/v], Gal), galactose + glucose (2% + 0.1%, [w/v], Gal + 0.1% Glu), or glucose (2%, [w/v], Glu) as carbon source. Transformation of yeast cells was performed by the lithium acetate method [36]. For drop-dilution assay, cells were grown on S-Glu-Ura media to an OD<sub>600</sub> of 1.0. The cells were then diluted serially in fivefold increments followed by spotting 5 μl of the diluted cells on solid media and further growth at the indicated temperatures.

### Recombinant DNA techniques

Plasmids encoding full-length and truncated PulD were kind gifts from Dr. Anthony Pugsley. All four secretin constructs were PCR amplified and the PCR products were inserted into the yeast expression vector pYX113 or pYX143. For PulD, the predicted signal sequence was removed. The PulD secretin was cloned as two variants, full length (PulD-FL) and truncated version (PulD<sub>28-42/259-660</sub>; PulD-T). Both variants were cloned into BamHI/NheI restriction site. The HA-tagged versions of InvG and SsaC were cloned using BamHI/XmaI restriction sites.

### Biochemical methods

Protein samples for immunodecoration were analysed on 8, 10, 12.5, or 15% SDS-PAGE and subsequently transferred onto nitrocellulose membranes by semi-dry western blotting. Proteins were detected by incubating the membranes first with primary antibodies and then with either horseradish peroxidase-coupled goat anti-rabbit, goat anti-mouse or goat anti-rat secondary antibodies. Due to the unusual stability of the PulD oligomers, the PulD samples were always treated with 2x Laemmli buffer containing 8 M urea, boiled for 10 min at 95°C, and analysed then by SDS-PAGE and immunoblotting.

Sub-cellular fractionation of yeast cells was performed as described before [32]. Isolation of mitochondria from yeast cells was performed by differential centrifugation, as previously described [37]. For the protease protection assay, 50 μg of mitochondria were resuspended in 100 μl of SEM buffer (250 mM sucrose, 1 mM EDTA, 10 mM MOPS, pH 7.2). As a control, mitochondria were treated with 1% Triton X-100 in SEM buffer and incubated on ice for 30 min. The samples were treated with Proteinase K (PK) at various concentrations on ice for 30 min. The proteolytic reaction was stopped with 5 mM Phenylmethylsulfonyl fluoride (PMSF). The samples were then precipitated with trichloroacetic acid (TCA) and resuspended in 40 μl of 2x Laemmli buffer, boiled for 10 min at 95°C, and analyzed by SDS-PAGE and immunoblotting.

To analyse whether proteins are membrane-embedded, alkaline extraction was performed. Mitochondria (50 μg) were resuspended in 100 μl of buffer containing 10 mM HEPES-KOH, 100 mM Na<sub>2</sub>CO<sub>3</sub>, pH 11.5 and incubated for 30 min on ice. The membrane fraction was pelleted by centrifugation (76000xg, 30 min, 2°C) and the supernatant fraction was precipitated with TCA. Both fractions were analyzed by SDS-PAGE and immunoblotting.

Assembly of native complexes was analyzed by BN-PAGE. Isolated mitochondria, microsomes, or bacterial membranes were solubilised with detergent-containing buffer (1% DDM, 1% digitonin, or 0.5% TritonX-100 in 20 mM Tris, 0.1 mM EDTA, 50 mM NaCl, 10% glycerol, pH 7.4) for 30 min at 4°C on an overhead shaker. After a clarifying spin (30,000xg, 15 min, 2°C), 10x sample buffer (5% [w/v] Coomassie brilliant blue G-250, 100 mM Bis-Tris, 500 mM 6-aminocaproic acid, pH 7.0) was added and the mixture was analysed by BN-PAGE containing either a 6–14% or 8–13% gradient of acrylamide [38]. Gels were analysed further by western blotting. The mixture Native Mark Unstained Protein Standard (Thermo Scientific) was used to monitor the migration of molecular weight marker proteins.

**TABLE 1: List of yeast strains used in this study.**

Name	Mating type	Genetic background	Reference
W303α	MATα	<i>ade2-1 can1-100 his3-11 leu2 3_112 trp1Δ2 ura3-52</i>	
JSY7452	MATα	<i>ade2-1 can1-100 his3-11,15 leu2-3 trp1-1 ura3-1</i>	[34]
YPH499	MATα	<i>ura3-52 lys2-801_amber ade2-101_ochre trp1-Δ63 his3-Δ200 leu2-Δ1</i>	
<i>tom20Δ</i>	MATα	W303α; <i>tom20Δ::HIS3</i>	[31]
<i>tom70/71Δ</i>	MATα	JSY7452; <i>tom70Δ::TRP1 tom71Δ::HIS3</i>	[34]
<i>mas37Δ</i>	MATα	YPH499; <i>mas37Δ::HIS3</i>	[35]

### Bacterial strains

All *Salmonella* strains were derived from the *S. typhimurium* strain SL1344 by standard allelic exchange procedures. Bacterial cultures were supplemented with streptomycin (50 µg/mL) and tetracycline (12.5 µg/mL). Molecular cloning was performed by standard Gibson cloning as per manufacturer's recommendations.

### Bacterial crude membrane preparation

*S. typhimurium* strains were grown in LB broth supplemented with 0.3 M NaCl at 37°C under low aerated conditions to enhance expression of genes of SPI-1. Overnight cultures were diluted to a final ratio of 1:50 into fresh LB-NaCl until the optical density reached an OD<sub>600</sub> 0.7–0.8. The equivalent of 15 OD units was harvested at 8000×g for 10 min and thereafter re-suspended in 750 µl Buffer K (50 mM triethanolamine, pH 7.5, 250 mM sucrose, 1 mM EDTA, 1 mM MgCl<sub>2</sub>, 10 µg/ml DNase, 10 mg/mL lysozyme, 1:100 protease inhibitor cocktail). The cell suspension was incubated on ice for 30 min. The samples were bead milled for 2 min to break the bacteria and subsequently centrifuged (10000×g, 10 min, 4°C) to pellet unbroken cells and debris. Crude membranes, present in the supernatant, were precipitated by centrifugation (52000 rpm, 50 min, 4°C, in a Beckman TLA-55 rotor) and used for BN-PAGE analysis.

### REFERENCES

- Green ER, and Meccas J (2016). Bacterial Secretion Systems: An Overview. **Microbiol Spectr** 4(1). doi: 10.1128/microbiolspec.VMBF-0012-2015
- Kubori T (2016). Life with Bacterial Secretion Systems. **PLoS Pathog** 12(8): e1005562. doi: 10.1371/journal.ppat.1005562
- Alvarez-Martinez CE, and Christie PJ (2009). Biological diversity of prokaryotic type IV secretion systems. **Microbiol Mol Biol Rev** 73(4): 775-808. doi: 10.1128/MMBR.00023-09
- Galan JE, and Wolf-Watz H (2006). Protein delivery into eukaryotic cells by type III secretion machines. **Nature** 444(7119): 567-73. doi: 10.1038/nature05272
- Korotkov KV, Sandkvist M, and Hol WG (2012). The type II secretion system: biogenesis, molecular architecture and mechanism. **Nat Rev Microbiol** 10(5): 336-51. doi:10.1038/nrmicro2762
- Johnson TL, Abendroth J, Hol WG, and Sandkvist M (2006). Type II secretion: from structure to function. **FEMS Microbiol Lett** 255(2): 175-86. doi: 10.1111/j.1574-6968.2006.00102.x
- Disconzi E, Guilvout I, Chami M, Masi M, Huysmans GH, Pugsley AP, and Bayan N (2014). Bacterial secretins form constitutively open pores akin to general porins. **J Bacteriol** 196(1): 121-8. doi: 10.1128/JB.00750-13
- Korotkov KV, Gonen T, and Hol WG (2011). Secretins: dynamic channels for protein transport across membranes. **Trends Biochem Sci** 36(8): 433-43. doi: 10.1016/j.tibs.2011.04.002
- Hardie KR, Lory S, and Pugsley AP (1996). Insertion of an outer membrane protein in *Escherichia coli* requires a chaperone-like protein. **EMBO J** 15(5): 978-88. doi: 10.1002/j.1460-2075.1996.tb00434.x

### ACKNOWLEDGMENTS

We thank Elena Kracker, Lara Sophie Rieder, Dr. Tobias Jores, and Dr. Thomas Ulrich for their technical help. We would like to thank Dr. Antony P. Pugsley for constructs of bacterial secretins and an antibody against PulD. This work was supported by the Deutsche Forschungsgemeinschaft (SFB766/B11 to D.R.).

### CONFLICT OF INTEREST

The authors declare no conflict of interests.

### COPYRIGHT

© 2019 Natarajan *et al.* This is an open-access article released under the terms of the Creative Commons Attribution (CC BY) license, which allows the unrestricted use, distribution, and reproduction in any medium, provided the original author and source are acknowledged.

Please cite this article as: Janani Natarajan, Anasuya Moitra, Sussanne Zabel, Nidhi Singh, Samuel Wagner and Doron Rapaport (2019). Yeast can express and assemble bacterial secretins in the mitochondrial outer membrane. **Microbial Cell** 7(1): 15-27. doi: 10.15698/mic2020.01.703

- Nouwen N, Stahlberg H, Pugsley AP, and Engel A (2000). Domain structure of secretin PulD revealed by limited proteolysis and electron microscopy. **EMBO J** 19(10): 2229-36. doi:10.1093/emboj/19.10.2229
- Linderoth NA, Model P, and Russel M (1996). Essential role of a sodium dodecyl sulfate-resistant protein IV multimer in assembly-export of filamentous phage. **J Bacteriol** 178(7): 1962-70. doi: 10.1128/jb.178.7.1962-1970.1996
- Chami M, Guilvout I, Gregorini M, Remigy HW, Muller SA, Valerio M, Engel A, Pugsley AP, and Bayan N (2005). Structural insights into the secretin PulD and its trypsin-resistant core. **J Biol Chem** 280(45): 37732-41. doi: 10.1074/jbc.M504463200
- Schraidt O, and Marlovits TC (2011). Three-dimensional model of *Salmonella's* needle complex at subnanometer resolution. **Science** 331(6021): 1192-5. doi:10.1126/science.1199358
- Berry JL, Phelan MM, Collins RF, Adomavicius T, Tonjum T, Frye SA, Bird L, Owens R, Ford RC, Lian LY, and Derrick JP (2012). Structure and assembly of a trans-periplasmic channel for type IV pili in *Neisseria meningitidis*. **PLoS Pathog** 8(9): e1002923. doi: 10.1371/journal.ppat.1002923
- Radics J, Konigsmair L, and Marlovits TC (2014). Structure of a pathogenic type 3 secretion system in action. **Nat Struct Mol Biol** 21(1): 82-7. doi: 10.1038/nsmb.2722
- Koo J, Burrows LL, and Howell PL (2012). Decoding the roles of pilotins and accessory proteins in secretin escort services. **FEMS Microbiol Lett** 328(1): 1-12. doi:10.1111/j.1574-6968.2011.02464.x
- Gu S, Rehman S, Wang X, Shevchik VE, and Pickersgill RW (2012). Structural and functional insights into the pilotin-secretin complex of the type II secretion system. **PLoS Pathog** 8(2): e1002531. doi: 10.1371/journal.ppat.1002531
- Guilvout I, Chami M, Berrier C, Ghazi A, Engel A, Pugsley AP, and Bayan N (2008). In vitro multimerization and membrane insertion of

- bacterial outer membrane secretin PulD. **J Mol Biol** 382(1): 13-23. doi: 10.1016/j.jmb.2008.06.055
19. Guilvout I, Nickerson NN, Chami M, and Pugsley AP (2011). Multimerization-defective variants of dodecameric secretin PulD. **Res Microbiol** 162(2): 180-90. doi: 10.1016/j.resmic.2011.01.006
20. Daefler S, Guilvout I, Hardie KR, Pugsley AP, and Russel M (1997). The C-terminal domain of the secretin PulD contains the binding site for its cognate chaperone, PulS, and confers PulS dependence on pIVf1 function. **Mol Microbiol** 24(3): 465-75. doi: 10.1046/j.1365-2958.1997.3531727.x
21. Nickerson NN, Tosi T, Dessen A, Baron B, Raynal B, England P, and Pugsley AP (2011). Outer membrane targeting of secretin PulD protein relies on disordered domain recognition by a dedicated chaperone. **J Biol Chem** 286(45): 38833-43. doi: 10.1074/jbc.M111.279851
22. Huysmans GH, Guilvout I, and Pugsley AP (2013). Sequential steps in the assembly of the multimeric outer membrane secretin PulD. **J Biol Chem** 288(42): 30700-7. doi:10.1074/jbc.M113.489112
23. Ochman H, Soncini FC, Solomon F, and Groisman EA (1996). Identification of a pathogenicity island required for *Salmonella* survival in host cells. **Proc Natl Acad Sci USA** 93(15): 7800-4. doi: 10.1073/pnas.93.15.7800
24. Crago AM, and Koronakis V (1998). *Salmonella* InvG forms a ring-like multimer that requires the InvH lipoprotein for outer membrane localization. **Mol Microbiol** 30(1): 47-56. doi: 10.1046/j.1365-2958.1998.01036.x
25. Marlovits TC, Kubori T, Sukhan A, Thomas DR, Galan JE, and Unger VM (2004). Structural insights into the assembly of the type III secretion needle complex. **Science** 306(5698): 1040-2. doi: 10.1126/science.1102610
26. Hu J, Worrall LJ, Hong C, Vuckovic M, Atkinson CE, Caveney N, Yu Z, and Strynadka NCJ (2018). Cryo-EM analysis of the T3S injectisome reveals the structure of the needle and open secretin. **Nat Commun** 9(1): 3840. doi: 10.1038/s41467-018-06298-8.
27. Collin S, Guilvout I, Nickerson NN, and Pugsley AP (2011). Sorting of an integral outer membrane protein via the lipoprotein-specific Lol pathway and a dedicated lipoprotein pilotin. **Mol Microbiol** 80(3): 655-65. doi: 10.1111/j.1365-2958.2011.07596.x.
28. Guilvout I, Chami M, Engel A, Pugsley AP, and Bayan N (2006). Bacterial outer membrane secretin PulD assembles and inserts into the inner membrane in the absence of its pilotin. **EMBO J** 25(22): 5241-9. doi: 10.1038/sj.emboj.7601402
29. Guilvout I, Brier S, Chami M, Hourdel V, Francetic O, Pugsley AP, Chamot-Rooke J, and Huysmans GH (2017). Prepore Stability Controls Productive Folding of the BAM-independent Multimeric Outer Membrane Secretin PulD. **J Biol Chem** 292(1): 328-338. doi: 10.1074/jbc.M116.759498
30. Ulrich T, and Rapaport D (2015). Biogenesis of beta-barrel proteins in evolutionary context. **Int J Med Microbiol** 305(2): 259-64. doi: 10.1016/j.ijmm.2014.12.009
31. Muller JE, Papic D, Ulrich T, Grin I, Schutz M, Oberhettinger P, Tommassen J, Linke D, Dimmer KS, Autenrieth IB, and Rapaport D (2011). Mitochondria can recognize and assemble fragments of a beta-barrel structure. **Mol Biol Cell** 22(10): 1638-47. doi:10.1091/mbc.E10-12-0943
32. Walther DM, Papic D, Bos MP, Tommassen J, and Rapaport D (2009). Signals in bacterial beta-barrel proteins are functional in eukaryotic cells for targeting to and assembly in mitochondria. **Proc Natl Acad Sci USA** 106(8): 2531-6. doi: 10.1073/pnas.0807830106
33. Schlossmann, J, Lill R, Neupert W, and Court DA (1996). Tom71, a novel homologue of the mitochondrial preprotein receptor Tom70. **J Biol Chem** 271(30): 17890-5. doi: 10.1074/jbc.271.30.17890.
34. Kondo-Okamoto N, Shaw JM, and Okamoto K (2008). Tetratricopeptide repeat proteins Tom70 and Tom71 mediate yeast mitochondrial morphogenesis. **EMBO Rep** 9(1): 63-9. doi: 10.1038/sj.embor.7401113
35. Habib SJ, Waizenegger T, Lech M, Neupert W, and Rapaport D (2005). Assembly of the TOB complex of mitochondria. **J Biol Chem** 280(8): 6434-40. doi: 10.1074/jbc.M411510200
36. Gietz RD, and Woods RA (2006). Yeast transformation by the LiAc/SS Carrier DNA/PEG method. **Methods Mol Biol** 313: 107-20. doi: 10.1385/1-59259-958-3:107
37. Daum G, Bohni PC, and Schatz G (1982). Import of proteins into mitochondria. Cytochrome b2 and cytochrome c peroxidase are located in the intermembrane space of yeast mitochondria. **J Biol Chem** 257(21): 13028-33. PMID: 6290489
38. Schagger H, Cramer WA and von Jagow G (1994). Analysis of molecular masses and oligomeric states of protein complexes by blue native electrophoresis and isolation of membrane protein complexes by two-dimensional native electrophoresis. **Anal Biochem** 217(2): 220-30. doi: 10.1006/abio.1994.1112



# The Biogenesis Process of VDAC – From Early Cytosolic Events to Its Final Membrane Integration

Anasuya Moitra and Doron Rapaport\*

Interfaculty Institute of Biochemistry, University of Tübingen, Tübingen, Germany

## OPEN ACCESS

### Edited by:

Vito De Pinto,  
University of Catania, Italy

### Reviewed by:

Eduardo Nestor Maldonado,  
Medical University of South Carolina,  
United States

Dejana Mokranjac,  
Ludwig Maximilian University  
of Munich, Germany

### \*Correspondence:

Doron Rapaport  
doron.rapaport@uni-tuebingen.de

### Specialty section:

This article was submitted to  
Mitochondrial Research,  
a section of the journal  
Frontiers in Physiology

**Received:** 29 June 2021

**Accepted:** 26 July 2021

**Published:** 12 August 2021

### Citation:

Moitra A and Rapaport D (2021)  
The Biogenesis Process of VDAC –  
From Early Cytosolic Events to Its  
Final Membrane Integration.  
*Front. Physiol.* 12:732742.  
doi: 10.3389/fphys.2021.732742

Voltage dependent anion-selective channel (VDAC) is the most abundant protein in the mitochondrial outer membrane. It is a membrane embedded  $\beta$ -barrel protein composed of 19 mostly anti-parallel  $\beta$ -strands that form a hydrophilic pore. Similar to the vast majority of mitochondrial proteins, VDAC is encoded by nuclear DNA, and synthesized on cytosolic ribosomes. The protein is then targeted to the mitochondria while being maintained in an import competent conformation by specific cytosolic factors. Recent studies, using yeast cells as a model system, have unearthed the long searched for mitochondrial targeting signal for VDAC and the role of cytosolic chaperones and mitochondrial import machineries in its proper biogenesis. In this review, we summarize our current knowledge regarding the early cytosolic stages of the biogenesis of VDAC molecules, the specific targeting of VDAC to the mitochondrial surface, and the subsequent integration of VDAC into the mitochondrial outer membrane by the TOM and TOB/SAM complexes.

**Keywords:** beta-barrels, chaperones, mitochondria, outer membrane, TOM complex, VDAC

## INTRODUCTION

Most of the outer membrane (OM) proteins in Gram-negative bacteria are membrane-embedded  $\beta$ -barrel proteins that are composed of anti-parallel  $\beta$ -strands forming a barrel shaped hydrophilic pore in the membrane. In eukaryotes, the presence of  $\beta$ -barrel proteins is restricted to the OM of mitochondria and chloroplasts that were derived from prokaryotic ancestors. The assembly of these proteins into their corresponding OM is in each case facilitated by a dedicated protein complex that contains a highly conserved central  $\beta$ -barrel protein termed Bama/YaeT/Omp85 in Gram-negative bacteria, Tob55/Sam50 in mitochondria, and probably OEP80 in plastids (Ulrich and Rapaport, 2015; Gross et al., 2021). These central components are related to each other and belong to the Omp85 superfamily (Gentle et al., 2005). Voltage Dependent Anion-selective Channels (VDACs) are abundant mitochondrial  $\beta$ -barrel proteins (Schein et al., 1976; Colombini, 1979). Their pore is composed of 19 anti-parallel  $\beta$ -strands whereas strands 1 and 19 are in parallel orientation to each other. VDAC, which was previously known as mitochondrial porin, functions as a channel for transport of metabolites, nucleotides, ions, and even small peptides (Benz, 1989). VDACs are found in mitochondria across the spectrum of life, from unicellular yeasts to plants and all higher eukaryotes. Bakers' yeast (*Saccharomyces cerevisiae*) has two genes encoding VDACs, *POR1* and *POR2*, while higher eukaryotes like humans have at least three isoforms, *VDAC1*, *VDAC2* and *VDAC3* and plants have up to five such genes (Young et al., 2007; Raghavan et al., 2012).

During the evolution of mitochondria from an ancient endosymbiont, most of the organellar genes, including those encoding predecessors of VDACS, were transferred to the nucleus, with the mitochondrial genome retaining the codes for only few key components of the respiratory chain complexes (Gray et al., 1999). VDACS are thus transcribed in the nucleus and translated on cytosolic ribosomes. Then, they need to be targeted to the correct sub-cellular organelle, namely the mitochondria, and ultimately integrated into the mitochondrial OM (MOM) with the help of dedicated import machineries. In this review, we will highlight recent studies that have discovered cytosolic factors associated with newly synthesized VDAC molecules, the elusive mitochondrial targeting information for VDAC, and finally the mechanisms of insertion and integration of VDAC into MOM.

## EARLY CYTOSOLIC EVENTS OF NEWLY SYNTHESIZED VDAC MOLECULES

The first challenge of the biogenesis of VDAC is to keep the newly synthesized molecules in an import competent conformation (Freitag et al., 1982; Rapaport and Neupert, 1999). The rather hydrophobic  $\beta$ -strands that build the transmembrane segments are prone to aggregation in the cytosol. Thus, the newly synthesized VDAC precursors must be bound by cytosolic chaperones to shield these hydrophobic patches, preventing the emerging nascent chain from engaging in unfavorable intra- and inter-molecular interactions (Kim et al., 2013). This association with chaperones maintains them in an import-competent conformation. Recent studies, using yeast as a model system, demonstrate that newly synthesized VDAC molecules dynamically interact with Hsp70 chaperones (Ssa1/2) and their Hsp40 co-chaperones Ydj1 and Sis1 (Figure 1; Jores et al., 2018). Inhibiting the activity of the cytosolic Hsp70 chaperone, preventing its docking to the mitochondrial receptor Tom70, or co-depleting both co-chaperones Ydj1 and Sis1 resulted in a significant reduction in *in vivo* and *in vitro* import of VDAC into yeast mitochondria. Experiments utilizing Hsp70 inhibitors and pull-down assays demonstrated that the interactions between VDAC and Hsp70 chaperones and their physiological role are also conserved in mammalian cells. Moreover, a  $\beta$ -hairpin motif of VDAC, hypothesized to be the mitochondrial targeting signal (see below), was sufficient for the interaction with these (co-) chaperones. It should be emphasized that these (co-) chaperones support the import of not only  $\beta$ -barrel proteins but are also involved in the biogenesis of many additional proteins. Hence, so far, a targeting factor, which is dedicated solely to  $\beta$ -barrel proteins was not identified. The abovementioned chaperones, based on the mitochondrial targeting information, relay the nascent precursors to the receptors of the translocase of the outer membrane (TOM) of mitochondria. Other  $\beta$ -barrel proteins like Tom40 and Tob55/Sam50 appear to follow the same route as VDAC (Jores et al., 2018).

Currently, it is not clear whether the aforementioned cytosolic factors support biogenesis solely by preventing premature unfavorable aggregation or whether they also facilitate specific targeting. The contribution of the chaperone anchor Tom70,

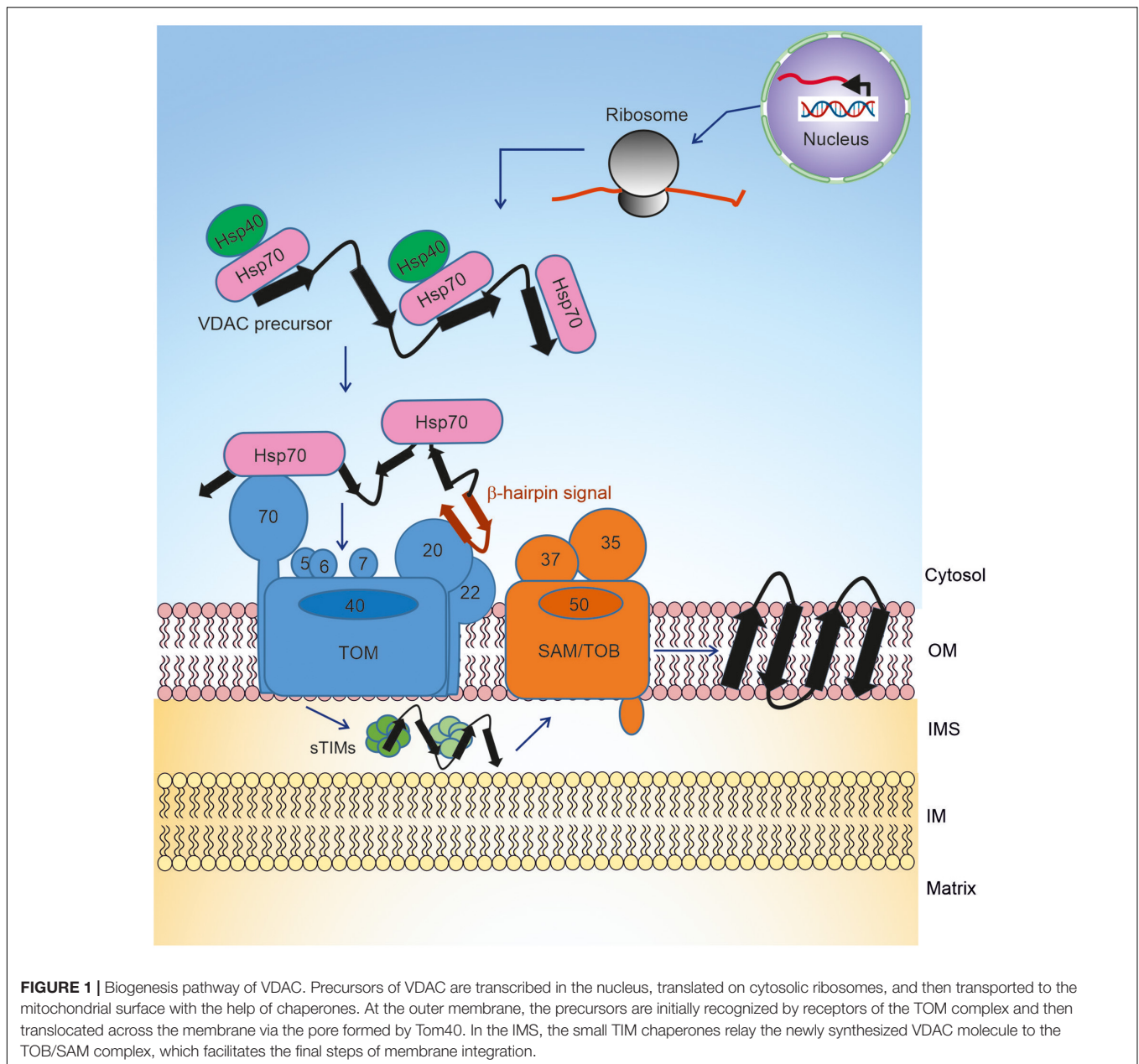
located at the mitochondrial surface, to the overall import process suggests that association with chaperones also increases the specificity of organellar targeting.

## TARGETING OF VDAC TO THE MITOCHONDRIAL SURFACE

Most mitochondrial precursor proteins contain a cleavable N-terminal presequence that targets them to mitochondria. However, like the other mitochondrial  $\beta$ -barrel proteins, VDAC lacks a cleavable targeting signal. Hence, it remained unclear how the targeting information for VDAC was encoded. Various studies showed that bacterial and chloroplast  $\beta$ -barrel proteins could be targeted and assembled into yeast mitochondria (Walther et al., 2009; Ulrich et al., 2012, 2014). Conversely, VDAC could also be integrated into bacterial outer membranes and form pores there (Walther et al., 2010), suggesting that the targeting information for  $\beta$ -barrel proteins is conserved from bacteria to mitochondria and thus functional in both systems. Since none of the studies could identify a definitive linear amino acid sequence as the targeting signal, it was hypothesized that the targeting signal may be a structural feature of the  $\beta$ -barrel proteins.

Truncation studies showed that the last C-terminal  $\beta$ -strand of mitochondrial  $\beta$ -barrel proteins contains a stretch of amino acids that facilitate their interaction with the TOB/SAM complex. These residues were called the  $\beta$ -signal (Kutik et al., 2008). However, deletion or mutation of the  $\beta$ -signal did not interfere with the initial targeting of newly synthesized  $\beta$ -barrel proteins to mitochondria. Studies involving a bacterial trimeric autotransporter Yersinia adhesion A (YadA), where each subunit contributes four  $\beta$ -strands to a 12-mer  $\beta$ -barrel structure, demonstrated that such proteins can be targeted to mitochondria upon their expression in yeast cells (Müller et al., 2011). This finding implies that even a partial  $\beta$ -barrel structure (like four  $\beta$ -strands) is sufficient for specific mitochondrial targeting. Hence, it was further tested whether a  $\beta$ -hairpin structural motif, which is composed of two  $\beta$ -strands and a loop and represents the most basic repeating structural motif of  $\beta$ -barrel proteins, could be the elusive mitochondrial targeting signal. To support this possibility, it was shown that a peptide corresponding to the last  $\beta$ -hairpin of human VDAC1 could competitively inhibit the *in vitro* import of mitochondrial  $\beta$ -barrels (Jores et al., 2016). Moreover, hybrid proteins of this  $\beta$ -hairpin fused to soluble passenger domains like GFP or DHFR were targeted to mitochondria upon their expression in yeast cells. Such  $\beta$ -hairpin motif has an amphipathic characteristic as eventually, upon its incorporation into a membrane-embedded  $\beta$ -barrel, one phase of the motif will face the lipid core and hence is hydrophobic, whereas the opposite one will be exposed to the pore lumen and thus is rather hydrophilic. Importantly, it was discovered that optimal mitochondrial targeting depends on relative elevated hydrophobicity of those amino acid residues that face the lipid core of the membrane (Jores et al., 2016).

In most eukaryotic cells, mitochondria are the only organelles containing  $\beta$ -barrel proteins. The problem of specific targeting gets an interesting twist in plant cells where



plastids can be an alternative destination for such proteins. Klinger et al. (2019) addressed this issue and found that the hydrophobicity is not sufficient for the discrimination of targeting to chloroplasts or mitochondria. By domain swapping between mitochondrial (atVDAC1) and chloroplast (psOEP24) targeted  $\beta$ -barrel proteins, they could demonstrate that the presence of a hydrophilic amino acid at the C-terminus of the penultimate  $\beta$ -strand is also required for mitochondrial targeting. A variant of the chloroplast  $\beta$ -barrel protein psOEP24, which mimics such profile, was efficiently targeted to mitochondria (Klinger et al., 2019).

Collectively, it seems that the combined contribution of several  $\beta$ -hairpin motifs with a highly hydrophobic face assures proper mitochondrial targeting of VDAC.

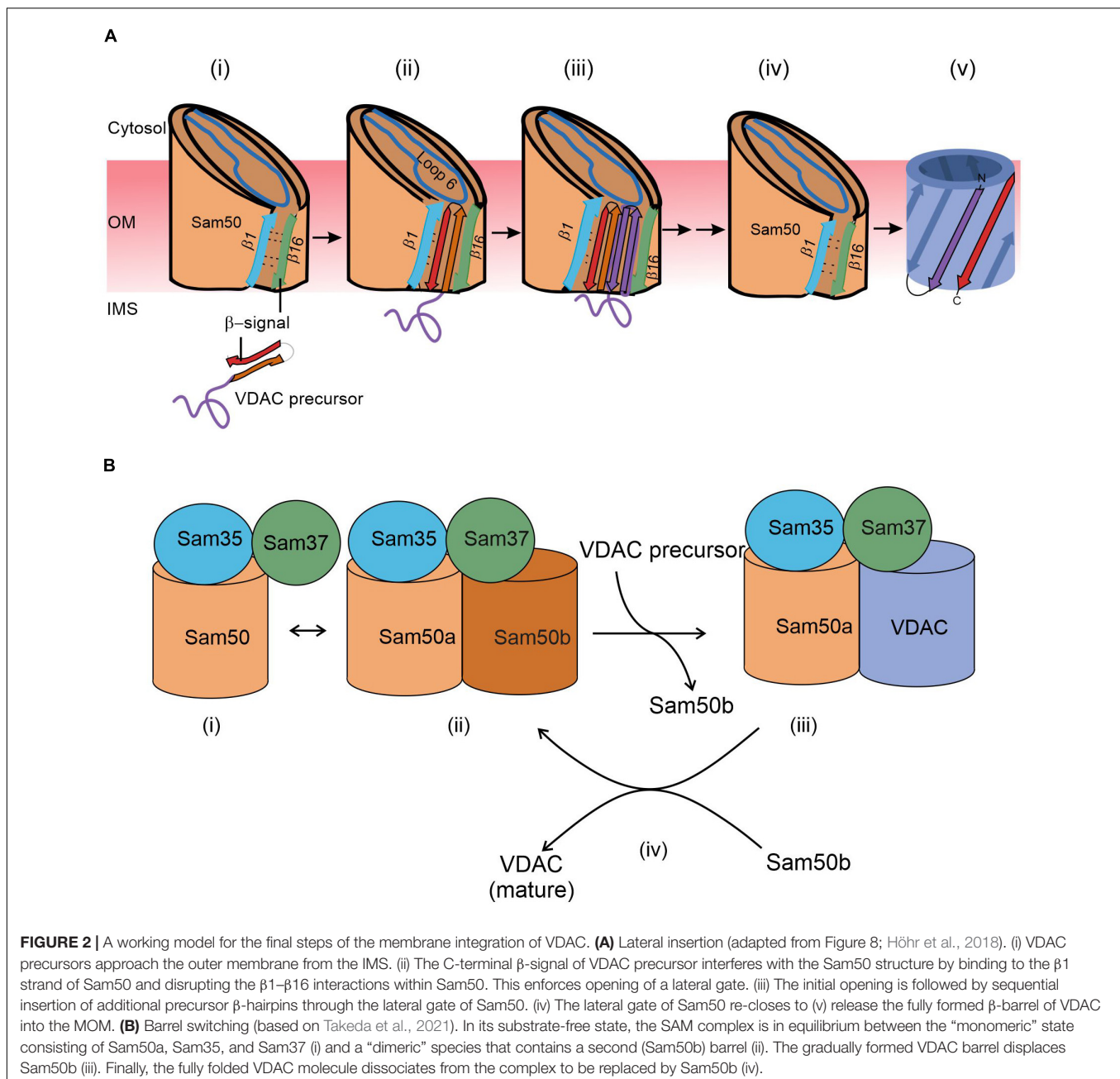
## MEMBRANE INTEGRATION OF VDAC BY THE TOM AND TOB/SAM COMPLEXES

Once the chaperone-associated VDAC precursors are targeted to mitochondria via the  $\beta$ -hairpin signal, they interact with the TOM complex at the mitochondrial surface to initiate organellar import (Figure 1). The TOM complex is comprised of the core complex and its peripheral import receptors. The core complex has a central translocon channel, formed by the integral  $\beta$ -barrel protein Tom40, along with several transmembrane accessory proteins namely Tom5, Tom6, Tom7, and Tom22 (Bausewein et al., 2017; Araiso et al., 2019; Tucker and Park, 2019). Tom20 and Tom70 are the receptors involved in the initial

recognition of multiple mitochondrial proteins (Neupert and Herrmann, 2007; **Figure 1**). Several studies hinted at the role of Tom20 in the recognition of  $\beta$ -barrel precursors (Rapaport and Neupert, 1999; Schleiff et al., 1999; Krimmer et al., 2001; Yamano et al., 2008). Using NMR, photo-crosslinking and fluorescence complementation assays, it was recently shown that the  $\beta$ -hairpin element of VDAC interacts with the mitochondrial import receptor Tom20 via the presequence binding region of the latter (Jores et al., 2016). Moreover, direct cross-linking of the  $\beta$ -hairpin motif to Tom70 and the observation that blocking this receptor interferes with the import of VDAC suggested that Tom70 also plays a role in the initial recognition of VDAC (Jores et al., 2016).

The involvement of Tom70 can be either via direct recognition of the substrate protein or by serving as a docking site for the chaperone-substrate complex.

Following recognition by the import receptors, the VDAC precursors are translocated across the MOM via the Tom40 channel by interacting with a series of binding sites, probably with increasing affinities (Hill et al., 1998). Upon its emergence at the intermembrane space (IMS), the translocated VDAC molecule interacts with the small chaperones of the translocase of the inner membrane (small TIMs). The IMS chaperone system includes the small Tim proteins, Tim8, Tim9, Tim10, and Tim13 (Koehler et al., 1998). These small chaperones form alternating circular



hexamers comprised of three subunits of Tim9 and Tim10, or three subunits of each Tim8 and Tim13 (Webb et al., 2006; Beverly et al., 2008). Site-specific cross-linking indicated that the small TIMs interact with the IMS-exposed part of the N-terminal extension of Tom40 (Shiota et al., 2015).

The small TIMs play an important role in the transfer of the  $\beta$ -barrel precursors of VDAC from the TOM complex to the sorting and assembly machinery (SAM) complex (Hoppins and Nargang, 2004; Wiedemann et al., 2004; **Figure 1**). The formation of a  $\beta$ -hairpin within the last two C-terminal  $\beta$ -strands of VDAC is crucial for the interaction of the precursors with the TIM chaperones. Structural and mechanistic studies revealed that TIM chaperones hold the VDAC protein precursors in a nascent chain-like extended conformation via multiple clamp-like binding sites (Weinhäupl et al., 2018). Such multiple weak and constantly reshuffling interactions ultimately allow for the efficient release of the precursor to the actual insertase, the SAM complex, which is also known as the topogenesis of outer-membrane  $\beta$ -barrel proteins (TOB) complex (**Figure 1**; Paschen et al., 2003; Wiedemann et al., 2003; Gentle et al., 2004). The Tim9/10 binding cleft for the  $\beta$ -barrel precursors has conserved hydrophobic residues for these interactions, and mutations in these residues are detrimental to the VDAC biogenesis and overall cell growth.

To facilitate a smooth transfer, the TOM and the TOB/SAM complex can form a super-complex bridged by the cytosolic domain of Tom22 and the peripheral TOB/SAM component, Mas37/Sam37 (Qiu et al., 2013). The core subunit of the TOB/SAM complex is the 16-stranded  $\beta$ -barrel protein Tob55/Sam50, that belongs to the Omp85 superfamily of proteins. Tob55/Sam50 has an N-terminal POTRA domain, which can bind the incoming substrate but is not essential for the  $\beta$ -barrel assembly process. In addition, the TOB/SAM complex harbors two cytosol-exposed peripheral subunits that are involved in formation of a TOM-TOB super-complex (Mas37/Sam37) and stabilization of the TOB/SAM bound form of the precursor (Tob38/Sam35).

Our understanding of the final steps in the biogenesis of the VDAC  $\beta$ -barrel precursors evolved dramatically in the last 5 years. Structural studies indicate the formation of a lateral gate between  $\beta$ -strands 1 and 16 of Sam50. Accordingly, and supported by intensive cross-linking assays, the lateral gate insertion model was put forward. This model suggests that the C-terminal  $\beta$ -signal of the precursor initiates opening of the gate by exchange with the endogenous Sam50  $\beta$ -signal. In addition, loop 6 of Sam50 was found to be crucial for the VDAC precursor transfer to the lateral gate (Höhr et al., 2018). An increasing number of  $\beta$  hairpin-like loops of the precursor insert and fold sequentially and accumulate at the lateral gate (**Figure 2A**). Finally, hydrogen bonds are formed between the first and last  $\beta$ -strand to close the newly folded VDAC  $\beta$ -barrel. Upon folding at Sam50, the full-length newly formed  $\beta$ -barrel protein is laterally released into the outer membrane and the Sam50 lateral gate closes (**Figure 2A**). The opening of the putative lateral gate obtained further support from a recent report on the atomic structure of the SAM complex (Diederichs et al., 2020). Membrane thinning in the vicinity of the lateral

gate can further facilitate insertion of the  $\beta$ -barrel protein into the lipid bilayer.

The membrane integration model recently obtained a new twist from structural studies. Based on detailed atomic structure of the SAM complex, the barrel swapping model envisions the SAM complex as formed by a SAM monomer (Sam50a along with Sam35 and Sam37) and a Sam50b second barrel (**Figure 2B**; Takeda et al., 2021). The precursor protein  $\beta$ -signal binds Sam50a as in the lateral gate insertion model. Then, the folded VDAC  $\beta$ -barrel slowly displaces Sam50b and takes its place. Sam37 that originally also interacts with Sam50b, gets gradually involved in interactions with the newly formed VDAC barrel (**Figure 2B**). Finally, this barrel dissociates from the SAM complex and is integrated into the MOM.

Of note, most of our current knowledge regarding the biogenesis of  $\beta$ -barrel proteins is based on biochemical and structural studies on fungal elements. While the atomic structure of the mammalian TOM complex appears to be rather similar to its fungal counterpart (Wang et al., 2020), not much is known about the SAM complex in higher eukaryotes. It is rather clear that the mammalian Sam50 is the central component of the complex. However, the precise functions of Metaxins1/2/3, which are homologous to yeast Sam35 and Sam37, is not clear yet.

## PERSPECTIVES

Our understanding of the factors and machineries involved in the assembly of VDAC proteins into the MOM has made tremendous progress in the last 20 years. We now have detailed atomic structures of the membrane-embedded TOM and SAM complexes, and the hexamer of the small TIM chaperones that transfer the substrate from the former to the latter. Challenges for the future include the characterization of the mammalian SAM complex and to decipher how the various biogenesis steps of VDAC are regulated and adapted to the cellular physiological conditions. Moreover, it will be interesting to determine if after its insertion into the OM, oligomerization, additional folding, or post-translational modifications are necessary for VDAC to become fully functional.

## AUTHOR CONTRIBUTIONS

AM and DR wrote the manuscript. Both authors contributed to the article and approved the submitted version.

## FUNDING

This work was supported by the Deutsche Forschungsgemeinschaft (RA1028/8-2 to DR) and the IMPRS “From Molecules to Organisms” (AM).

## ACKNOWLEDGMENTS

We thank Dr. Kai S. Dimmer for his comments on this manuscript.

## REFERENCES

- Araiso, Y., Tsutsumi, A., Qiu, J., Imai, K., Shiota, T., Song, J., et al. (2019). Structure of the mitochondrial import gate reveals distinct preprotein paths. *Nature* 575, 395–401. doi: 10.1038/s41586-019-1680-7
- Bausewein, T., Mills, D. J., Langer, J. D., Nitschke, B., Nussberger, S., and Kühlbrandt, W. (2017). Cryo-EM structure of the TOM core complex from *Neurospora crassa*. *Cell* 170, 693–700.e697.
- Benz, R. (1989). "Porins from mitochondrial and bacterial outer membranes: structural and functional aspects," in *Anion Carriers of Mitochondrial Membranes*, eds A. Azzi, K. A. Nałęcz, M. J. Nałęcz, and L. Wojtczak (Berlin: Springer).
- Beverly, K. N., Sawaya, M. R., Schmid, E., and Koehler, C. M. (2008). The Tim8-Tim13 complex has multiple substrate binding sites and binds cooperatively to Tim23. *J. Mol. Biol.* 382, 1144–1156. doi: 10.1016/j.jmb.2008.07.069
- Colombini, M. (1979). A candidate for the permeability pathway of the outer mitochondrial membrane. *Nature* 279, 643–645. doi: 10.1038/279643a0
- Diederichs, K. A., Ni, X., Rollauer, S. E., Botos, I., Tan, X., King, M. S., et al. (2020). Structural insight into mitochondrial  $\beta$ -barrel outer membrane protein biogenesis. *Nat. Commun.* 11:3290.
- Freitag, H., Neupert, W., and Benz, R. (1982). Purification and characterisation of a pore protein of the outer mitochondrial membrane from *Neurospora crassa*. *Eur. J. Biochem.* 123, 629–636. doi: 10.1111/j.1432-1033.1982.tb06578.x
- Gentle, I., Gabriel, K., Beech, P., Waller, R., and Lithgow, T. (2004). The Omp85 family of proteins is essential for outer membrane biogenesis in mitochondria and bacteria. *J. Cell Biol.* 164, 19–24. doi: 10.1083/jcb.200310092
- Gentle, I. E., Burri, L., and Lithgow, T. (2005). Molecular architecture and function of the Omp85 family of proteins. *Mol. Microbiol.* 58, 1216–1225. doi: 10.1111/j.1365-2958.2005.04906.x
- Gray, M. W., Burger, G., and Lang, B. F. (1999). Mitochondrial evolution. *Science* 283, 1476–1481.
- Gross, L. E., Klinger, A., Spies, N., Ernst, T., Flinner, N., Simm, S., et al. (2021). Insertion of plastidic  $\beta$ -barrel proteins into the outer envelopes of plastids involves an intermembrane space intermediate formed with Toc75-V/OEP80. *Plant Cell* 33, 1657–1681. doi: 10.1093/plcell/koab052
- Hill, K., Model, K., Ryan, M. T., Dietmeier, K., Martin, F., Wagner, R., et al. (1998). Tom40 forms the hydrophilic channel of the mitochondrial import pore for preproteins. *Nature* 395, 516–521. doi: 10.1038/26780
- Höhr, A. I. C., Lindau, C., Wirth, C., Qiu, J., Stroud, D. A., Kutik, S., et al. (2018). Membrane protein insertion through a mitochondrial  $\beta$ -barrel gate. *Science* 359:eah6834. doi: 10.1126/science.aah6834
- Hoppins, S. C., and Nargang, F. E. (2004). The Tim8-Tim13 complex of *Neurospora crassa* functions in the assembly of proteins into both mitochondrial membranes. *J. Biol. Chem.* 279, 12396–12405. doi: 10.1074/jbc.m313037200
- Jores, T., Klinger, A., Groß, L. E., Kawano, S., Flinner, N., Duchardt-Ferner, E., et al. (2016). Characterization of the targeting signal in mitochondrial  $\beta$ -barrel proteins. *Nat. Commun.* 7:12036.
- Jores, T., Lawatscheck, J., Beke, V., Franz-Wachtel, M., Yunoki, K., Fitzgerald, J. C., et al. (2018). Cytosolic Hsp70 and Hsp40 chaperones enable the biogenesis of mitochondrial  $\beta$ -barrel proteins. *J. Cell Biol.* 217:3091. doi: 10.1083/jcb.201712029
- Kim, Y. E., Hipp, M. S., Bracher, A., Hayer-Hartl, M., and Hartl, F. U. (2013). Molecular chaperone functions in protein folding and proteostasis. *Annu. Rev. Biochem.* 82, 323–355. doi: 10.1146/annurev-biochem-060208-092442
- Klinger, A., Gosch, V., Bodensohn, U., Ladig, R., and Schleiff, E. (2019). The signal distinguishing between targeting of outer membrane  $\beta$ -barrel protein to plastids and mitochondria in plants. *Biochim. Biophys. Acta Mol. Cell Res.* 1866, 663–672. doi: 10.1016/j.bbamcr.2019.01.004
- Koehler, C. M., Jarosch, E., Tokatlidis, K., Schmid, K., Schweyen, R. J., and Schatz, G. (1998). Import of mitochondrial carriers mediated by essential proteins of the intermembrane space. *Science* 279, 369–373. doi: 10.1126/science.279.5349.369
- Krimmer, T., Rapaport, D., Ryan, M. T., Meisinger, C., Kassenbrock, C. K., Blachly-Dyson, E., et al. (2001). Biogenesis of porin of the outer mitochondrial membrane involves an import pathway via receptors and the general import pore of the TOM complex. *J. Cell Biol.* 152, 289–300. doi: 10.1083/jcb.152.2.289
- Kutik, S., Stojanovski, D., Becker, L., Becker, T., Meinecke, M., Krüger, V., et al. (2008). Dissecting membrane insertion of mitochondrial  $\beta$ -barrel proteins. *Cell* 132, 1011–1024. doi: 10.1016/j.cell.2008.01.028
- Müller, J. E., Papic, D., Ulrich, T., Grin, I., Schütz, M., Oberhettinger, P., et al. (2011). Mitochondria can recognize and assemble fragments of a  $\beta$ -barrel structure. *Mol. Biol. Cell* 22, 1638–1647. doi: 10.1091/mbc.e10-12-0943
- Neupert, W., and Herrmann, J. M. (2007). Translocation of proteins into mitochondria. *Annu. Rev. Biochem.* 76, 723–749. doi: 10.1146/annurev-biochem.76.052705.163409
- Paschen, S. A., Waizenegger, T., Stan, T., Preuss, M., Cyrklaff, M., Hell, K., et al. (2003). Evolutionary conservation of biogenesis of  $\beta$ -barrel membrane proteins. *Nature* 426, 862–866. doi: 10.1038/nature02208
- Qiu, J., Wenz, L. S., Zerbes, R. M., Oeljeklaus, S., Bohnert, M., Stroud, D. A., et al. (2013). Coupling of mitochondrial import and export translocases by receptor-mediated supercomplex formation. *Cell* 154, 596–608. doi: 10.1016/j.cell.2013.06.033
- Raghavan, A., Sheiko, T., Graham, B. H., and Craigen, W. J. (2012). Voltage-dependant anion channels: novel insights into isoform function through genetic models. *Biochim. Biophys. Acta Biomembr.* 1818, 1477–1485. doi: 10.1016/j.bbamem.2011.10.019
- Rapaport, D., and Neupert, W. (1999). Biogenesis of Tom40, core component of the TOM complex of mitochondria. *J. Cell Biol.* 146, 321–331. doi: 10.1083/jcb.146.2.321
- Schein, S. J., Colombini, M., and Finkelstein, A. (1976). Reconstitution in planar lipid bilayers of a voltage-dependent anion-selective channel obtained from paramecium mitochondria. *J. Membr. Biol.* 30, 99–120. doi: 10.1007/bf01869662
- Schleiff, E., Silviu, J. R., and Shore, G. C. (1999). Direct membrane insertion of voltage-dependent anion-selective channel protein catalyzed by mitochondrial Tom20. *J. Cell Biol.* 145, 973–978. doi: 10.1083/jcb.145.5.973
- Shiota, T., Imai, K., Qiu, J., Hewitt, V. L., Tan, K., Shen, H. H., et al. (2015). Molecular architecture of the active mitochondrial protein gate. *Science* 349, 1544–1548. doi: 10.1126/science.aac6428
- Takeda, H., Tsutsumi, A., Nishizawa, T., Lindau, C., Busto, J. V., Wenz, L.-S., et al. (2021). Mitochondrial sorting and assembly machinery operates by  $\beta$ -barrel switching. *Nature* 590, 163–169. doi: 10.1038/s41586-020-03113-7
- Tucker, K., and Park, E. (2019). Cryo-EM structure of the mitochondrial protein-import channel TOM complex at near-atomic resolution. *Nat. Struct. Mol. Biol.* 26, 1158–1166. doi: 10.1038/s41594-019-0339-2
- Ulrich, T., Gross, L. E., Sommer, M. S., Schleiff, E., and Rapaport, D. (2012). Chloroplast  $\beta$ -barrel proteins are assembled into the mitochondrial outer membrane in a process that depends on the TOM and TOB complexes. *J. Biol. Chem.* 287, 27467–27479. doi: 10.1074/jbc.m112.382093
- Ulrich, T., Oberhettinger, P., Schütz, M., Holzer, K., Ramms, A. S., Linke, D. I., et al. (2014). Evolutionary conservation in biogenesis of  $\beta$ -barrel proteins allows mitochondria to assemble a functional bacterial trimeric autotransporter protein. *J. Biol. Chem.* 289, 29457–29470. doi: 10.1074/jbc.m114.565655
- Ulrich, T., and Rapaport, D. (2015). Biogenesis of beta-barrel proteins in evolutionary context. *Int. J. Med. Microbiol.* 305, 259–264. doi: 10.1016/j.ijmm.2014.12.009
- Walther, D. M., Bos, M. P., Rapaport, D., and Tommassen, J. (2010). The mitochondrial porin, VDAC, has retained the ability to be assembled in the bacterial outer membrane. *Mol. Biol. Evol.* 27, 887–895. doi: 10.1093/molbev/msp294
- Walther, D. M., Papic, D., Bos, M. P., Tommassen, J., and Rapaport, D. (2009). Signals in bacterial beta-barrel proteins are functional in eukaryotic cells for targeting to and assembly in mitochondria. *Proc. Natl. Acad. Sci. U.S.A.* 106, 2531–2536. doi: 10.1073/pnas.0807830106
- Wang, W., Chen, X., Zhang, L., Yi, J., Ma, Q., Yin, J., et al. (2020). Atomic structure of human TOM core complex. *Cell Discov.* 6:67.
- Webb, C. T., Gorman, M. A., Lazarou, M., Ryan, M. T., and Gulbis, J. M. (2006). Crystal structure of the mitochondrial chaperone TIM9•10 reveals a Six-bladed  $\alpha$ -propeller. *Mol. Cell* 21, 123–133. doi: 10.1016/j.molcel.2005.11.010
- Weinhäupl, K., Lindau, C., Hessel, A., Wang, Y., Schütze, C., Jores, T., et al. (2018). Structural basis of membrane protein chaperoning through the mitochondrial intermembrane space. *Cell* 175, 1365–1379.e1325.

- Wiedemann, N., Kozjak, V., Chacinska, A., Schönfish, B., Rospert, S., Ryan, M. T., et al. (2003). Machinery for protein sorting and assembly in the mitochondrial outer membrane. *Nature* 424, 565–571. doi: 10.1038/nature01753
- Wiedemann, N., Truscott, K. N., Pfannschmidt, S., Guiard, B., Meisinger, C., and Pfanner, N. (2004). Biogenesis of the protein import channel Tom40 of the mitochondrial outer membrane: intermembrane space components are involved in an early stage of the assembly pathway. *J. Biol. Chem.* 279, 18188–18194. doi: 10.1074/jbc.m400050200
- Yamano, K., Yatsukawa, Y., Esaki, M., Hobbs, A. E., Jensen, R. E., and Endo, T. (2008). Tom20 and Tom22 share the common signal recognition pathway in mitochondrial protein import. *J. Biol. Chem.* 283, 3799–3807. doi: 10.1074/jbc.m708339200
- Young, M. J., Bay, D. C., Hausner, G., and Court, D. A. (2007). The evolutionary history of mitochondrial porins. *BMC Evol. Biol.* 7:31. doi: 10.1186/1471-2148-7-31

**Conflict of Interest:** The authors declare that the research was conducted in the absence of any commercial or financial relationships that could be construed as a potential conflict of interest.

**Publisher's Note:** All claims expressed in this article are solely those of the authors and do not necessarily represent those of their affiliated organizations, or those of the publisher, the editors and the reviewers. Any product that may be evaluated in this article, or claim that may be made by its manufacturer, is not guaranteed or endorsed by the publisher.

Copyright © 2021 Moitra and Rapaport. This is an open-access article distributed under the terms of the Creative Commons Attribution License (CC BY). The use, distribution or reproduction in other forums is permitted, provided the original author(s) and the copyright owner(s) are credited and that the original publication in this journal is cited, in accordance with accepted academic practice. No use, distribution or reproduction is permitted which does not comply with these terms.